

Chapter 7

HOUSE AND TERRAIN SHIELDING

William A. Woolson, Michael L. Gritzner, Stephen D. Egbert,
James A. Roberts, and Mark D. Otis
Science Applications International Corporation

Shoichiro Fujita
Radiation Effects Research Foundation

This chapter describes the research to produce models for calculating the shielding by houses for atomic bomb survivors who were in or near Japanese residential houses. The shielding data will be used in the revised dosimetry system for those survivors with nine-parameter assignments and also for those with globe information ("nine parameter" and "globe" are explained later). The nine-parameter shielding method was used primarily for survivors who were inside or very close outside Japanese residences. The globe technique was used primarily for survivors not in houses but shielded by terrain or by nearby Japanese houses.

The mathematical procedures used to perform this shielding analysis are described in Appendix 7-1 which also describes the validation of these procedures by comparisons with measurements of the shielding provided by Japanese houses during Operation BREN in Nevada in the early 1960s.¹

The calculations reported here provide the radiation fields as perturbed from the free field (see Editor's Note) by the presence of Japanese residential houses with mud-plaster walls and tile roofs. The result of the calculations is an energy- and angle-differential fluence with the same resolution as the free-field calculation. The kerma at a point in the perturbed field can be calculated by integrating the product of the perturbed field and the appropriate energy-dependent kerma-response function over energy and angle (see Editor's Note). Organ doses are computed by coupling the energy- and angle-differential fluence as perturbed by the house with an adjoint Monte Carlo calculation that describes the transport of the radiation through the body to the particular organ (see Chapter 8).

Note that this procedure differs from the previous (T65D) procedure¹ that accounted for the shielding by the house and body by the use of so-called "transmission factors", which are simply multiplicative factors of the free-field kerma. Although transmission factors (TF)

can be computed with the techniques described here, the procedure for the revised dosimetry system performs more detailed calculations that can give the complete energy- and angle-differential fluence at any site. The calculational procedure includes more accuracy in house models, in the ground-range effects on the radiation field, in the generation of secondary gamma rays in the house and body by neutrons, and in determining the effects of the orientation, size, and posture of the survivor.

The house shielding calculations reported here were performed with an adjoint Monte Carlo technique that simulates actual individual radiation particle transport in reverse time (see Appendix 7-1). The use of the Monte Carlo method permits modeling the structure of the Japanese house containing the survivor and nearby houses in great detail. The procedure includes not only the nearest house or the house containing the survivor, it calculates the effects of several surrounding houses arranged in a so-called "cluster". These geometry models are constructed by combination of simple geometric shapes such as spheres and parallelepipeds using logical operations (such as "and" and "or"). In principle, the neighborhood of each survivor could be modeled in this detail and calculations performed to provide the person's particular house shielding. This would involve a great deal of effort. However, it is hoped that by carefully choosing typical house clusters, it will be possible to provide, with a limited set of calculations, a model for the house shielding that is sufficiently accurate to incorporate all the information embodied in the codified nine-parameter data and globe data.

In addition to developing accurate geometry models of typical Japanese neighborhoods, it is important to produce accurate models of the material composition of typical Japanese houses. This includes the composition of the walls, the interior partitions, and the roof construction. The amount of shielding afforded by Japanese houses is directly dependent on the elemental composition of these materials and their thickness (areal density). A section of this report describes a comprehensive sensitivity analysis that was performed to understand the effect of variations in the material composition and in the mass per unit area on the overall house shielding.

The house shielding model for the new dosimetry system is currently constrained to use information concerning the survivor that is available in the RERF computerized data bases. This constraint forces reliance on the nine-parameter and globe data that were developed for the T65D dosimetry. There is no constraint, however, to use these data in the same manner as for T65D. A considerable portion of the research involved calculating the nine parameters and globe parameters for locations within the clusters and then analyzing the shielding calculations with respect to the nine parameters and globe data to determine functions and models that could represent the variation in shielding.

BACKGROUND

The initial concern about the accuracy of the T65D dosimetry system for A-bomb survivors was focused on the free-in-air (FIA) values, particularly the kerma in tissue due to neutrons at Hiroshima as reported by Loewe and Mendelsohn.² An analysis by Marcum³ also questioned the gamma-ray TF applied to the FIA kerma due to gamma rays in the T65D correction for house shielding. The average gamma-ray TF in T65D reported by Milton and Shohoji⁴ were 0.90 for Hiroshima and 0.81 for Nagasaki. Marcum estimated that the average

gamma-ray TF should be quite a bit lower: 0.55 for Hiroshima and 0.50 for Nagasaki. A more detailed analysis by Woolson et al⁵ supported the original claim by Marcum. Thus, early attempts to evaluate the impact of the new dosimetry used the kerma values of Loewe and the TF of Marcum.

The T65D TF for house shielding were based on experiments with the BREN reactor and a large ⁶⁰Co source, as discussed in Appendix 7-1, in Auxier,¹ and in Woolson et al⁵, in which radiation-analog Japanese houses were exposed to the sources mounted in a 465 m high tower. The neutron TF were obtained by taking the ratio of the neutron kerma measured inside the house to the FIA neutron kerma measured at the same ground range without the presence of the house. Likewise, reported gamma-ray TF were the ratio of the gamma-ray kerma inside the house to FIA gamma-ray kerma. The measured TF were then parameterized into the nine-parameter formula for direct application in the T65D. The nine parameters presumably captured the relevant information about the survivor's location in a house to represent the shielding of the survivor.

The problem with this approach for application to the A-bomb survivors primarily rests with direct use of gamma-ray TF obtained in the BREN experiments to determine the shielding of the prompt gamma rays and the gamma rays induced in the air, ground, and buildings by neutrons (the shielding of the gamma rays from the fission products was represented by the ⁶⁰Co data). Note that the measured gamma-ray TF depends on the magnitude of the FIA neutron fluence because the gamma-ray kerma measured inside houses includes gamma rays from neutron inelastic and capture interactions with the house materials. Since measured gamma-ray TF are not, then, independent of the existing neutron field, these TF should only be applied to situations that have the same relative neutron and gamma-ray environment. Unfortunately, the neutron fluence produced by the BREN reactor in the vicinity of the mock houses was, relative to the gamma-ray fluence, much larger than was produced by either of the A-bombs near houses in Hiroshima and Nagasaki. These neutrons at the BREN experiments produced relatively more capture gamma rays in the house materials that were measured by detectors inside the houses along with the attenuated incident gamma rays. Because of the excessive number of neutrons at BREN, this secondary gamma-ray component resulted in large measured TF. Since this component was not present in such magnitude at Hiroshima or Nagasaki, the T65D gamma-ray TF were too large, as was suggested by Marcum.

In addition to this large bias in the T65D gamma-ray TF, there were other problems with the treatment of shielding in the T65D dosimetry. In T65D, the TF do not depend on distance. The hardening of the neutron spectrum and the shift in elevation angle (the line from the survivor to the burst point) with ground range produce changes in the shielding for which T65D did not account. There are also inconsistencies in the nine-parameter and globe methods for shielding because of the use of different data bases and model assumptions for the two methods in T65D. Also, the TF approach does not provide for the kerma produced by secondary gamma rays from neutron interactions in the materials of the house and body.

The primary reason, however, for the revision of the T65D shielding model is the need for more detailed dosimetric data at specific organs within the body to account for the orientation, posture, size, and sex of the survivor. Also needed are estimates of the energy-differential fluence of neutrons and gamma rays and a breakdown of the kerma into individual neutron

and gamma-ray components. This level of detail requires that the house shielding model provide the energy- and angle-differential fluence distribution at the location of the survivor in or near houses for subsequent computation of the shielding by the body. Thus, simple kerma TF cannot be used, as in T65D, to describe the house shielding; the complete radiation field inside the house must be provided. A methodology for producing these detailed shielding descriptions was presented by Woolson et al⁵ and accepted by the US Department of Energy (DOE) Working Group on A-bomb dosimetry and by Japanese scientists on the Review Committee to Evaluate the Radiation Dose from the Atomic Bomb. This report describes the research using that methodology to generate the detailed house shielding model for the revised A-bomb dosimetry.

METHOD FOR SHIELDING CALCULATIONS

The theoretical basis for, and a complete description of, the method used to evaluate the shielding of the survivors by the Japanese houses and to produce the data base for the house shielding in the revised dosimetry is provided in Appendix 7-1.

The shielding calculations were performed in computerized geometrical models of typical Japanese residential neighborhoods. The models consist of clusters of six or more houses. These computer models of house geometries contain the roofs, walls, interior partitions, windows, doors, floors, and the relative location of the houses with respect to each other. The Monte Carlo method is used to simulate the repeated scatterings of neutrons and gamma rays through these geometries. Without describing in detail the distinctions between forward and adjoint modes for Monte Carlo simulations, the calculations were performed in the adjoint mode in which simulation begins at the detector* location, particles move back in reverse time, "upscatter" to higher energies when they interact with house materials, and exit the cluster model by crossing an outer cylindrical surface. Some of the starting gamma rays upscatter to become neutrons that exit the cylindrical surface, thus simulating secondary gamma-ray production in the houses. The scatterings and distances between collisions are randomly sampled in the Monte Carlo simulation according to the nuclear cross sections for the house materials and the configuration geometry.

Data for each particle simulation generated during the Monte Carlo computer calculation are saved on what is called the "leakage" tape. In the reverse time, or adjoint mode, a particle leaking from the system by crossing the outer cylindrical surface portrays a particle incident on the surface in normal forward time (forward mode) that arrives at the detector location with the energy and angle used to commence the particular adjoint history. Thus, the leakage tape records, in essence, the location, energy, and angle of the incident neutrons and gamma rays and the resultant energy and angle at the detector of the particles and secondary particles generated in the house materials.

Typically, leakage tapes from a Monte Carlo run for house shielding will contain about 40,000 individual particle simulations or histories. These histories provide the effect of

*Many analysts who make Monte Carlo calculations of the type reported here use the word "detector" in a generalized sense for the object in which they calculate the radiation field. The detector might, in different cases, be an actual instrument, a small mass of material, or an organ in a person's body. The word "receptor" is often used in the same sense in purely radiological studies.

shielding of the free-field radiation by the house cluster. From the free-field data, it is possible to compute the number of neutrons or gamma rays in a given energy band and in a given angular band that would cross particular points on the cylindrical surface surrounding the cluster. A data processing code examines the leakage tape for histories that fall into these particular energy, angle, and surface bands, and links their histories with the free field to compute the field at the shielded detector location. In effect, the shielding calculations continue the radiation transport from the free field into the house cluster. By saving the Monte Carlo simulations on tape, many different shielding estimates can be performed by linking (or folding) the shielding tape leakage data with the free field at different ground ranges and for different orientations of the cluster with respect to the burst point.

This approach assumes the radiation incident on the imaginary cylindrical coupling surface surrounding the cluster calculated without the cluster present (i.e., air over flat ground geometry) is not too different from the actual incident radiation with the cluster present. Discrepancies would arise from differences in the radiation that interacts inside the cylindrical volume (with or without the cluster), escapes the volume, and then scatters back into the volume once again. Comparisons of calculations using this technique with data from the BREN Japanese house experiments discussed in Appendix 7-1 show excellent agreement and indicate that the approximation is a good one. Furthermore, since the burst points at Hiroshima and Nagasaki were over 500 m above the ground, most of the energetic incident radiation came from the air, unperturbed by the ground, and that portion of the incident radiation that interacted with the ground and houses in the far field should not be too different from the same in a flat ground model. The near field air-ground-house interactions are treated, of course, in the cluster calculation.

CLUSTER MODELS

Cluster Design

During the process of validating the computer procedure (Appendix 7-1), it was found that the radiation field is perturbed not only by the house containing the survivor but also by houses adjacent to the survivor's house. Thus, it is necessary to model clusters (or groups) of Japanese houses to calculate the full shielding effect. The shielding offered by a house other than the house containing the survivor is called the mutual shielding effect. Since the Monte Carlo shielding calculations can be folded with the free field at any ground range and for any orientation of the cluster with respect to the burst point, the clusters were selected to include as many different shielding situations as possible (e.g., two-story house shielding a single-story house, a house shielded by a house across the street, etc.). To be as realistic as possible in the design of house clusters, the models selected were from actual histories of survivor situations.

A housing cluster model is produced by first generating models for the individual houses, then combining these mathematical models for individual houses into an appropriate arrangement with the houses properly spaced for street width and separation distances of neighboring houses. The individual houses are modeled with the combinatorial geometry technique, which produces a mathematical representation of the house geometry through logical operations on a set of simple bodies.

One can model objects in great detail with this method. The models used in this study considered the following: exterior doors and windows, walls, passageways, verandas, interior partitions and openings, first and second flooring, tatami, closets, alcoves, and roofs. The large overhead beams in typical Japanese houses were not modeled, and the closets were empty in this analysis. The models of individual houses were checked by generating computer-drawn views of the models from specified viewpoints. Any discrepancy between the pictured results and the desired design could be fixed and the procedure repeated until the final model had the desired input design.

The mathematical models of the individual houses were specified relative to a cartesian origin. The cluster model was constructed from the individual house models by referencing the origin of each house model to its position in the cluster frame of reference. In this way, clusters of any size could be constructed subject to the limitation of the available computer memory and the increased run time for larger geometry models.

Each volumetric region of the geometry model for the cluster must have a specified composition consisting of partial element densities. The computer code uses the input partial densities of a given material to form the macroscopic cross sections required in the transport simulation. The cross-section data consist of both the total macroscopic cross section for the given material and the energy- and angle-differential scattering cross sections.

The mathematical model of the Japanese house cluster and the material description for each region of the cluster are the basic input data for the adjoint Monte Carlo simulation to calculate the perturbation of the free field due to the presence of houses in the vicinity of the survivor.

Six-House Cluster

The first house cluster used to perform shielding calculations is called the six-house cluster. It consists of two two-story houses and four one-story houses with three houses aligned on each side of a street. The layout model was based on a shielding history from Hiroshima in Nishi Temma-cho shown in Figure 1. This model was selected because it provided the opportunity to study a variety of shielding situations, depending on the orientation of the cluster relative to the burst point (in the shielding calculations the orientation of the house cluster with respect to the burst point can be varied arbitrarily). Two computer-generated views of the mathematical model of the six-house cluster are shown in Figure 2.

With this configuration, the effects of mutual shielding by one- and two-story houses could be studied. The combinations include (depending on the orientation with respect to the burst point) two-story unshielded, single-story unshielded, two-story shielded by a two-story, two-story shielded by a one-story house, one-story shielded by a two-story house, one-story shielded by a one-story house, one-story shielded by one- and two-story houses across the street, and two-story shielded by a one-story house across the street. The presumption is, of course, that most of the mutual shielding is done by the most adjacent house along the line of sight to the bomb.

During visits to Hiroshima and Nagasaki, measurements of the dimensions of common features of several Japanese houses existing at the time of the bombing were made. The wall thickness, partition height, roof slope, and room layout were ascertained. These measurements were compared with the same features of the house models used during Operation

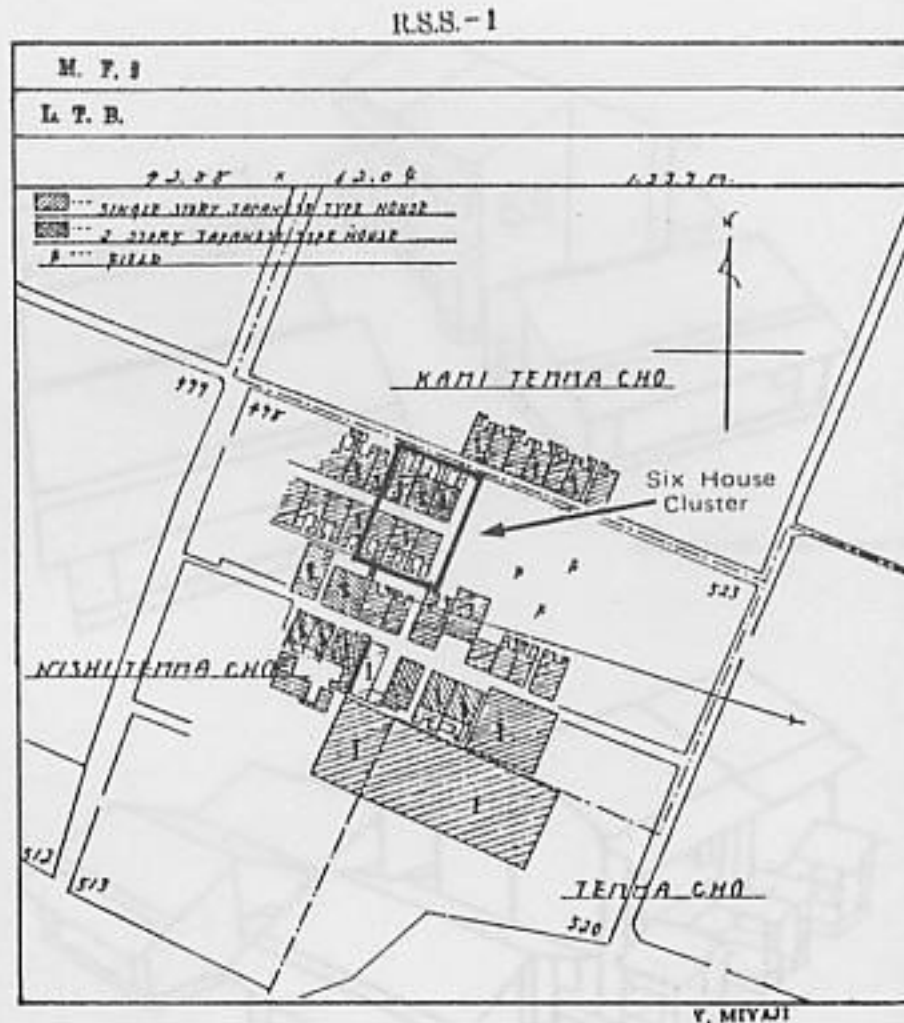


Figure 1. Nishi Temma-cho housing clusters and the six-house cluster used in the shielding calculations

BREN (Appendix 7-1). It was found that the dimensions among the Japanese houses were remarkably uniform and that the BREN houses agreed with Japanese houses (Table 1). For this reason, the house models (size dimensions only) generated for the BREN measurements were used in the six-house cluster. Thus, the two-story house in the cluster is BREN House B, and the one-story house is BREN House A. Note that only the geometry models for House A and House B were used. The materials discussed in the next section for the six-house cluster were selected to be representative of Japanese house composition, rather than the cement-asbestos board used in Operation BREN experiments.

The locations selected for calculation of the radiation fields in the houses are shown in the plan of the house cluster in Figure 3. The notation used in Operation BREN was adopted for specifying the survivor's location. A point is identified by a house number (1 to 6), the house type (A or B), followed by a slash (/), and then a letter to indicate the location in the house. Thus, the point denoted by 4A/E means the point is in house 4, which is type A (single story), at location E. These points were selected to provide a sufficient data base to cover the important ranges of the nine parameters.

Points were also selected at various locations in the street of the six-house cluster for

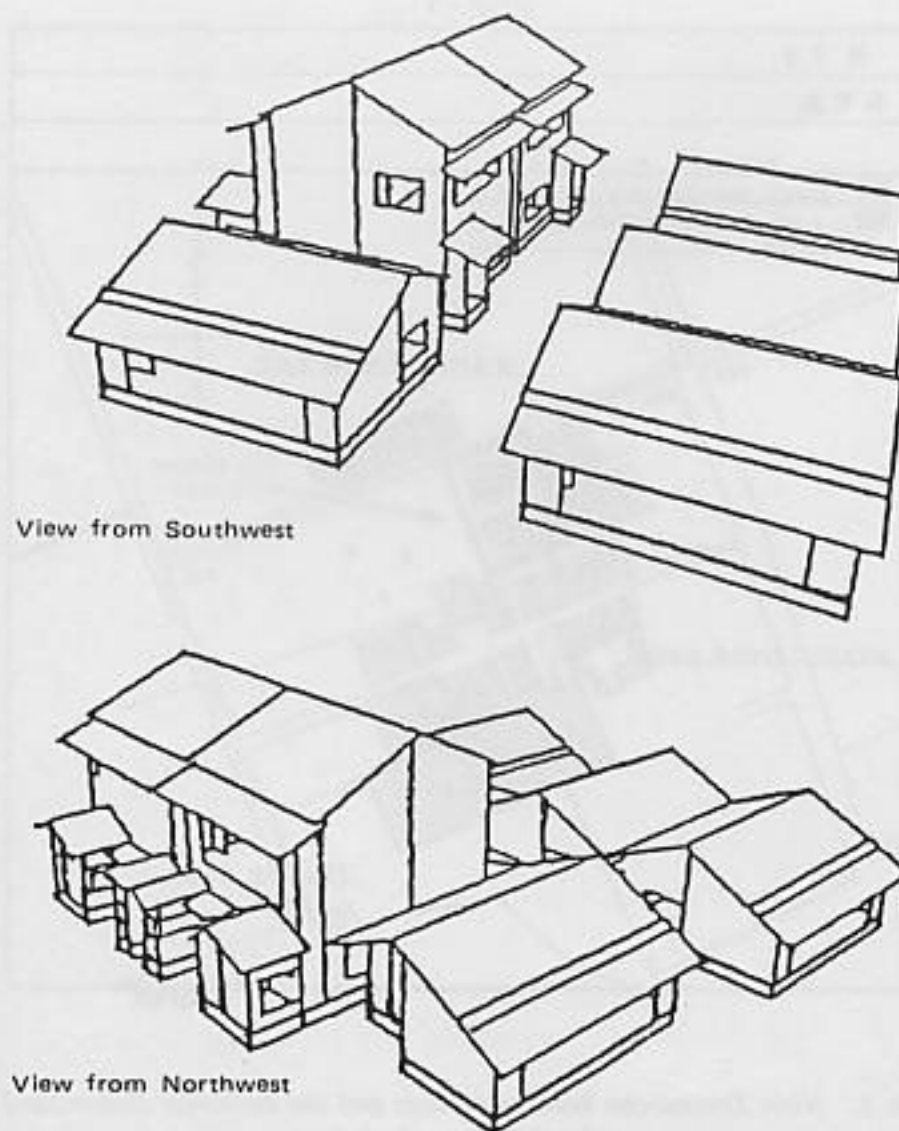


Figure 2. Combinatorial geometry of the six-house cluster model

Table 1. Dimensions of Model Japanese Houses (cm)

House Type	Roof Peak	Length	Width	Second Story Floor Height	Partition Height
Single story house A	475	872	700	—	270
Two story house B	915	858 ^a	675	400	315
Tenement (one unit)	860	700 ^a	500	360	300

^aMain portion of house

globe data analysis. Survivors with globe data were primarily in the streets and shielded by nearby residential houses. The points are depicted in Figure 4. The first four detector locations on Figure 4 were calculated with only House 5B present in the computational model, as indicated by parentheses.

Tenement Cluster

A third of the survivors with nine parameters were in tenement houses at the time of the

HOUSE AND TERRAIN SHIELDING

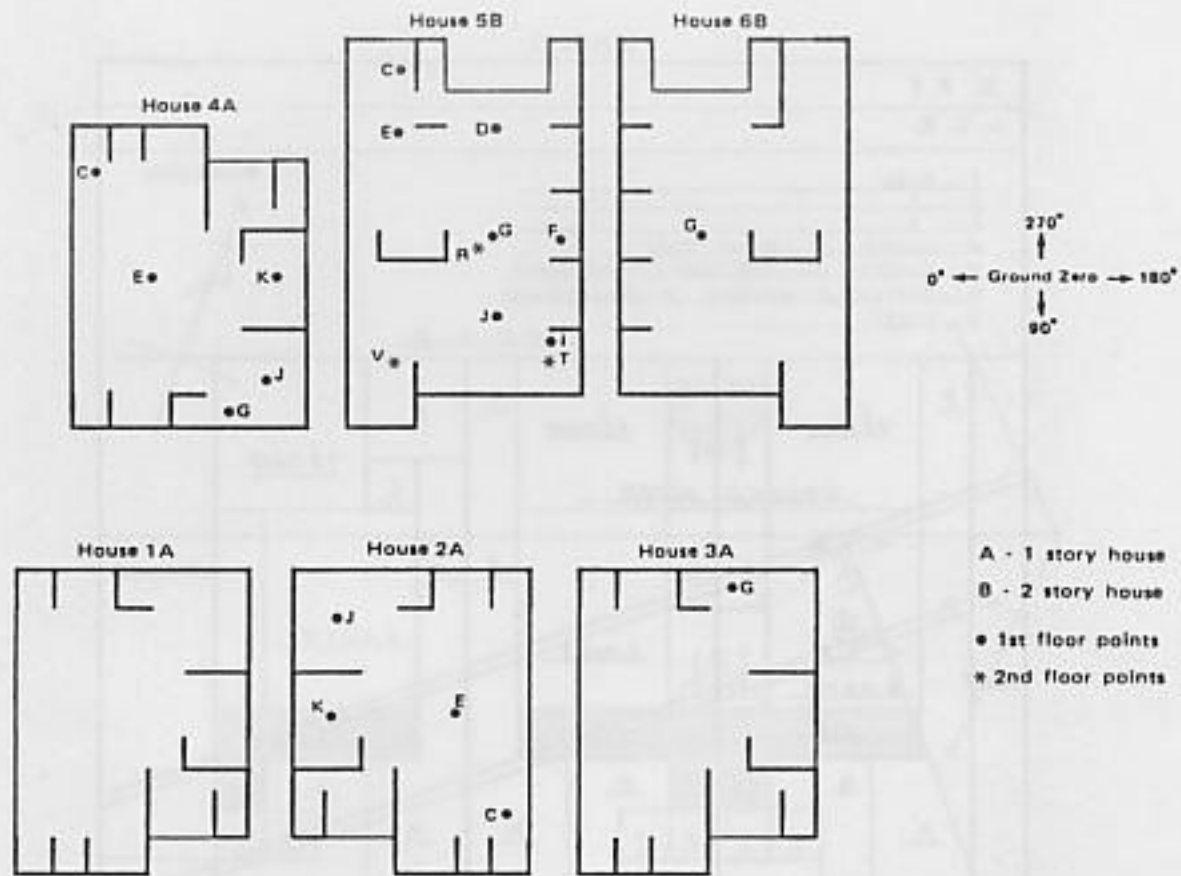


Figure 3. Plan of the six-house cluster showing location of detectors

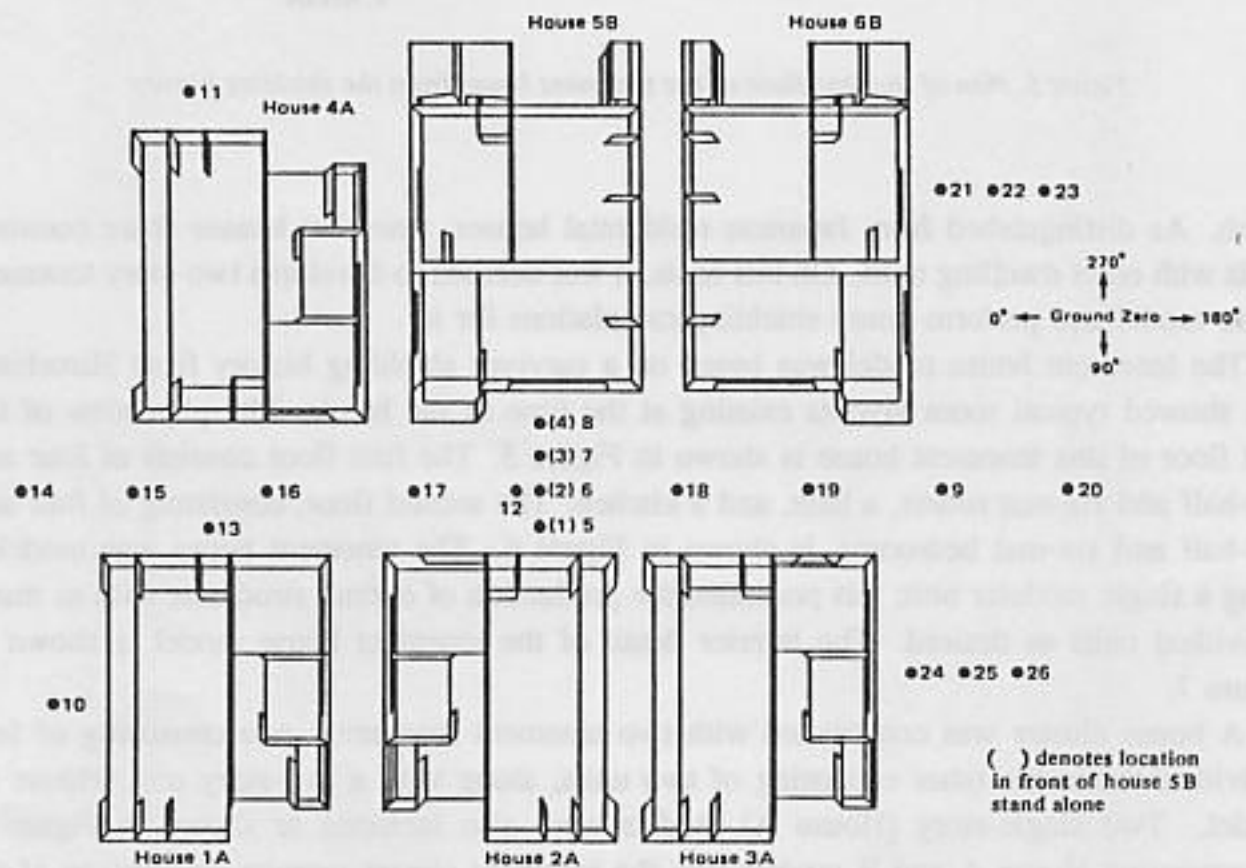


Figure 4. Six-house cluster showing location of detectors for globe shielding study

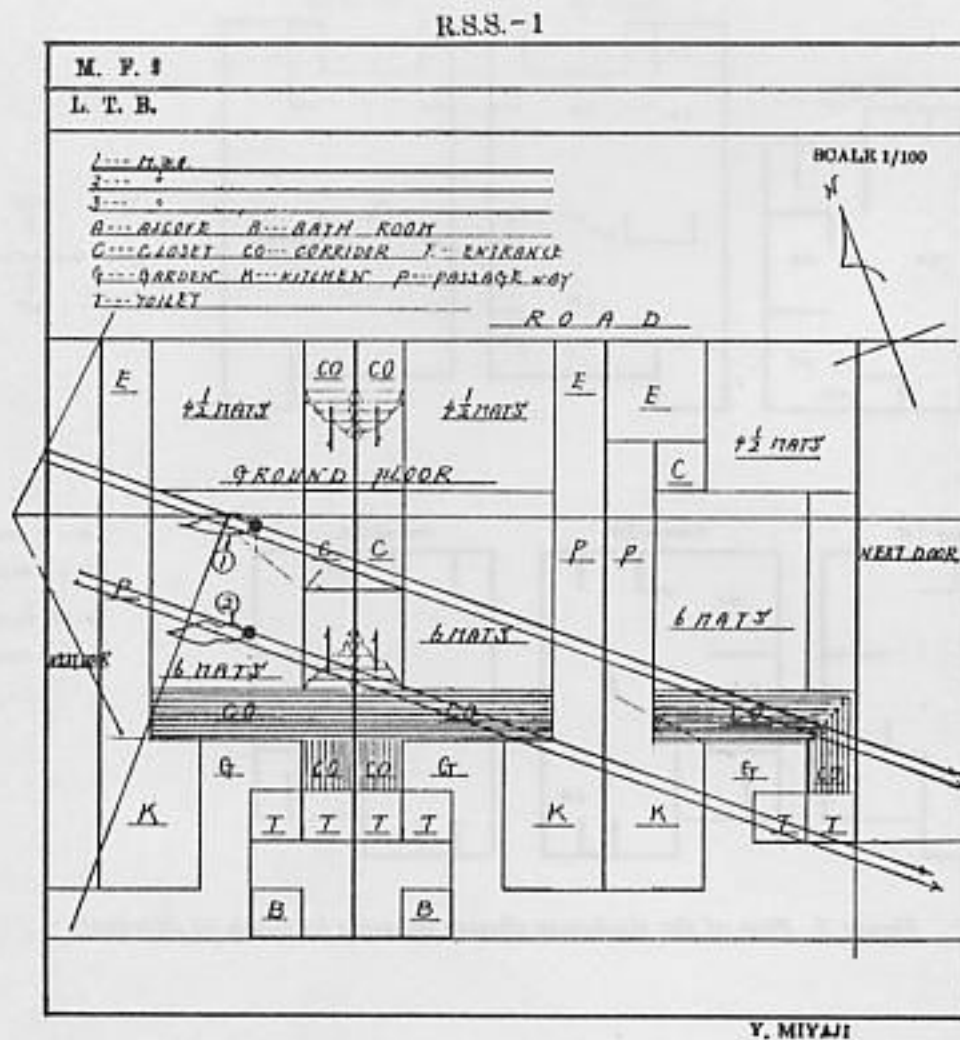


Figure 5. Plan of the first floor of the tenement house from the shielding history

bomb. As distinguished from Japanese residential houses, tenement houses share common walls with other dwelling units. On this basis, it was decided to develop a two-story tenement house model and perform house shielding calculations for it.

The tenement house model was based on a survivor shielding history from Hiroshima that showed typical room layouts existing at the time of the bomb. The plan view of the first floor of this tenement house is shown in Figure 5. The first floor consists of four and one-half and six-mat rooms, a bath, and a kitchen. The second floor, consisting of four and one-half and six-mat bedrooms, is shown in Figure 6. The tenement house was modeled using a single modular unit; this permitted the production of overall structures with as many individual units as desired. The interior detail of the tenement house model is shown in Figure 7.

A house cluster was constructed with two tenement structures: one consisting of four individual units; the other consisting of two units, along with a two-story unit (House B) model. Two single-story (House A) models were also included as shown in Figure 8. Incorporating House A and B models into the tenement cluster permits comparison of the TF calculated for this model and for the six-house cluster model. The house designations and location of detectors used in the tenement cluster are shown in Figure 9.

HOUSE AND TERRAIN SHIELDING

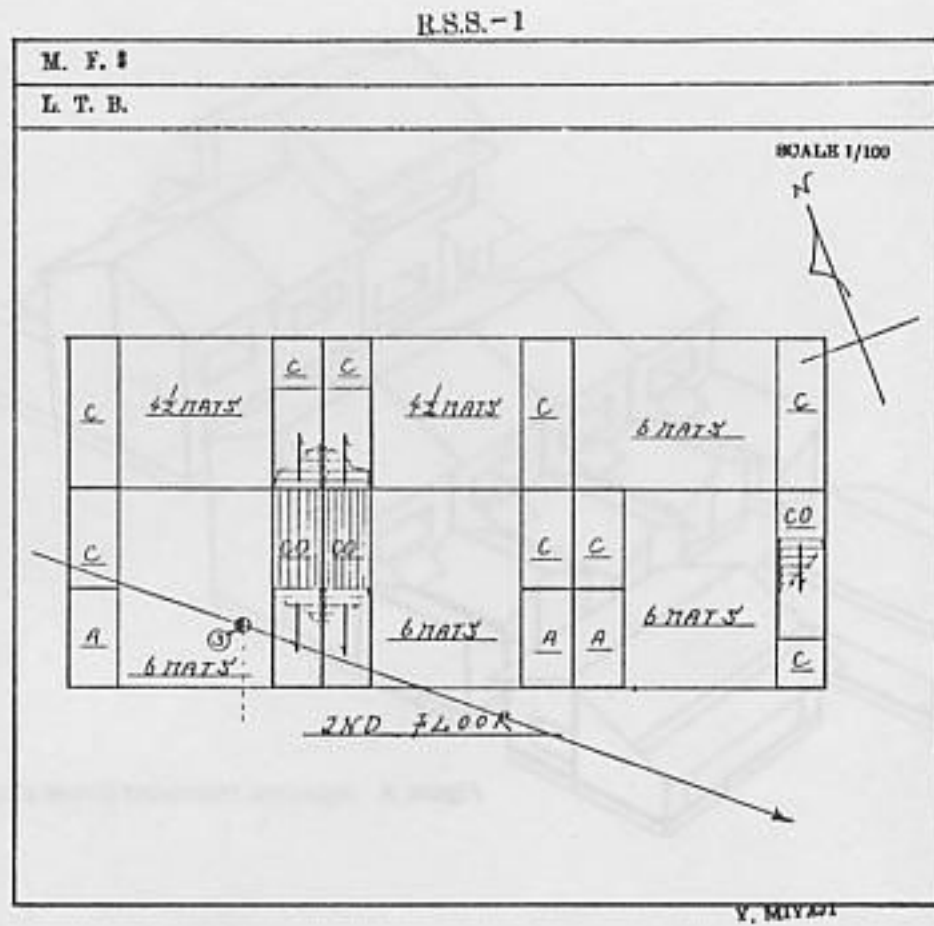


Figure 6. Plan of the second floor of the tenement house from the shielding history

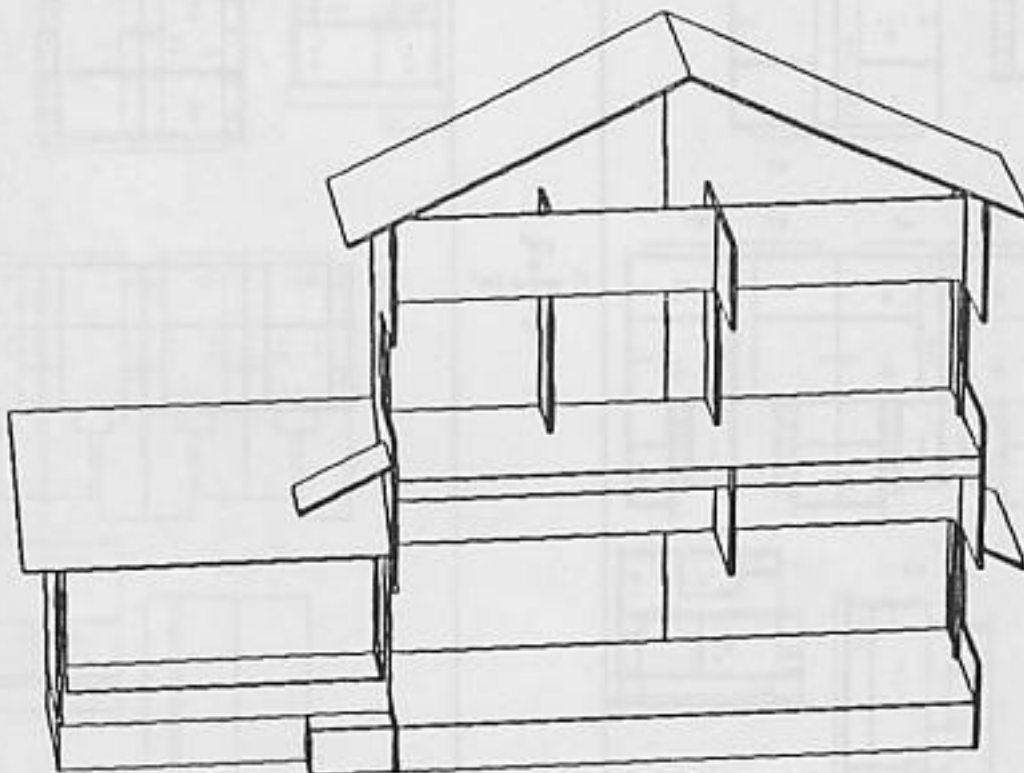


Figure 7. Interior detail of the tenement house model

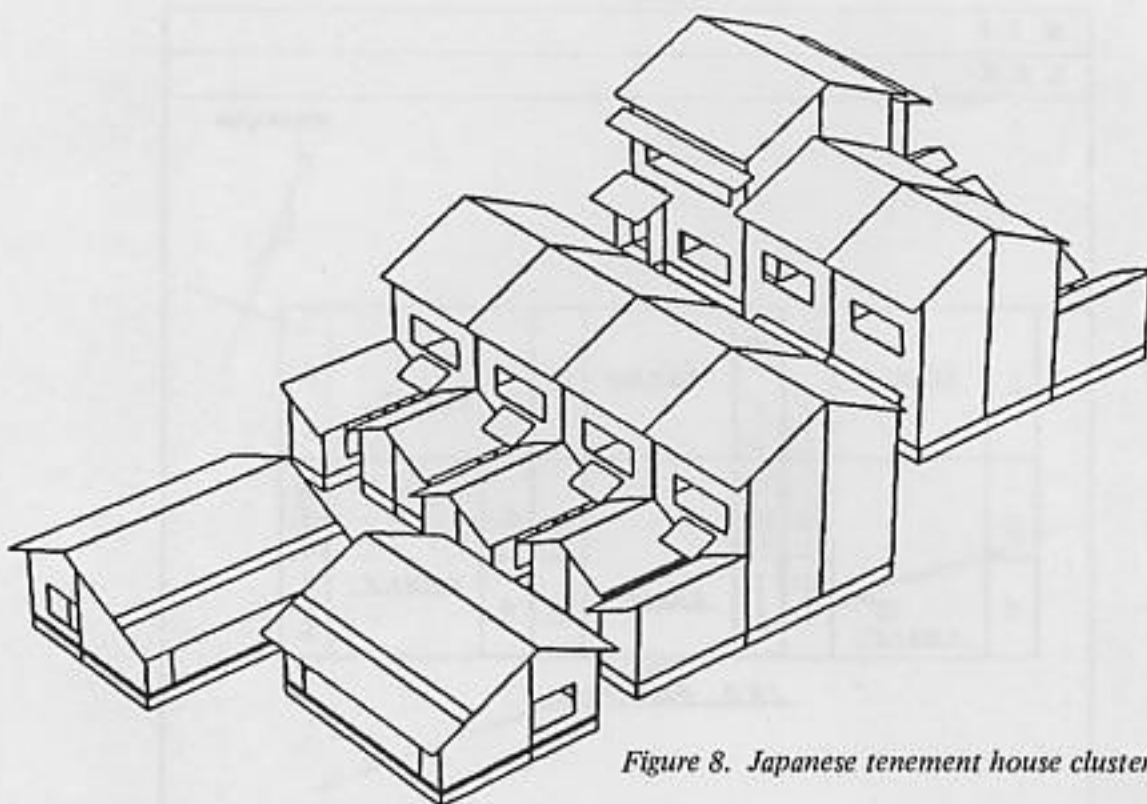


Figure 8. Japanese tenement house cluster model



Figure 9. Plan of the tenement house cluster with location of detectors. The left-hand view shows the house designations used in detector identification

Materials for House Shielding


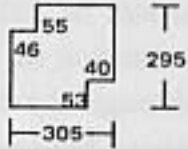
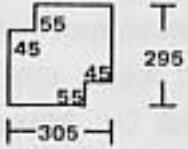
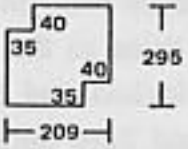
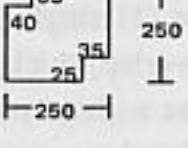
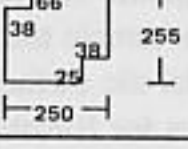
The attenuation of incident neutrons and gamma rays and the production of secondary gamma rays in the house depend directly on the material models used in the transport calculations. The elemental compositions, densities, and thicknesses must be as realistic as possible to insure accurate results. Several different house material models were used during the course of the calculational effort to develop the house shielding data of the new dosimetry system. During this development an extensive analysis of the sensitivity of the dosimetry to material selection was conducted (described later). Here the material models that were used in the final house shielding calculations are defined. Because the final material models differ from models used previously,⁶ the results presented will be different.

Depending on distance from hypocenter, a significant fraction of the radiation received by survivors in Japanese houses penetrated the houses through the roof. Thus, it is very important to develop a good model for the roof of Japanese houses. Resource materials available at RERF Hiroshima, previous Atomic Bomb Casualty Commission (ABCC) reports, and T65D reference reports indicated that the typical Japanese roof consisted of a thin wood subroof followed by a continuous bed of mud-plaster on which roof tiles were laid in an interlocking pattern. However, in June 1984, working with Dr. Maruyama of the National Institute of Radiological Sciences (NIRS), and Mr. Yamada of RERF, it was found that the tiles were laid on strips of mud rather than a continuous bed. Mr. Yamada consulted a carpenter, Mr. Takeuchi, who built houses in Japan prior to the war. Mr. Takeuchi demonstrated the procedure in which the tiles are interlocked and the method of laying them in strips of mud. A mud strip about 10 cm wide and 2 cm thick runs along the roof fall line, and the tiles are centered on this mud strip. This creates five separate radiation penetration regions on a typical Japanese roof. They are (1) single-tile thickness without mud, (2) single-tile thickness with mud, (3) double-tile (overlap) thickness without mud, (4) double-tile thickness with mud, and (5) triple-tile thickness without mud.

Various samples of Japanese roof tiles were assembled and measurements made to determine the area fractions for each of these five separate regions. The results are summarized in Tables 2 and 3. Table 2 provides the dimensions of six sample tiles, the area per tile for each of the penetration regions, and the percent of the total tile surface area for each of the regions. Tiles 3 and 5 were selected as representative tiles for Hiroshima and Nagasaki. A sensitivity analysis, using several calculational approaches, was conducted to determine the best calculational model dealing with five separate regions for each tile face of the roof.

The final model selected for the calculations was based on the Hiroshima tile case 5. The five roof material regions were constructed corresponding to each of the different mass penetrations over the tile face (single-tile thickness, single tile plus 2 cm of mud, double-tile thickness, double-tile thickness plus mud, and triple-tile thickness). When a particle in the Monte Carlo simulation encounters the roof, a random number determines which portion of the tile the particle encounters based on the area percentages for each of the regions (see Table 2, case 5). Thus, for example, about 27% of the incident particles encounter a double-tile thickness. Throughout the scattering in the roof, it is assumed that the particle stays in this selected region, that is, the particle cannot escape from one tile region into another. This procedure is preferable over an averaged-mass roof model. An averaged-mass will not give the average radiation transported, because the attenuation and scattering are not linear,

Table 2. Calculation of the Area and Percent of Roof Covered by Different Thicknesses of Tile and Mud for 10 cm Wide Mud Strips

Tile Size	Thickness	Area (cm ²)	%
1. Japanese Handbook 'Standard' Tile			
	Single	171	30.8
	Single+Mud	152	27.4
	Double	135.4	24.4
	Double+Mud	70	12.6
	Triple	26.6	4.8
2. RERF Reference Tile (probably Nagasaki)			
	Single	102.5	20.6
	Single+Mud	79	15.9
	Double	163.3	33.0
	Double+Mud	108	21.8
	Triple	43.2	8.7
3. Nagasaki Tile (NIRS Sample)			
	Single	86.25	17.9
	Single+Mud	75	15.6
	Double	160.25	33.3
	Double+Mud	110	22.9
	Triple	49.5	10.3
4. Nagasaki Tile (NIRS Sample)			
	Single	59.75	15.5
	Single+Mud	145	37.7
	Double	79	20.5
	Double+Mud	75	19.5
	Triple	26.25	6.8
5. Hiroshima Tile (NIRS Sample)			
	Single	59.25	17.2
	Single+Mud	70	20.3
	Double	93.25	27.1
	Double+Mud	90	26.2
	Triple	31.50	9.2
6. Hiroshima Tile (From Warehouse of Mr. Takeuchi, Hiroshima)			
	Single	54.02	15.5
	Single+Mud	73	21.0
	Double	95.08	27.3
	Double+Mud	91	26.2
	Triple	34.58	10.0

but exponential with mass thickness.

The wood subroof was modeled as 2 cm thick with a wood density of 0.5 g cm^{-3} . It was assumed that the moisture in the wood was 15% of the dry wood weight. The mud for setting the tiles was presumed to be 2 cm thick with a density of 1.5 g cm^{-3} . The moisture content in the mud was assumed to be 8% of the dry mud weight. The tile material was assumed to be the same composition as the mud but at a density of 1.7 g cm^{-3} with a thickness of 1.8 cm. The composition of these materials is given in Table 4 along with the composition for the air, ground, and wall material.

The wall material in Table 4 is composed of the same material used in the roof mud with the addition of 25% by volume of organic material to model the bamboo lath used in the wall construction. The air and the ground in Table 4 are the same as those used in the

Table 3. Summary Japanese House Roof Tile Data

Case	Description	Tiles per 3.3 m ² ^a	Exposed Area (cm ²)	Exposed Length (cm)
1	Japanese handbook	60	555	22.2
2	RERF reference	66	496	18.7
3	Nagasaki tile (NIRS)	69	481	18.5
4	Nagasaki tile (NIRS)	86	385	22.0
5	Hiroshima tile (NIRS)	96	344	16.0
6	Hiroshima tile (Takeuchi)	95	348	16.4

^aA standard area unit in Japanese construction.

Table 4. Composition of Materials Used in Shielding Calculations

Element	Elemental Composition (atoms/g material $\times 10^{24}$)				
	Air	Ground	Roof Wood	Roof Tile & Mud	Wall
H	1.137 (-3)	1.826 (-2) ^a	4.050 (-2)	4.956 (-3)	8.301 (-3)
C		4.356 (-4)	2.131 (-2)	2.533 (-4)	2.215 (-3)
N	3.230 (-2)	0	3.655 (-4)	0	3.406 (-5)
O	9.260 (-3)	2.227 (-2)	1.878 (-2)	1.868 (-2)	1.871 (-2)
Na		3.130 (-4)		3.597 (-4)	3.264 (-4)
Mg		5.380 (-5)		2.765 (-4)	2.509 (-4)
Al		1.212 (-3)		4.373 (-3)	3.968 (-3)
Si		5.426 (-3)		3.714 (-3)	3.365 (-3)
Ar	1.950 (-4)	0		0	0
K		4.182 (-4)		7.101 (-4)	6.443 (-4)
Ca		9.791 (-5)		1.988 (-4)	1.804 (-4)
Ti		1.385 (-5)		1.359 (-4)	1.266 (-4)
Fe		1.405 (-4)		2.792 (-4)	2.534 (-4)
Density (g/cm ³)	1.176 (-3)	1.5	0.5	1.7/1.5 Tile/Mud	1.5

^aRead as 1.826×10^{-2}

ground-level free-field calculations at Hiroshima (see Chapter 3.)

Narrow-beam measurements of the attenuation of wall and tile samples from Japanese residential houses were made by Maruyama (NIRS) and Shreve (Science Applications International Corporation SAIC). Both these measurements used well-collimated gamma-ray sources and NaI scintillation detectors to eliminate multi-scattered gamma rays as much as possible in order to obtain the true total cross section for the incident beam across the material thickness. Results from these measurements are presented in Table 5 for ⁶⁰Co (highest energy, 1.33 MeV) and ¹³⁷Cs (0.662 MeV). Also presented in Table 5 is the attenuation, A, computed by

$$A = e^{-\Sigma_t X} \quad (1)$$

where Σ_t is the total group-averaged cross section used in the transport calculations for the energy band containing the ⁶⁰Co or ¹³⁷Cs line and X is the material thickness. Considering

Table 5. Gamma-ray Attenuation of Japanese House Materials

Material	NIRS Measurements		SAIC Measurements	SAIC Model	
	0.662 MeV	1.33 MeV	1.33 MeV	Group 13 (0.45-0.7 MeV)	Group 11 (1-1.5 MeV)
Plaster wall	0.53 ^a	0.64	0.66 ^b	0.50	0.62
Nagasaki tile	0.82 ^c	0.89	0.92	—	—
Hiroshima tile	0.77 ^d	0.87	0.89	0.78	0.84

^a 5.7 cm thick sample from Hiroshima.^b 6.0 cm thick sample from Hiroshima.^c Average of two samples.^d Average of three samples.

NIRS measurements from Maruyama et al, Informal Report 1984.

the group averaging and the nature of the experiments, the comparisons between the model and the measurements are reasonable.

SENSITIVITY TO MODELING OF CONSTRUCTION MATERIALS

Methods

Shielding provided by any structure depends on the materials it contains, the thickness of walls and roofs, and other details of construction. Every effort was made to model the cluster as accurately as possible by using representative Japanese dwellings. But some simplifying assumptions were required, and the accuracy of these assumptions will influence the results of the shielding calculations. A sensitivity analysis on materials and construction was conducted to determine the sensitivity of house shielding to variations in the model assumptions.

Appropriate ranges of variation were estimated for several parameters describing construction materials. These parameters included the physical thickness of exterior and interior walls, the fraction of straw, lath, and other organic materials in these walls, water content of roof and wall material, thickness of roofing mud and tile, and the fraction of silicon in roof and wall mud, as shown in Table 6. The nominal value of each parameter, used in all previous calculations, lies at mid-range in each case. The ranges of wall and roof dimensions were determined on the basis of information obtained from RERF. Ranges for water and silicon content were based on known values for clays. The roof was assumed to consist of a uniform layer of mud covered with a single layer of roofing tile.

The sensitivity analysis used 25 sets of parameter values randomly selected from these ranges. Sampling was done in a highly stratified manner to insure coverage of all of each range even for this small number of sets. Each set of values was used in the cluster model for an adjoint Monte Carlo radiation calculation at a point in the cluster. When coupled with the radiation spectrum at a particular city, ground range, and orientation of the cluster, this set of calculations yielded a distribution of TF for each component of the spectrum. The fractional standard deviation (FSD) of these distributions will be used throughout this report as measures of uncertainty in transmission.

The sensitivity of the model to any particular parameter will be expressed in terms of the

Table 6. Range of Parameter Values Used for Uncertainty Analysis of House Construction for the Uniform Roof Model

Parameter	Symbol	Range
Outside wall thickness (cm)	OWT	5.0-9.0
Outside wall, % organic ^a	OWO	10-20
Interior wall thickness (cm)	IWT	5.0-9.0
Interior wall, % organic ^a	IWO	10-20
% H ₂ O for clay, mud, tile ^b	H2O	6-10
Roof mud thickness (cm)	RMT	1.0-6.0
Tile thickness (cm) ^c	RTT	1.7-4.0
% Si in mud (roof and wall) ^d	SIM	40-70

^aPercent of thickness contributed by all organic material including clapboard, rice straw, and bamboo lath

^bClay contains $\geq 4\%$ bound water by weight. The maximum of 10% assumes some water in other portions of house (i.e., joints, beams)

^cSingle-layer tiles range from 1.7 to 2 cm. The maximum includes extensive overlap.

^d40% Si by weight corresponds to clay with no sand. 70% corresponds to a 50/50 mix of clay and sand.

rank partial correlation coefficient (RPCC) of each parameter with a particular TF. The RPCC is a robust, nonparametric statistic used to indicate the presence or absence of correlation.⁷ The values for each variate in a multivariate data set are replaced by their respective rank or order. Thus, for example, if the sample values for some variate were (0.53, 0.72, 0.30, 0.62), the rank values would be (2, 4, 1, 3). The RPCC were computed for the multivariate set of ranks by the standard procedures for partial correlations.

Results are presented here for point E in house 4, (Figure 10) at several orientations of the cluster with respect to the burst point. For orientation of 0°, this location is unshielded by other structures. For 180°, it is heavily shielded by an adjacent, two-story building. Other orientations provide intermediate degrees of shielding. Thus, this one location in the cluster gives information representative of a wide range of shielding situations.

The Uniform Roof Model

Transmission factors and their uncertainties are presented for several cluster orientations at a range of 1090 m from the hypocenter in Hiroshima (Table 7). For each component of the radiation field, Table 7 lists the TF resulting from the nominal values of all parameters, the average TF for the 25 calculations using randomly chosen parameters, and the FSD of the 25 calculations. The standard deviation may be obtained by multiplying average TF and FSD. The TF and average TF values are, in general, not equal. This is not a surprising outcome. The nominal parameter values can be taken to be the mean of the randomly sampled values. Generally, a function of the means of several numbers is not equal to the mean of the function of those numbers. No average TF is significantly different from the TF as measured by a t-test at the 0.05 level.

Uncertainty due to the house construction model at Hiroshima and at this range is typically about 13% for neutrons, 11% for prompt gamma rays, and 14% for delayed gamma rays. The differences between the prompt and delayed gamma-ray components are due to differences in their energies and directions. At the time these calculations were performed

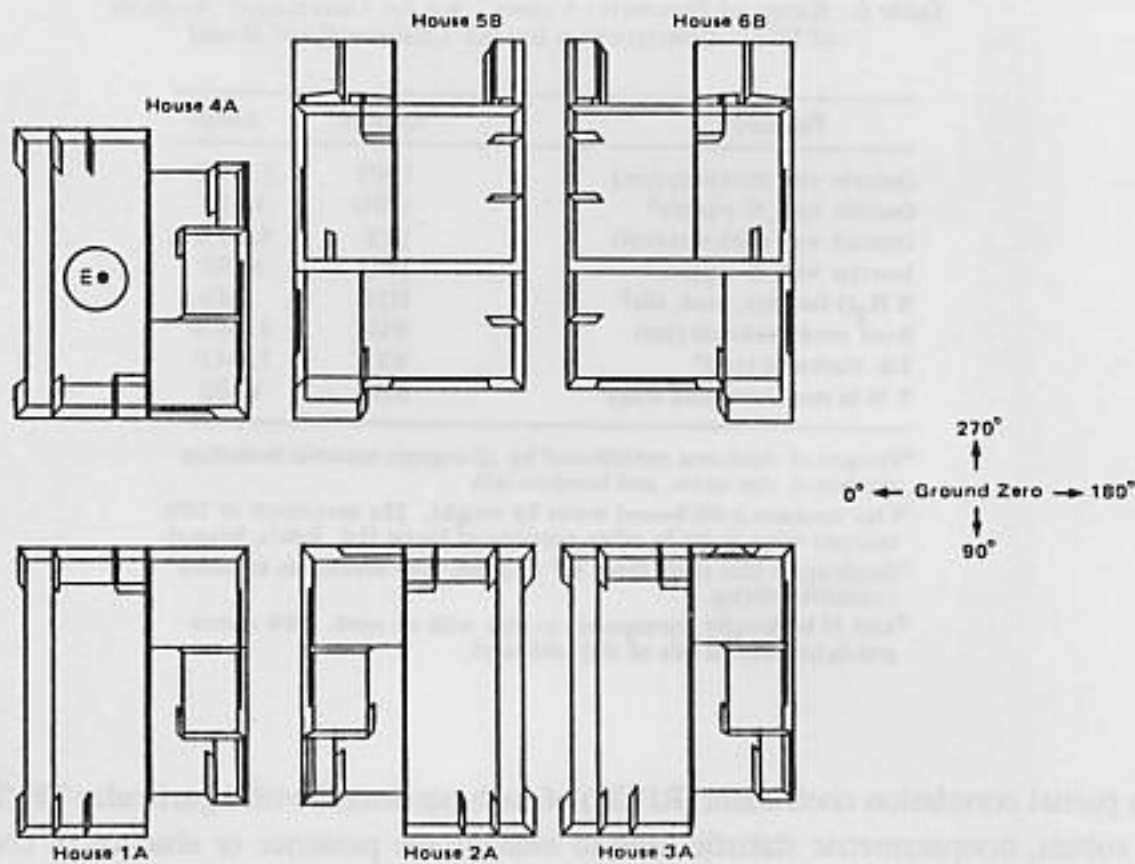


Figure 10. Six-house cluster showing the detector location used in the uncertainty calculations and the orientation angles

the delayed gamma-ray model did not include corrections for air-over-ground effects. When these corrections were estimated, both the TF and average TF for delayed gamma rays increased to nearly the values for the prompt gamma rays.

Correlation of parameter values with TF allows a measure of the amount of uncertainty contributed by each parameter. This is a measure of the sensitivity of the model to each parameter. It has the advantage of allowing all parameters to be tested simultaneously with a minimum number of calculations. The RPCC are presented in Table 8 along with their significance level. Those for which the significance level was greater than 0.05 have such a weak association with transmission that variation of the parameter has little or no effect on the result.

For Hiroshima at 1090 m from the hypocenter organic materials in the inner and outer walls and variation in clay and mud do not greatly influence radiation transmission. As expected, water content does not affect either prompt or delayed gamma-ray transmission, although it has some influence on neutron transmission.

From Table 8, the parameters most strongly associated with the TF for all components of the spectrum are those describing the construction of the roof (roof mud thickness and roof tile thickness). This was expected because much of the radiation fluence is directed downward, hence shielded by the roof.

To examine possible changes in model sensitivity with distance from the hypocenter

Table 7. Transmission Factors and Uncertainties for the Uniform Roof Model, Hiroshima at 1090 m

Orientation	Neutrons			Prompt Gamma rays			Delayed Gamma rays ^a		
	TF	\overline{TF}^b	FSD	TF	\overline{TF}^b	FSD	TF	\overline{TF}^b	FSD
0°	.453	.428	.101	.587	.685	.072	.462	.547	.098
45	.404	.383	.116	.554	.581	.093	.417	.436	.137
90	.339	.318	.134	.452	.448	.125	.363	.348	.165
135	.296	.278	.149	.369	.372	.145	.271	.285	.166
180	.279	.261	.149	.251	.269	.142	.188	.200	.168
225	.318	.293	.143	.381	.391	.106	.274	.285	.137
270	.383	.348	.126	.536	.528	.077	.381	.394	.119
315	.432	.406	.113	.558	.612	.090	.428	.482	.109

n = 25

^aNot corrected for ground effects. ^bAverage TF

Table 8. Rank Correlation of Parameters with Transmission Factor Uncertainty for the Uniform Roof Model, Hiroshima at 1090 m

Orientation	Neutrons			Prompt Gamma rays			Delayed Gamma rays				
	Parameter	RPCC	α	Parameter	RPCC	α	Parameter	RPCC	α		
0°	RMT	-.822	.01	RMT	-.917	.001	RMT	-.848	.01		
	IWT	-.628	.01								
	H2O	-.602	.02								
	RTT	-.484	.05								
90	RMT	-.934	.001	RMT	-.879	.01	RMT	-.727	.01		
	H2O	-.791	.01		RTT	-.571		.02	RTT	-.569	.02
	RTT	-.738	.01		IWT	-.516		.05	IWT	-.483	.05
	IWT	-.557	.02								
180	RMT	-.952	.001	RMT	-.860	.001	RMT	-.914	.01		
	H2O	-.710	.01		RTT	-.447		.05	RTT	-.560	.02
	RTT	-.671	.01								
	IWT	-.638	.01								
270	RMT	-.930	.001	RMT	-.791	.01	RMT	-.897	.01		
	H2O	-.571	.02		RTT	-.499		.05	RTT	-.478	.05
	RTT	-.505	.05		IWT	-.474		.05			
	IWT	-.501	.05								

(ground range), these calculations were repeated using the Hiroshima spectrum at 1500 m (Table 9). All neutron TF and average TF increased with increasing ground range. This is due to a hardening of the spectrum (i.e., selective removal of less penetrating radiation from the radiation field, as the ground range increases). The uncertainty due to house shielding, as given by FSD, showed no significant change, nor did the pattern of sensitivity to individual parameters (Table 10). No systematic changes in either transmission or sensitivity to shielding parameters were seen for gamma-ray components.

To examine the effects on house shielding resulting from differences in radiation fields at the two cities, these calculations were repeated using the Nagasaki spectrum at 1090 m from the hypocenter (Table 11). Here, again, an increase in transmission was observed for neutrons, in this case due to differences in the neutron spectra between the two cities. The

Table 9. Transmission Factors and Uncertainties for the Uniform Roof Model, Hiroshima at 1500 m

Orientation	Neutrons			Prompt Gamma rays			Delayed Gamma rays ^a		
	TF	\overline{TF}^b	FSD	TF	\overline{TF}^b	FSD	TF	\overline{TF}^b	FSD
0°	.488	.469	.092	.628	.738	.108	.496	.574	.095
45	.431	.413	.110	.578	.606	.092	.418	.440	.132
90	.356	.329	.130	.419	.406	.123	.321	.316	.152
135	.306	.284	.145	.354	.338	.159	.260	.263	.167
180	.282	.264	.147	.221	.222	.144	.174	.173	.173
225	.329	.304	.139	.379	.375	.105	.282	.281	.121
270	.407	.373	.119	.552	.532	.064	.389	.400	.092
315	.464	.442	.102	.588	.628	.088	.430	.489	.107

n = 25

^aNot corrected for ground effects. ^bAverage TF

Table 10. Rank Correlation of Parameters with Transmission Factor Uncertainty for the Uniform Roof Model, Hiroshima at 1500 m

Orientation	Neutrons			Prompt Gamma rays			Delayed Gamma rays			
	Parameter	RPCC	α	Parameter	RPCC	α	Parameter	RPCC	α	
0°	RMT	-.706	.01	RMT	-.865	.001	6	-.760	.01	
	IWT	-.667	.01							
	H2O	-.611	.02							
90	RMT	-.907	.01	RMT	-.778	.01	RTT	-.604	.05	
	H2O	-.817	.01		RTT	-.635	.01	RMT	-.602	.05
	IWT	-.732	.01				IWT	-.583	.05	
	RTT	-.523	.05							
180	RMT	-.951	.001	RMT	-.764	.01	RMT	-.883	.01	
	H2O	-.715	.01					RTT	-.482	.05
	RTT	-.686	.01							
	IWT	-.588	.02							
270	RMT	-.894	.01	RMT	-.722	.01	RMT	-.803	.01	
	H2O	-.604	.02		OWT	-.492		.05		
	IWT	-.563	.02							
	RTT	-.460	.05							
315	RMT	-.930	.001	RMT	-.895	.01	RMT	-.717	.01	
	IWT	-.575	.02							
	H2O	-.549	.02							
	RTT	-.452	.05							

patterns of parameter sensitivity were similar for the two cities (Table 12). For Nagasaki, a greater influence of wall thickness is evident in orientation with shielding from adjacent buildings. This is due to a lower height of burst, resulting in more radiation passing through walls at any given ground range.

The Tile Roof Model

The foregoing uncertainty analysis gave average FSD of about 13% for neutrons, 11% for prompt gamma-rays, and 14% for delayed gamma-ray TF regardless of ground range and

Table 11. Transmission Factors and Uncertainties for the Uniform Roof Model, Nagasaki at 1090 m

Orientation	Neutrons			Prompt Gamma rays			Delayed Gamma rays ^a		
	TF	TF ^b	FSD	TF	TF ^b	FSD	TF	TF ^b	FSD
0°	.498	.490	.091	.591	.726	.076	.470	.558	.097
45	.441	.421	.109	.558	.596	.101	.406	.432	.133
90	.366	.337	.129	.438	.427	.130	.340	.329	.160
135	.315	.292	.147	.369	.355	.158	.259	.269	.163
180	.290	.272	.145	.212	.225	.148	.172	.182	.172
225	.338	.313	.139	.376	.373	.109	.262	.273	.131
270	.419	.383	.117	.545	.527	.075	.374	.384	.110
315	.476	.451	.101	.564	.620	.097	.423	.482	.110

^aNot corrected for ground effects. ^bAverage TF

Table 12. Rank Correlation of Parameters with Transmission Factor Uncertainty for the Uniform Roof Model, Nagasaki at 1090 m

Orientation	Neutrons			Prompt Gamma rays			Delayed Gamma rays				
	Parameter	RPCC	α	Parameter	RPCC	α	Parameter	RPCC	α		
0°	RMT	-.722	.01	RMT	-.855	.001	RMT	-.824	.001		
	IWT	-.716	.01								
	H2O	-.668	.01								
	RTT	-.435	.05								
90	RMT	-.903	.001	RMT	-.785	.001	RMT	-.670	.01		
	H2O	-.815	.001		RTT	-.650		.01	RTT	-.584	.01
	RTT	-.723	.001		IWT	-.599		.01	IWT	-.506	.02
	IWT	-.519	.02		OWT	-.484		.02			
	OWT	-.456	.05								
180	RMT	-.926	.001	RMT	-.739	.001	RMT	-.909	.001		
	H2O	-.666	.01					RTT	-.536	.02	
	RTT	-.619	.01								
	IWT	-.571	.01								
	OWT	-.440	.05								
270	RMT	-.895	.001	RMT	-.750	.001	RMT	-.881	.001		
	H2O	-.568	.01		OWT	-.440		.05	RTT	-.490	.05
	IWT	-.538	.02		IWT	-.423		.05			

city. This uncertainty was most strongly associated with shielding parameters describing roof construction. In an effort to reduce the uncertainty in shielding calculations, an attempt was made to define better the ranges of roof parameters. As a result, an important error was discovered in all previous descriptions of Japanese roof construction, as described previously. It had been assumed to this point that mud used for securing roof tiles was laid down in a continuous sheet over the entire roof. But in fact, narrow strips of mud were used at the point of contact between the roof and each row of tiles. This does more than simply reduce the average amount of shielding material on the roof. It has important consequences for radiation shielding calculations because it results in significant "thin" and "thick" areas on the roof. The pattern of overlap of tiles becomes important, particularly in the areas between mud strips. It became clear that a rigorous treatment of the tiled roof would influence not

Table 13. Range of Parameter Values Used for Uncertainty Analysis of House Construction for the Tiled Roof Model

Parameter	Symbol	Range
% H ₂ O for clay, ^a mud, tile (by weight)	H2O	6-10
% H ₂ O for local ground (by weight) ^b	H2OG	18-30
Wall thickness	WT	5.6-8.4
Mud width (cm)	MW	9-11
Mud thickness (cm)	MT	1.5-2.5
Tile thickness (cm)	TT	1.6-1.8
Tile density (g/cm ³)	TD	
Hiroshima		1.6-1.8
Nagasaki		1.4-1.8

^a Clay contains $\geq 4\%$ bound water by weight. The maximum of 10% assumes some water in other portions of house.

^b Water content of ground and house material are correlated ($r \approx .80$)

Table 14. Transmission Factors and Uncertainties for the Tiled Roof Model, Hiroshima at 1000 m

Orientation	Neutrons			Prompt Gamma rays			Delayed Gamma rays ^a		
	TF	TF ^b	FSD	TF	TF ^b	FSD	TF	TF ^b	FSD
0°	.486	.462	.046	.671	.668	.023	.539	.534	.055
45	.447	.420	.042	.607	.629	.033	.492	.488	.054
90	.385	.367	.045	.561	.544	.048	.447	.430	.069
135	.331	.328	.048	.453	.436	.050	.337	.326	.081
180	.309	.302	.055	.328	.330	.064	.248	.241	.070
225	.346	.344	.062	.433	.447	.052	.332	.330	.071
270	.410	.405	.065	.605	.601	.041	.472	.462	.059
315	.460	.452	.055	.665	.643	.031	.486	.513	.060

^aNot corrected for ground effects. ^bAverage TF

only the uncertainty, but also would affect the shielding results themselves, probably raising estimated doses by reducing shielding in Japanese houses.

Tile patterns turned out to be slightly different in the two cities. Each city used slightly different tile sizes, hence a different number of mud strips was required. Two tiled roof models were developed to test the importance of these differences (cases 3 and 5, Table 2).

An uncertainty and sensitivity analysis was done using the two new tiled roof models. Physical parameters were varied as before. Since organic materials in the walls and the fraction of sand in clays had not proved significant, they were eliminated from this analysis. Several new parameters were added (Table 13). Some of these were required to test various features of the tiled roof models. These were the width and thickness of the mud strips. Since tiles in the two cities were found to be slightly different, different tile densities were used for each model. Interior and exterior wall thicknesses were combined into a single parameter rather than allowing them to vary independently. In addition, water content in the local ground around the cluster was varied to see what influence it had on neutron TF.

When calculations were done for Hiroshima, using the appropriate roof model and radiation spectrum at 1000 m (Table 14), all TF and average TF increased over those obtained

Table 15. Rank Correlation of Parameters with Transmission Factor Uncertainty for the Tiled Roof Model, Hiroshima at 1000 m

Orientation	Neutrons			Prompt Gamma rays			Delayed Gamma rays		
	Parameter	RPCC	α	Parameter	RPCC	α	Parameter	RPCC	α
0°	WT	-.737	.01	MW	-.568	.05	WT	-.794	.01
	TT	-.539	.05						
	H2OG	-.524	.05						
90	WT	-.789	.01	WT	-.929	.01	WT	-.754	.02
180	WT	-.779	.01	WT	-.744	.02	WT	-.782	.01
270	WT	-.797	.01				WT	-.530	.05

Table 16. Transmission Factors and Uncertainties for the Tiled Roof Model, Hiroshima at 2000 m

Orientation	Neutrons			Prompt Gamma rays			Delayed Gamma rays ^a		
	TF	\overline{TF}^b	FSD	TF	\overline{TF}^b	FSD	TF	\overline{TF}^b	FSD
0°	.547	.546	.044	.750	.741	.030	.580	.577	.060
45	.485	.478	.039	.618	.650	.049	.476	.474	.061
90	.403	.396	.038	.410	.427	.069	.348	.349	.087
135	.350	.349	.041	.417	.387	.070	.320	.301	.075
180	.322	.328	.047	.247	.251	.120	.204	.198	.083
225	.378	.379	.058	.385	.403	.087	.301	.305	.074
270	.464	.461	.062	.583	.588	.056	.454	.455	.066
315	.521	.527	.049	.674	.660	.032	.525	.533	.056

^aNot corrected for ground effects. ^bAverage TF

using the uniform roof model. All FSD decreased to the 5 to 7% range for all radiation components. These results are related. Reduced shielding can be expected to increase the TF. In addition, uncertainties in the thinner shield should have a much smaller influence on the TF.

Since much of the transmission takes place through the thinnest portions of the roof (one layer of roofing tile), variation in roof parameters should have little effect on average transmission. Sensitivity analysis confirms this expectation. Most of the uncertainty in TF is now associated with wall thickness (Table 15). To examine ground-range effects, these calculations were also done at 2000 m (Table 16). Once again, the hardening of the neutron spectrum resulted in increased TF with increased range. Gamma-ray TF are increased for unshielded orientations (0°) and decreased for shielded orientations (180°) due to the lowered angle of the line of sight with increased range. These changes also occurred with the uniform roof model but to a lesser degree. The changes are another consequence of the increased relative importance of wall shielding due to reduced roof shielding. Uncertainties once again showed no significant change with a change in ground range.

At 2000 m ground range, no shielding parameters were strongly enough associated with uncertainty in the TF to meet the 0.05 significance level criterion.

The Nagasaki roof model was submitted to an identical analysis using the Nagasaki

Table 17. Transmission Factors and Uncertainties for the Tiled Roof Model, Nagasaki at 1000 m

Orientation	Neutrons			Prompt Gamma rays			Delayed Gamma rays ^a		
	TF	\overline{TF}^b	FSD	TF	\overline{TF}^b	FSD	TF	\overline{TF}^b	FSD
0°	.534	.520	.043	.700	.697	.036	.564	.535	.060
45	.472	.462	.049	.616	.638	.059	.502	.469	.070
90	.400	.382	.059	.516	.514	.046	.428	.392	.084
135	.350	.350	.061	.431	.423	.067	.321	.306	.095
180	.334	.325	.065	.284	.280	.088	.242	.217	.109
225	.384	.368	.059	.389	.421	.048	.309	.316	.059
270	.456	.447	.047	.551	.601	.033	.434	.456	.045
315	.507	.501	.047	.654	.652	.021	.517	.509	.057

^aNot corrected for ground effects. ^bAverage TF

Table 18. Rank Correlation of Parameters with Transmission Factor Uncertainty for the Tiled Roof Model, Nagasaki at 1000 m

Orientation	Neutrons			Prompt Gamma rays			Delayed Gamma rays		
	Parameter	RPCC	α	Parameter	RPCC	α	Parameter	RPCC	α
0°	WT	-.539	.05	MW	-.550	.05	WT	-.581	.05
90	WT	-.831	.01	WT	-.813	.01	WT	-.729	.02
				MW	-.710	.02			
180	WT	-.864	.01	WT	-.825	.01	WT	-.725	.02
270	WT	-.625	.02						

Table 19. Comparison of Hiroshima and Nagasaki Style Roof Tile Models, Hiroshima Spectrum at 1000 m

Orientation	Nagasaki Style Roof			Hiroshima Style Roof		
	Neutrons	Gamma rays		Neutrons	Gamma rays	
		Prompt	Delayed ^a		Prompt	Delayed ^a
0°	.476	.681	.568	.486	.671	.539
45	.434	.621	.521	.447	.607	.492
90	.377	.548	.466	.325	.561	.447
135	.331	.449	.349	.331	.453	.337
180	.318	.335	.266	.309	.328	.248
225	.356	.428	.331	.346	.433	.332
270	.412	.577	.458	.410	.605	.472
315	.457	.659	.535	.460	.665	.486

^aNot corrected for ground effects.

spectrum at 1000 m ground range (Table 17). As before, neutron TF were higher than for Hiroshima at the same range. Differences between high- and low-shielded orientations for gamma-ray TF were more pronounced as a result of a lower height of burst point. The FSD were very similar for all radiation components. Sensitivity to house shielding parameters was also similar to that for Hiroshima at 1000 m (Table 18). Once again, wall thickness dominates and roof parameters are not significant.

Table 20. Comparison of Hiroshima and Nagasaki Style Roof Tile Models, Nagasaki Spectrum at 1000 m

Orientation	Nagasaki Style Roof			Hiroshima Style Roof		
	Neutrons	Gamma rays		Neutrons	Gamma rays	
		Prompt	Delayed ^a		Prompt	Delayed ^a
0°	.534	.700	.564	.528	.694	.550
45	.427	.616	.502	.478	.609	.485
90	.400	.516	.428	.406	.506	.417
135	.350	.431	.321	.345	.442	.321
180	.334	.284	.242	.317	.281	.228
225	.384	.389	.309	.368	.399	.315
270	.456	.551	.434	.444	.587	.454
315	.507	.654	.517	.500	.662	.521

^aNot corrected for ground effects.

Since the shielding for the tiled roof model is not sensitive to roof parameters, it can be expected that the differences in tile pattern between the two cities would have little influence on the TF. To test this expectation, TF for both roof models were calculated using both radiation environments (Tables 19 and 20). No differences were observed between the roof models that are significant given the 5 to 7% uncertainties in the TF for each shielding model. Differences resulting from the two spectra, however, are significant. For this reason, it was decided that a single tiled roof model would be adequate for calculations of house shielding at both cities. The model designed to represent Hiroshima roof styles was adopted for all further cluster calculations.

RESULTS OF CALCULATIONS

Results of the shielding calculations for the six-house cluster, the tenement cluster, and the terrain shielding model follow. These data were used to develop models to account for the shielding for survivors with nine-parameter and globe data for the new dosimetry system. The nine-parameter and globe modeling efforts are discussed in the subsequent sections.

The purpose of this section is to show the variation of the shielding effect of Japanese houses as a function of several variables and to show that this variation is consistent with the understanding of the shielding properties of Japanese houses. These variables include the location of the detector point, the orientation of the cluster, and ground range from the burst point.

The calculational method generates the energy- and angle-differential fluence distribution at the shielded location. These fluence distributions are too voluminous and detailed to allow inference of the shielding effects. To facilitate presentation of the information and to aid in understanding the shielding, the results are presented in the form of TF for the kerma in tissue ("transmission factor"). This TF is the ratio of the kerma at the shielded location to the kerma at the same position in space without the shield present. The kerma without the shield is the free-field or FIA kerma (see Editor's Note). Chapter 8 deals with the shielding by the body; hence the kerma without the shield (the body) is either the free-field kerma

or, more often, the kerma as affected by the presence of buildings. In any case, TF near unity indicate little attenuation by a shield, while small TF indicate large attenuations by the shield.

Secondary gamma rays are produced by neutrons that interact with house materials that are not present in the free field. For this component of the kerma at a shielded location, the TF is defined as the ratio of the kerma at the detector location due to the gamma rays produced in the house to the free-field kerma due to neutrons at the same position in space.

Although kerma TF facilitate the study of the attenuation by houses by reducing the shielding effects to a single measure, neither the models discussed later nor the dosimetry system use them *per se*.

Historically, the house shielding work initially focused on results from the six-house cluster; the six-house data were subjected to close scrutiny to understand the significant variations with parameters and to assess consistency in these variations. Following this investigation, results for the tenement cluster, survivor location in the open in the six-house cluster, and the terrain locations were examined in relation to the initial six-house data. This report on the calculational results reflects the emphasis on the data analysis for the six-house cluster.

The Six-House Cluster

A total of 21 detector points in the six-house cluster, shown in Figure 3, were chosen for calculations. A separate Monte Carlo calculation was made for each detector location. Results for these 21 detector locations, when folded with the free field at different orientations of the cluster with respect to the source, cover part of the range of the nine parameters to help develop a model of the house shielding for the dosimetry system for subjects with nine-parameter data. The calculations provide results for neutrons, secondary gamma rays produced by neutrons in the air, ground, and house, gamma rays from the bomb, and gamma rays from fission products in the bomb debris. In the following discussion, "prompt" gamma rays include the gamma rays from the bomb and secondary gamma rays induced in the air and ground, but not in the house, by neutrons. To discuss the results, seven detector locations are used for calculation of the TF. These seven locations are identified in Figure 11 by the larger circle enclosing a computed neutron TF at that location at 700 m ground range at Nagasaki. The following six topics concerning the TF are discussed:

1. Comparison between Hiroshima and Nagasaki.
2. The variation with location and ground range.
3. The variation with orientation.
4. The variation with the floor of the detector location.
5. Comparison of delayed radiation versus prompt radiation TF.
6. Results for secondary gamma rays produced in the house.

It was found that the data on TF studied in the framework of these six topics form a remarkably consistent set of results. The FSD of the Monte Carlo calculations were generally less than 5% for neutrons, prompt gamma rays, and delayed gamma rays. The calculations

Table 21. Comparison of Transmission Factors for Hiroshima and Nagasaki

Ground Range	Neutrons		Prompt Gamma rays		Delayed Gamma rays	
	Hiroshima	Nagasaki	Hiroshima	Nagasaki	Hiroshima	Nagasaki
Single Story (2A/E-180°)						
700 m	0.357	0.416	0.542	0.561	0.492	0.483
1000	0.363	0.404	0.538	0.518	0.478	0.477
1500	0.384	0.411	0.520	0.485	0.507	0.482
2000	0.407	0.426	0.518	0.522	0.478	0.470
Two-Story (5B/G-180°)						
700	0.236	0.270	0.355	0.323	0.248	0.231
1000	0.242	0.272	0.362	0.356	0.248	0.250
1500	0.259	0.280	0.386	0.375	0.271	0.266
2000	0.275	0.289	0.390	0.380	0.293	0.292

of the secondary gamma rays produced in the house had FSD that were generally less than 15%.

Comparison of the Transmission Factors between Hiroshima and Nagasaki. A comparison of the TF for neutrons, prompt gamma rays, and delayed gamma rays is presented in Table 21 which contains data for a single-story house and a bottom floor location in a two-story house at four ground ranges from 700 to 2000 m. The results in the table show only minor differences in the TF between Hiroshima and Nagasaki. The TF for neutrons at Nagasaki is generally greater than that at Hiroshima, indicative of the harder transported spectrum for Nagasaki. The TF for prompt gamma rays in Table 21 do not exhibit a discernible trend within the statistical uncertainty of the results. The TF for delayed gamma rays for Hiroshima is slightly larger than for Nagasaki because of the difference in the source spectrum between the ^{235}U fission products for Hiroshima and the ^{239}Pu and ^{238}U fission products for Nagasaki. Comparisons between Hiroshima and Nagasaki can also be made by examining Figures 11 to 30, discussed below.

Variation with Location and Ground Range. Figures 11 to 30 present TF computed at the seven locations for two orientations and for two ground ranges (700 and 2000 m). The orientation of the cluster with respect to the source can be ascertained from the figure by examining the direction of the "To Source" arrow. Selected TF are presented for neutrons and prompt gamma rays for the Hiroshima and Nagasaki sources.

As an example, Figure 11 presents the neutron TF computed for Nagasaki at 700 m ground range with the orientation referred to as the 0° degree orientation (see Figure 3). Note the difference in the TF computed at 2A/E and 4A/E. The presence of house 1A clearly reduces the TF for location E in house 2A compared to the unshielded identical location in house 4A. Location G in house 5B is shielded by a one-story house, while the same location in house 6B is shielded by a two-story house. This causes the reduction in TF in house 6 compared to house 5. Locations 5B/V and 5B/R are second-story locations (indicated by small internal circles) and here the TF is greater than on the first floor, as expected.

HOUSE AND TERRAIN SHIELDING

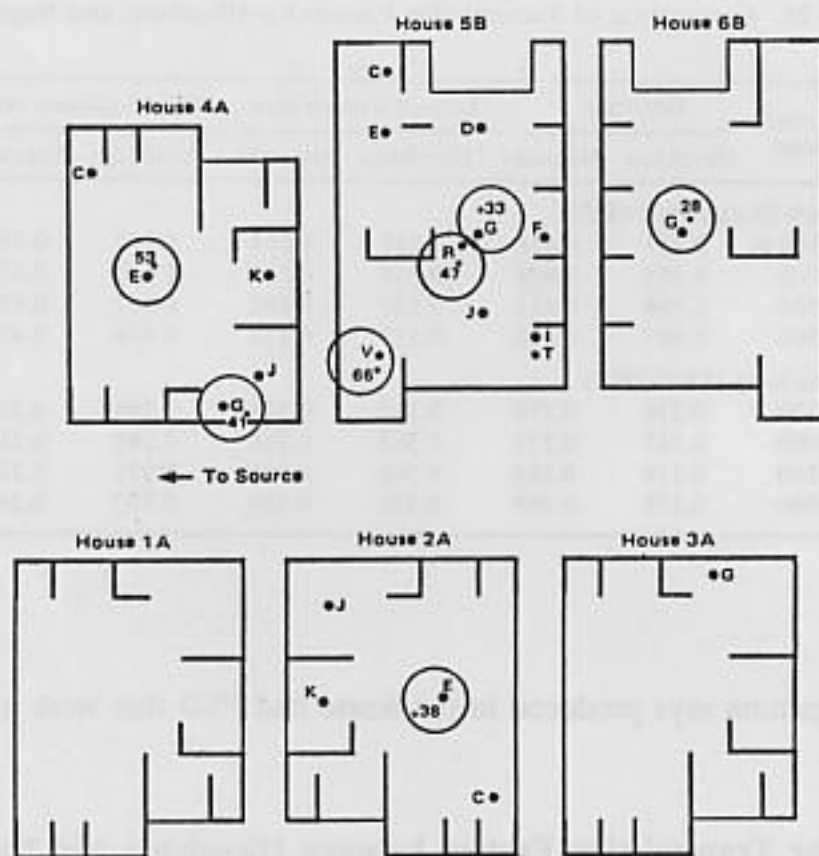


Figure 11. Transmission factors for neutrons for the free field, Nagasaki, 700 m ground range, hypocenter at 0°. House A, one story; B, two stories

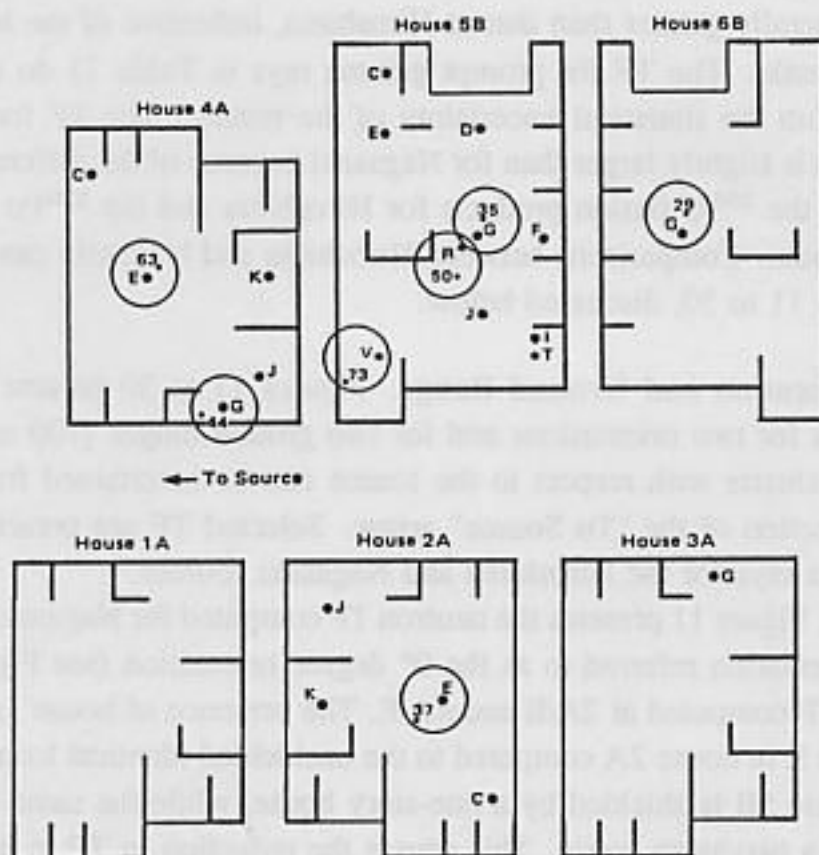


Figure 12. Transmission factors for neutrons for the free field, Nagasaki, 2000 m ground range, hypocenter at 0°

HOUSE AND TERRAIN SHIELDING

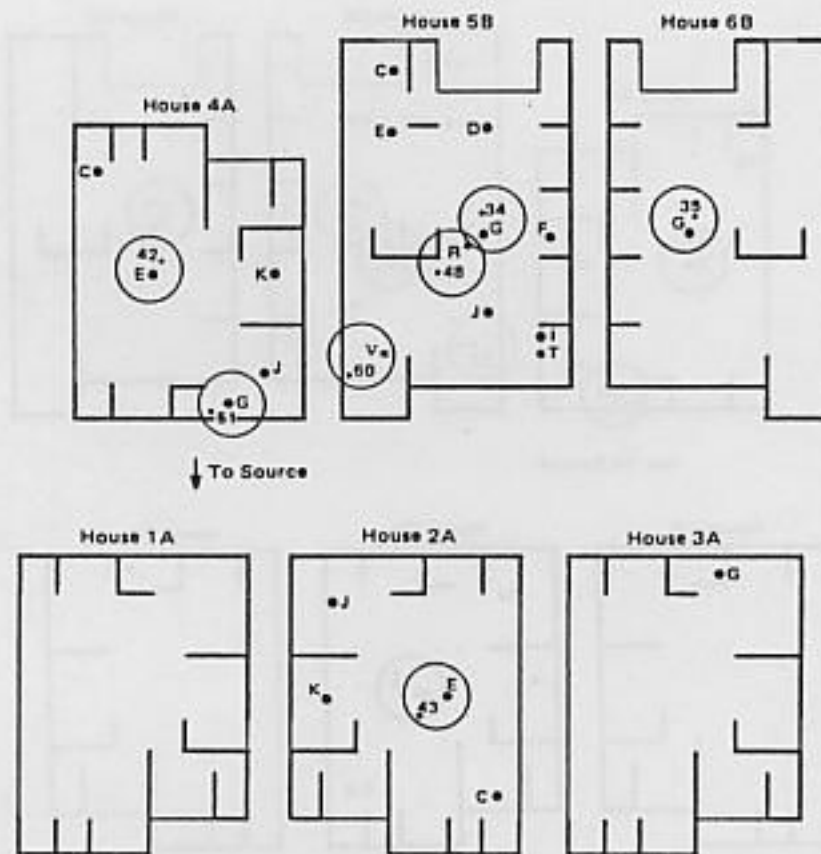


Figure 13. Transmission factors for neutrons for the free field, Nagasaki, 700 m ground range, hypocenter at 90°

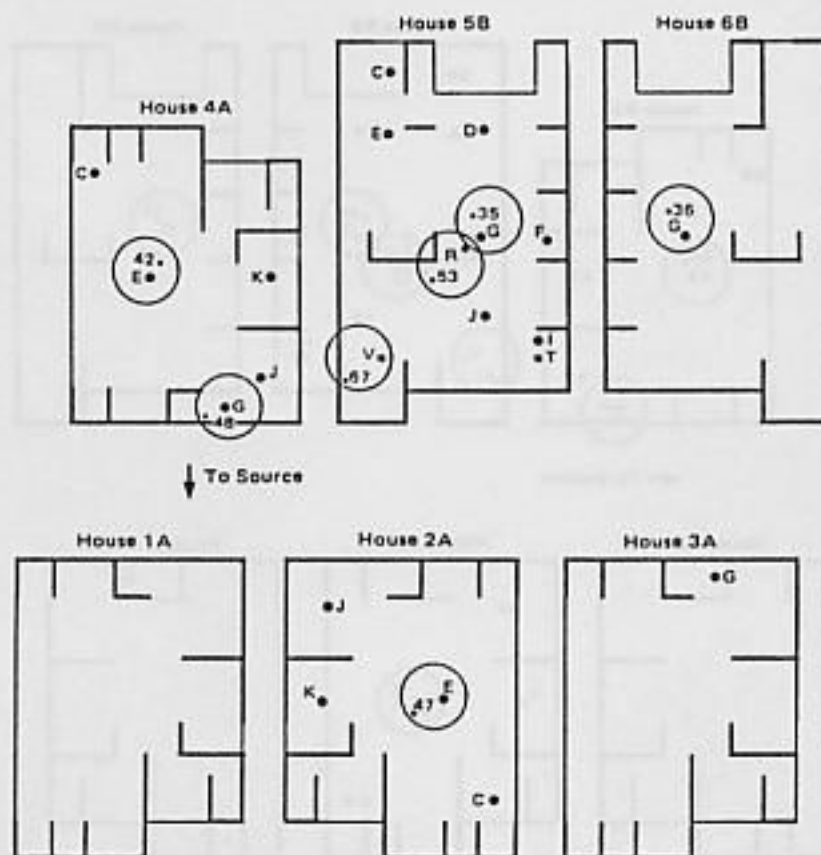


Figure 14. Transmission factors for neutrons for the free field, Nagasaki, 2000 m ground range, hypocenter at 90°

HOUSE AND TERRAIN SHIELDING

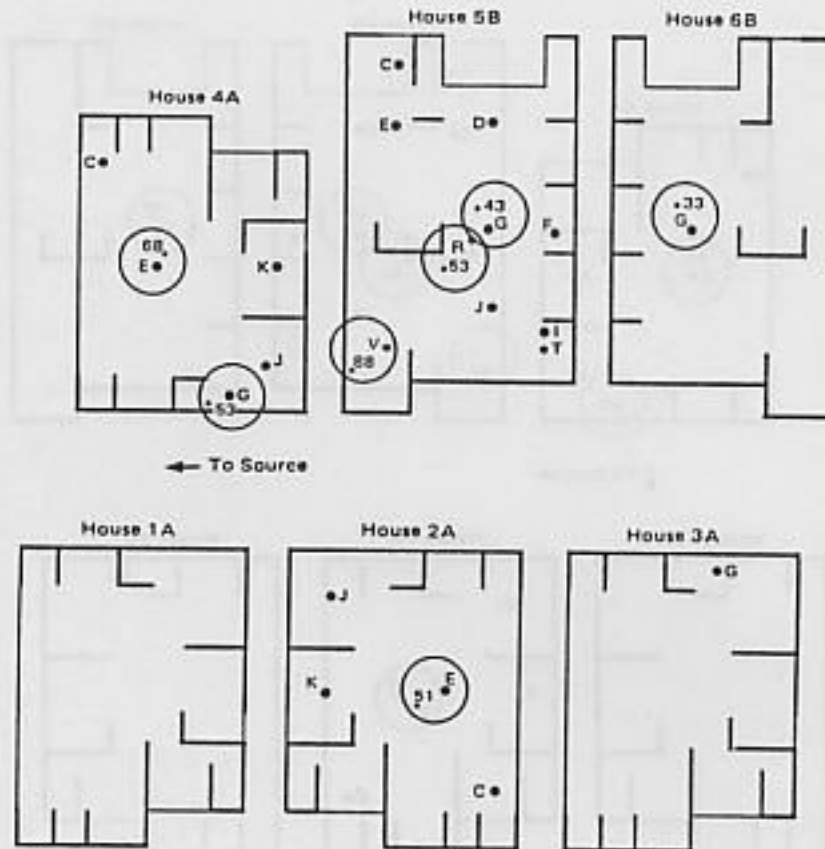


Figure 15. Transmission factors for prompt gamma rays for the free field, Nagasaki, 700 m ground range, hypocenter at 0°

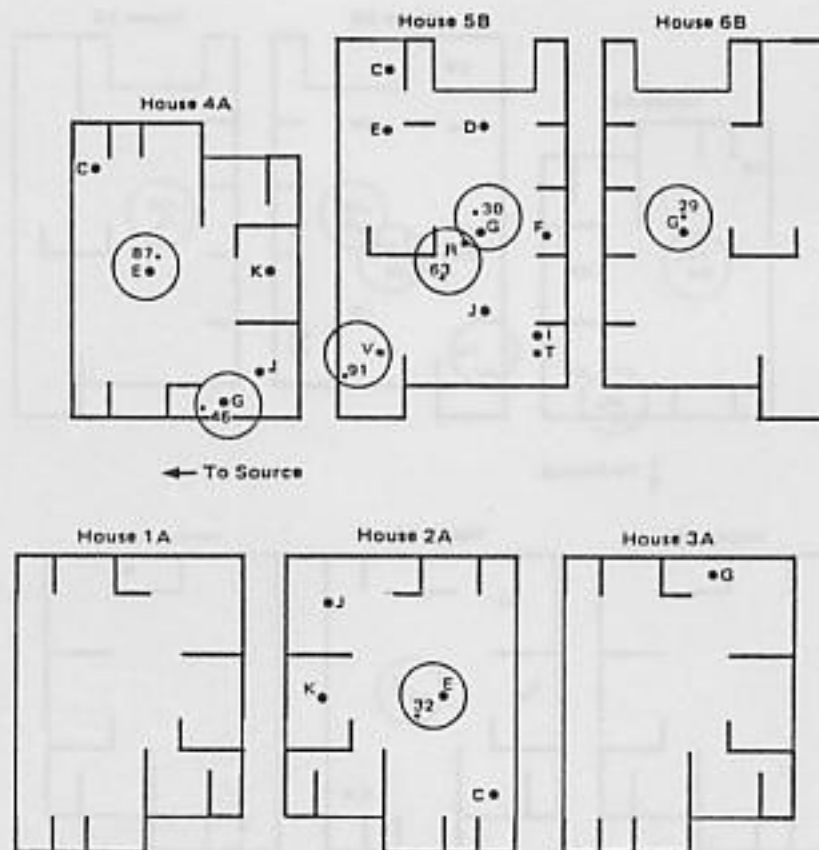


Figure 16. Transmission factors for prompt gamma rays for the free field, Nagasaki, 2000 m ground range, hypocenter at 0°

HOUSE AND TERRAIN SHIELDING

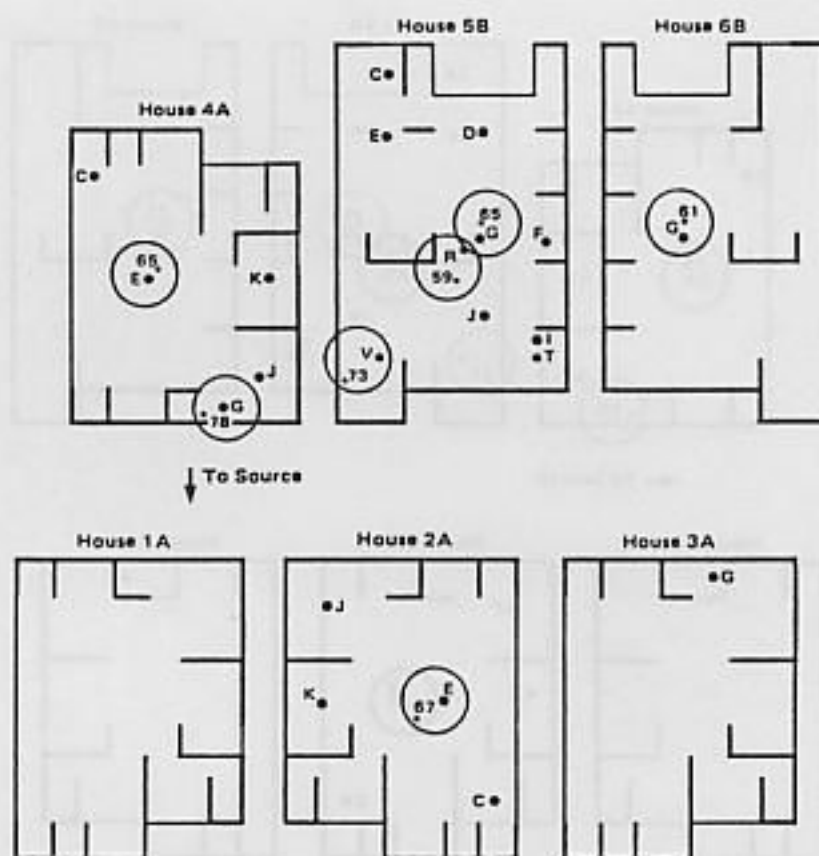


Figure 17. Transmission factors for prompt gamma rays for the free field, Nagasaki, 700 m ground range, hypocenter at 90°

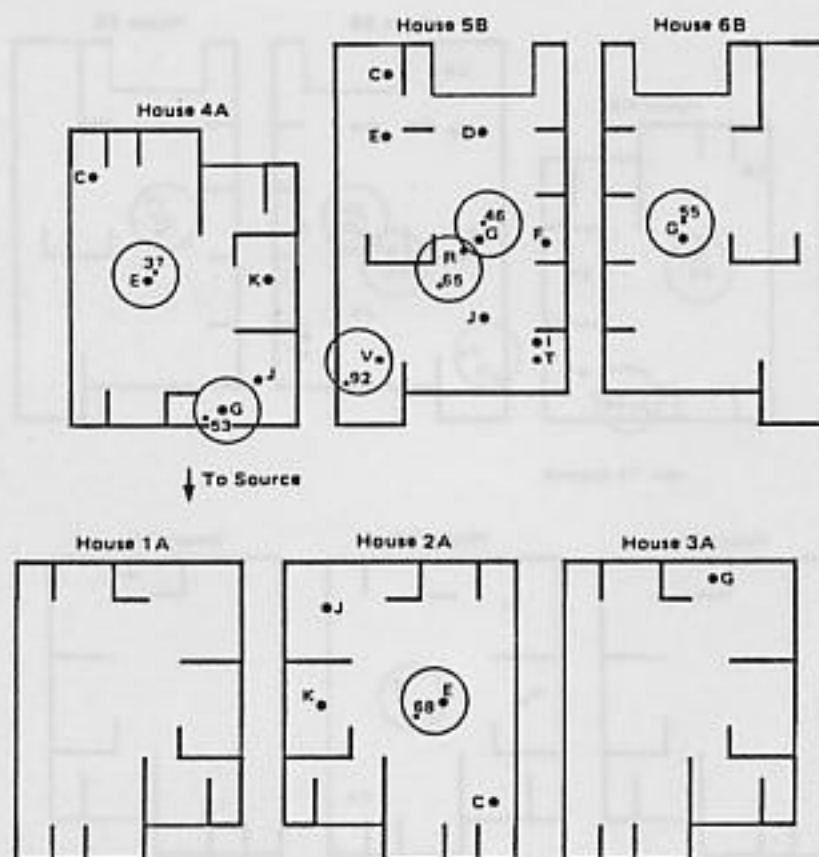


Figure 18. Transmission factors for prompt gamma rays for the free field, Nagasaki, 2000 m ground range, hypocenter at 90°

HOUSE AND TERRAIN SHIELDING

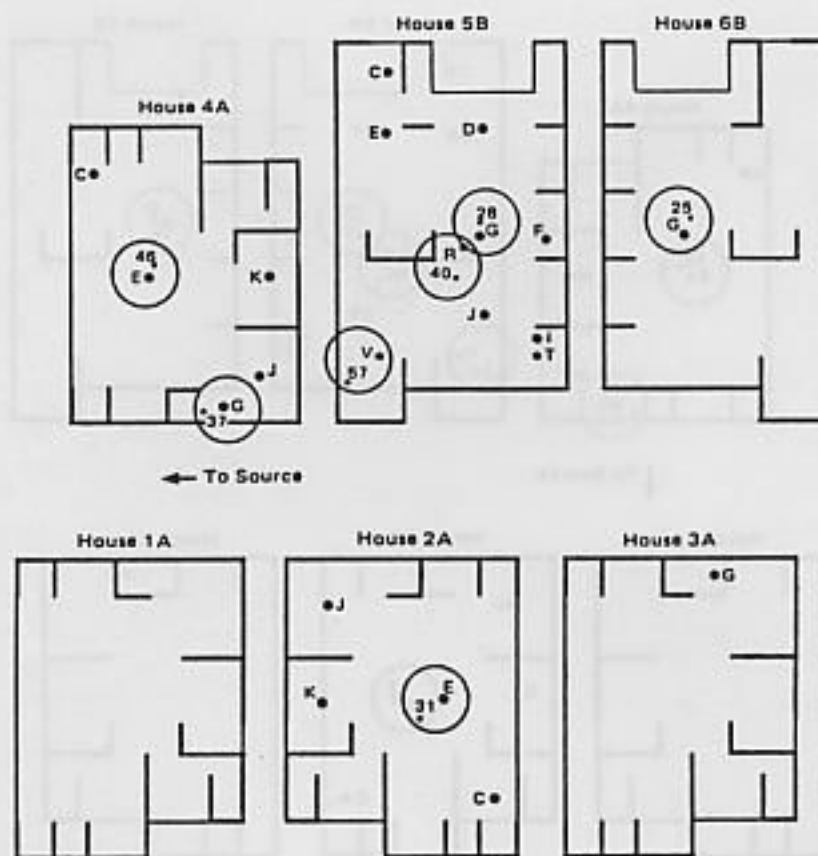


Figure 19. Transmission factors for neutrons for the free field, Hiroshima, 700 m ground range, hypocenter at 0°

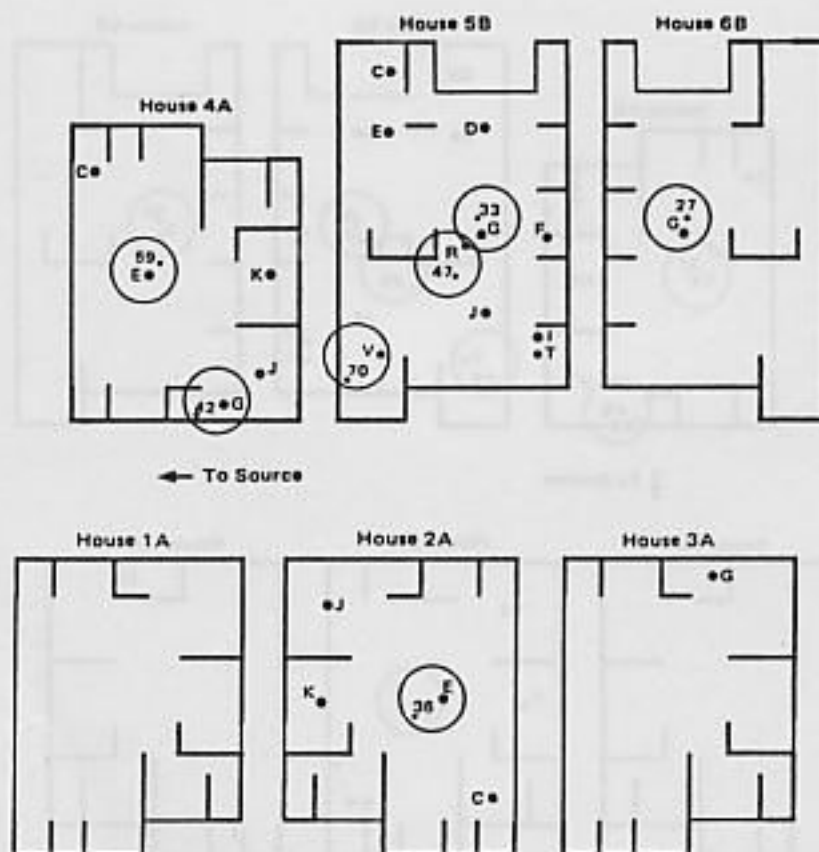


Figure 20. Transmission factors for neutrons for the free field, Hiroshima, 2000 m ground range, hypocenter at 0°

HOUSE AND TERRAIN SHIELDING

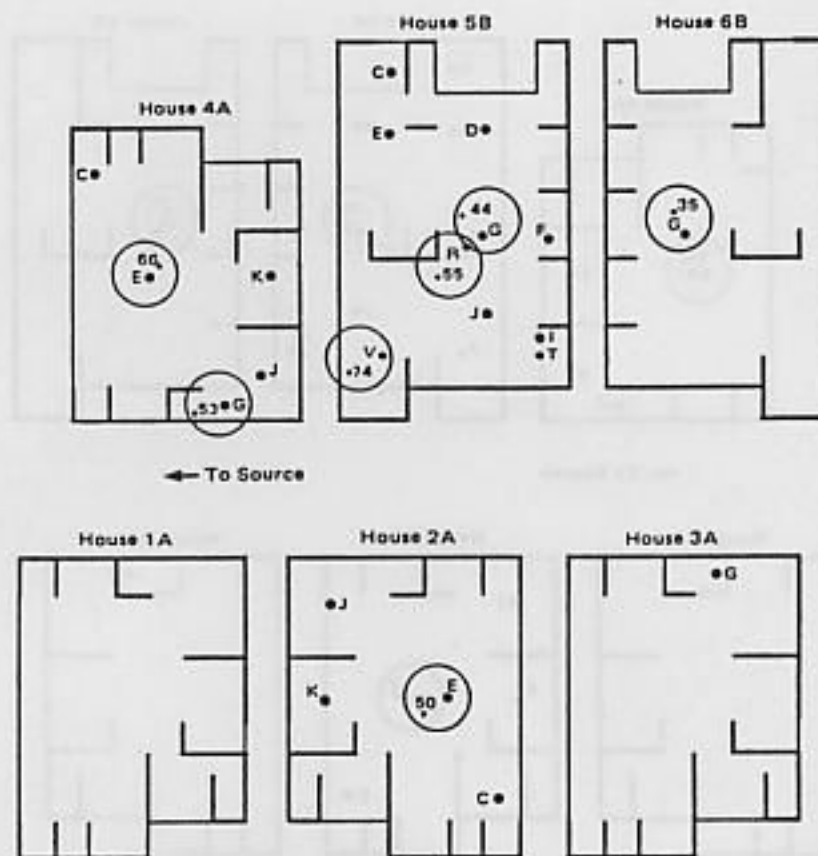


Figure 21. Transmission factors for prompt gamma rays for the free field, Hiroshima, 700 m ground range, hypocenter at 0°

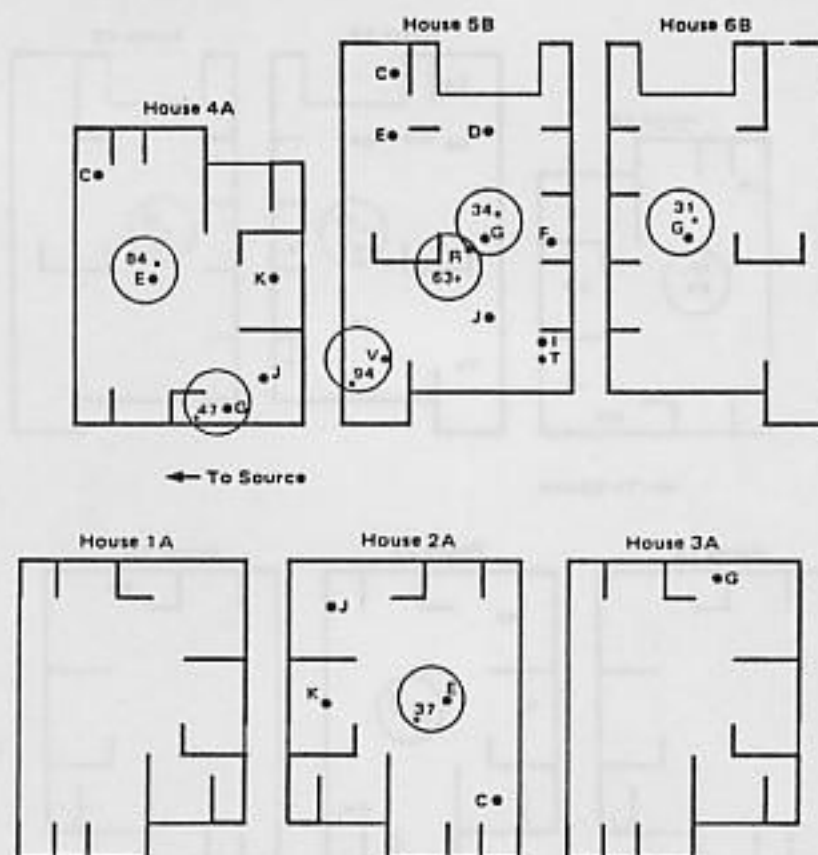


Figure 22. Transmission factors for prompt gamma rays for the free field, Hiroshima, 2000 m ground range, hypocenter at 0°

HOUSE AND TERRAIN SHIELDING

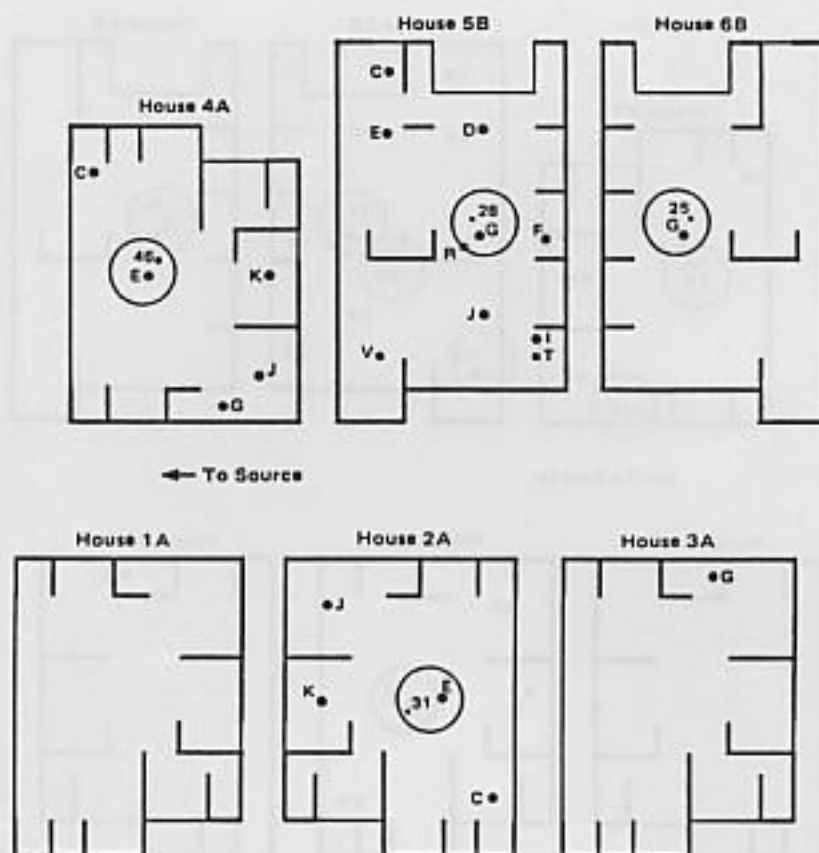


Figure 23. Transmission factors for neutrons for the free field, Hiroshima, 700 m ground range, hypocenter at 0°

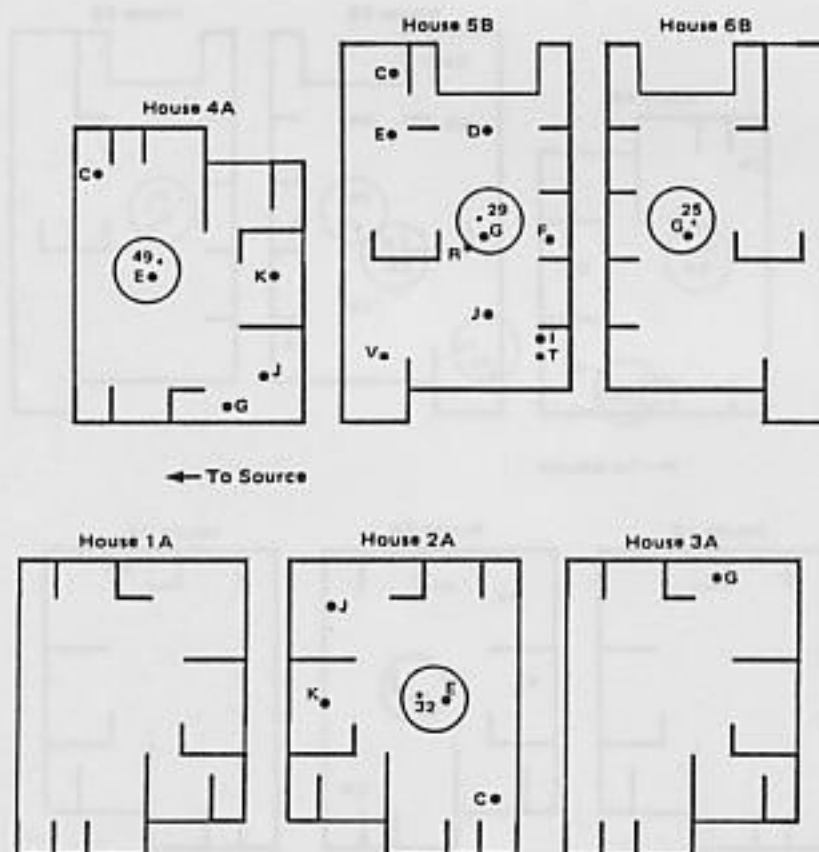


Figure 24. Transmission factors for neutrons for the free field, Hiroshima, 1000 m ground range, hypocenter at 0°

HOUSE AND TERRAIN SHIELDING

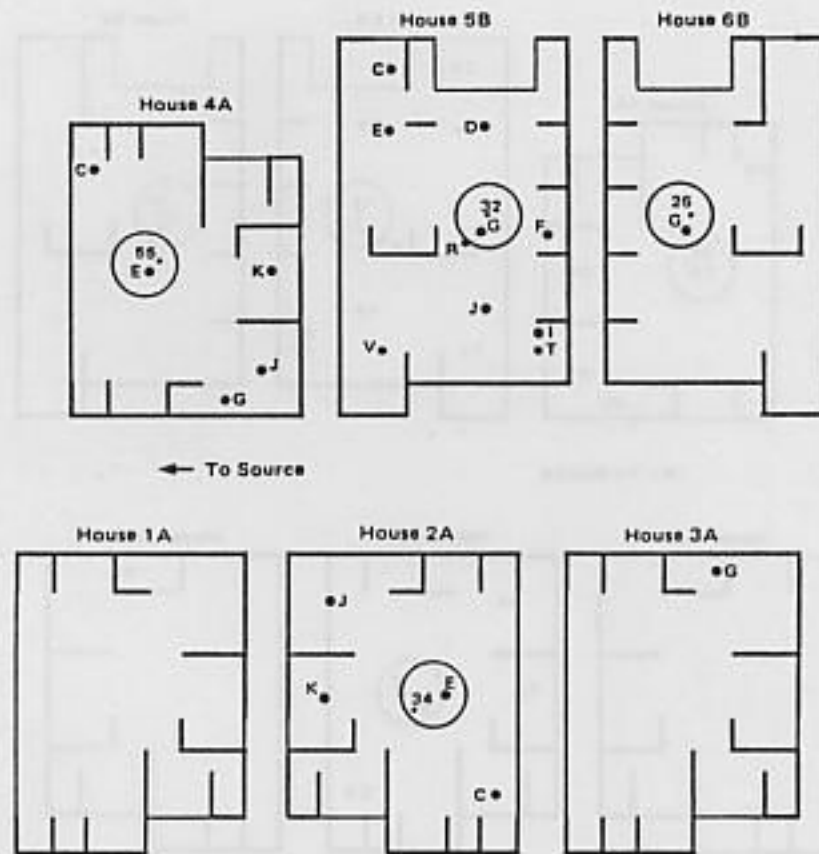


Figure 25. Transmission factors for neutrons for the free field, Hiroshima, 1500 m ground range, hypocenter at 0°

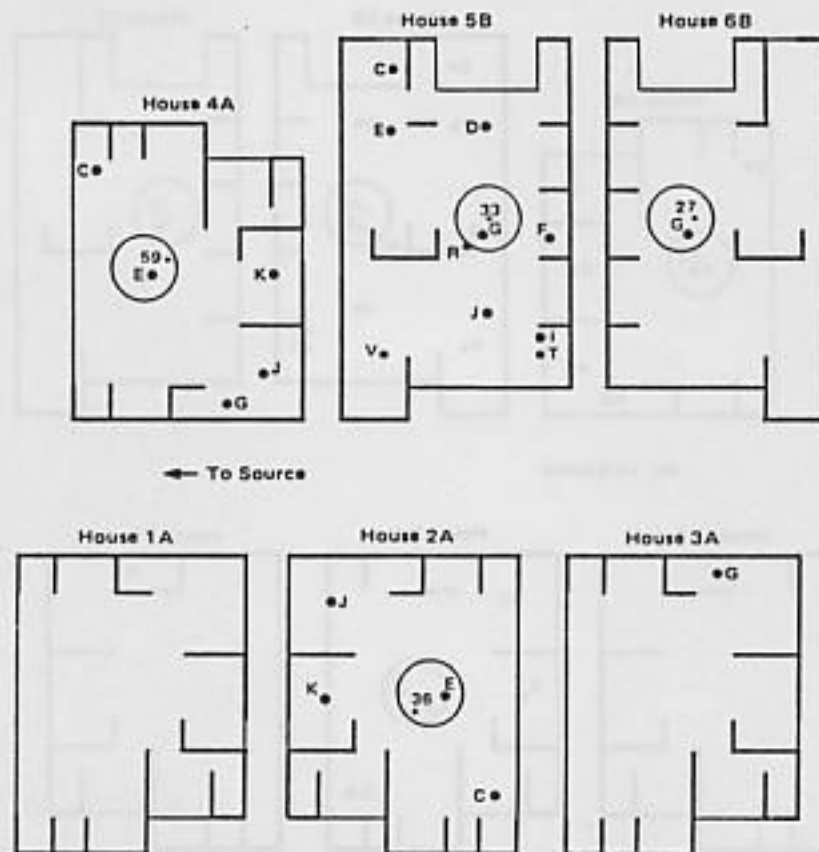


Figure 26. Transmission factors for neutrons for the free field, Hiroshima, 2000 m ground range, hypocenter at 0°

HOUSE AND TERRAIN SHIELDING

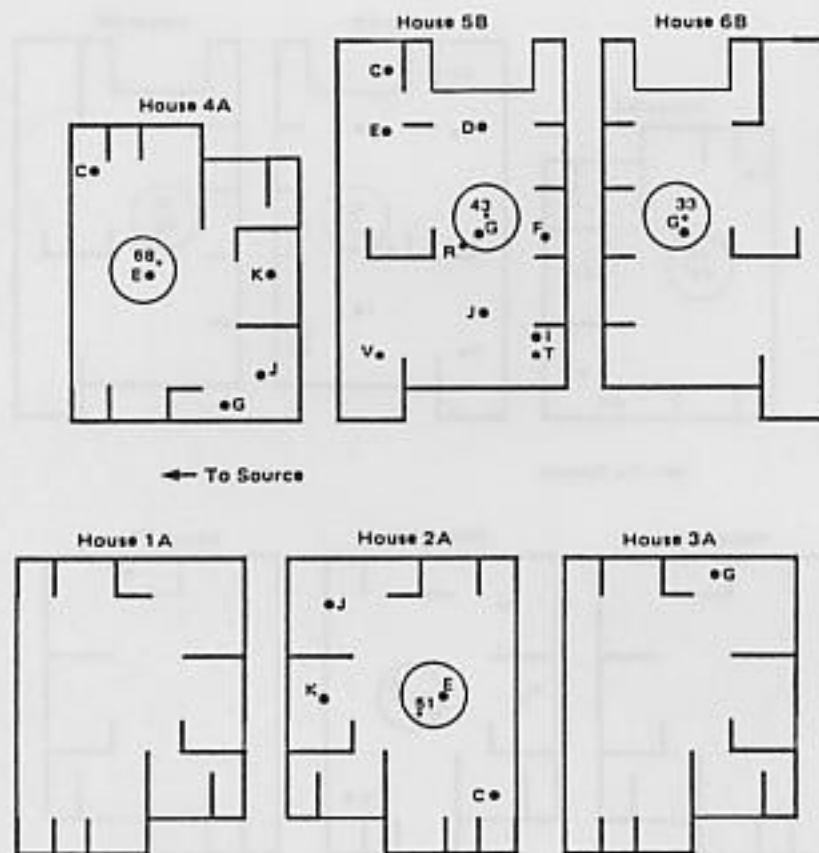


Figure 27. Transmission factors for prompt gamma rays for the free field, Nagasaki, 700 m ground range, hypocenter at 0°

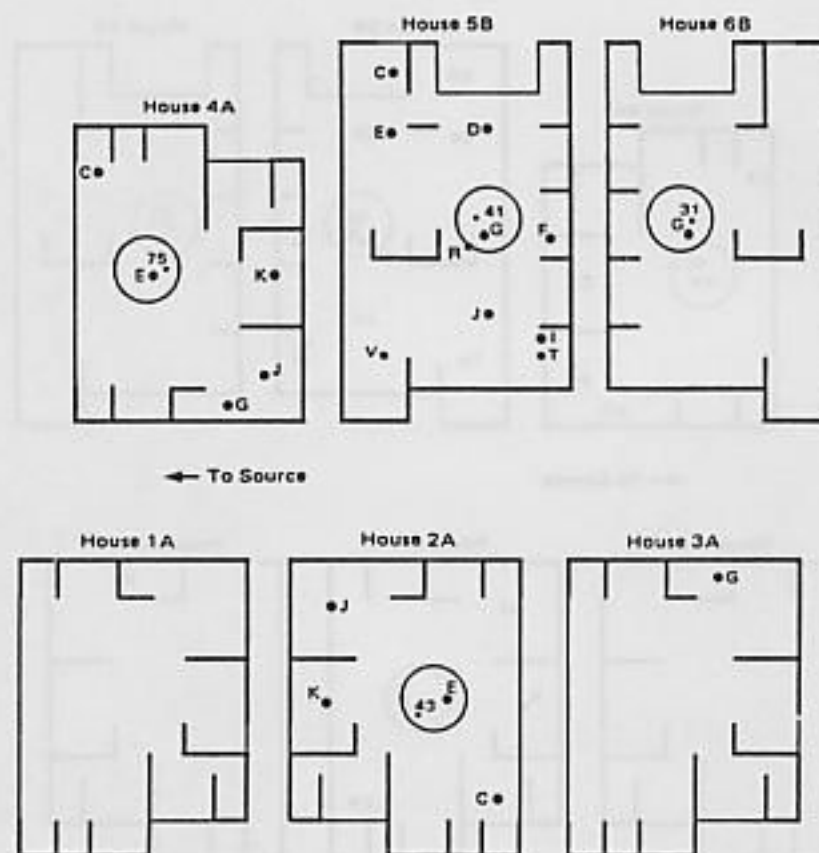


Figure 28. Transmission factors for prompt gamma rays for the free field, Nagasaki, 1000 m ground range, hypocenter at 0°

HOUSE AND TERRAIN SHIELDING

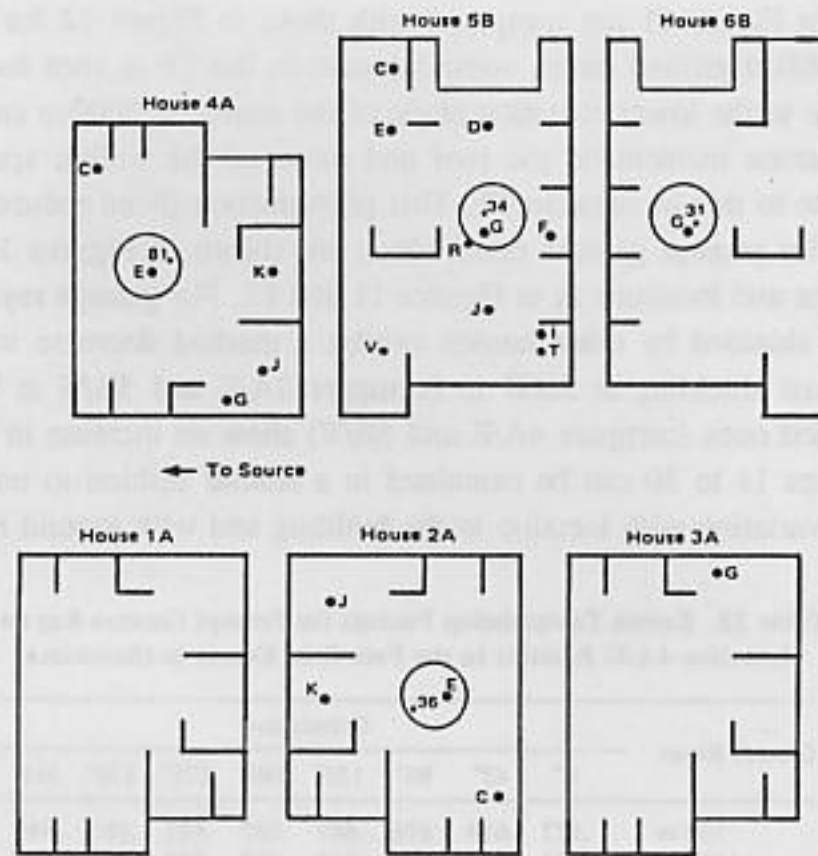


Figure 29. Transmission factors for prompt gamma rays for the free field, Nagasaki, 1500 m ground range, hypocenter at 0°

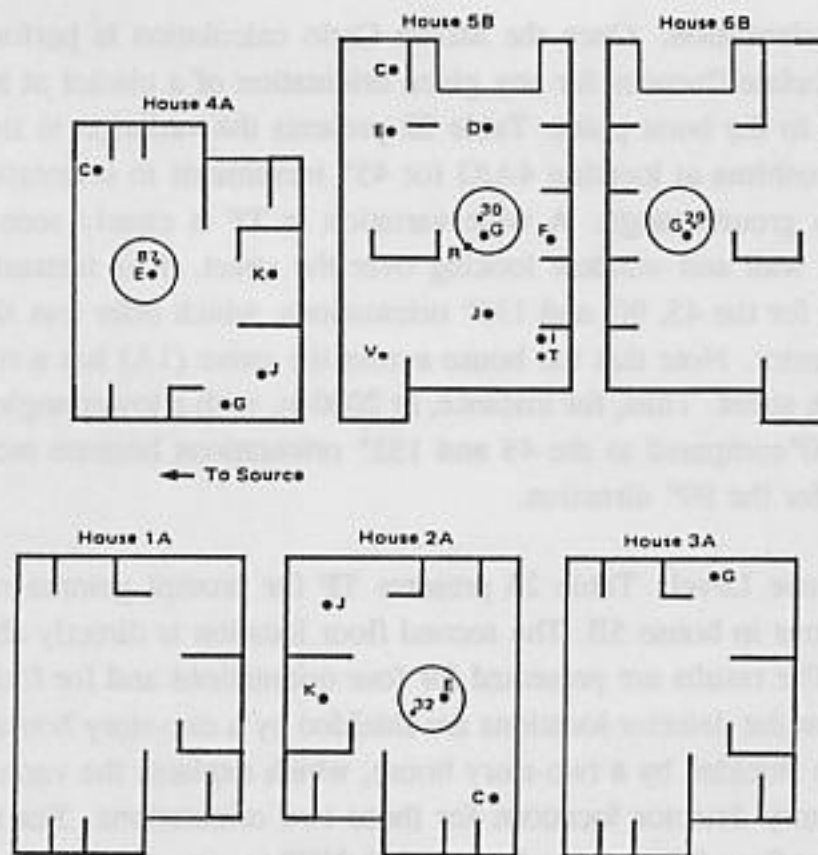


Figure 30. Transmission factors for prompt gamma rays for the free field, Nagasaki, 2000 m ground range, hypocenter at 0°

If the results in Figure 11 are compared with those in Figure 12 for the same source location, but at 2000 m ground range, some increase in the TF is seen for some locations. The increase is due to the lower elevation angle of the source at 2000 m compared to 700 m (giving fewer neutrons incident on the roof and more on the walls); spectrum hardening may also contribute to this increase in TF. This phenomenon (from reduced incident angle) is more apparent for prompt gamma rays, which are shown in Figures 15 and 16 for the same ground ranges and locations as in Figures 11 and 12. For gamma rays, however, those locations that are shielded by other houses exhibit a marked decrease in the TF because of additional mutual shielding at 2000 m (compare 2A/E and 5B/G at 700 and 2000 m) while the unshielded ones (compare 4A/E and 5B/V) show an increase in the TF. The data presented in Figures 11 to 30 can be examined in a similar fashion to understand most of the effects of the variation with location in the building and with ground range.

Table 22. Kerma Transmission Factors for Prompt Gamma Rays at Location 4A/G Relative to the Free-field Kerma in Hiroshima

Ground Range	Orientation							
	0°	45°	90°	135°	180°	225°	270°	315°
700 m	.527	.614	.676	.667	.507	.427	.485	.499
1000	.524	.647	.690	.718	.510	.374	.482	.498
1500	.488	.650	.615	.662	.479	.317	.486	.480
2000	.468	.626	.566	.592	.451	.299	.500	.477

Variation with Orientation. Once the Monte Carlo calculation is performed, the results can be used to calculate fluences for any given orientation of a cluster at any given ground range with respect to the burst point. Table 22 presents the variation in the TF for prompt gamma rays at Hiroshima at location 4A/G for 45° increments in orientation at 700, 1000, 1500, and 2000 m ground range. A wide variation in TF is clearly seen at this location, which is next to a wall and window looking over the street. It is interesting to study the results in Table 22 for the 45, 90, and 135° orientations, which offer less shielding between the source and detector. Note that the house across the street (1A) has a roof peak running perpendicular to the street. Thus, for instance, at 2000 m, with a lower angle to the burst, the TF is reduced at 90° compared to the 45 and 135° orientations because more of the source is shielded by 1A for the 90° direction.

Variation with Floor Level. Table 23 presents TF for prompt gamma rays for first and second floor locations in house 5B. The second floor location is directly above the location on the first floor. The results are presented for four orientations and for four ground ranges. At the 0° orientation the detector locations are shielded by a one-story house and at the 180° orientation they are shielded by a two-story house, which explains the variation between the first- and second-story detector locations for those two orientations. For the 90 and 275° orientations, the first floor TF increase from 700 to 1000 m ground range because the shift in elevation of the burst point from 40° (700 m) to 30° (1000 m) causes the primary shielding to shift from the roof to the walls. The 90° orientation is shielded by a single-story house across

Table 23. Kerma Transmission Factors for Prompt Gamma Rays at Location 5B/G (First Floor) and 5B/R (Second Floor) Relative to the Free-field Kerma in Hiroshima

Ground Range	Orientation							
	0°		90°		180°		270°	
	1st ^a	2nd	1st	2nd	1st	2nd	1st	2nd
700 m	.436	.548	.536	.594	.355	.461	.593	.631
1000	.425	.571	.602	.624	.362	.413	.634	.713
1500	.385	.607	.585	.643	.386	.354	.630	.796
2000	.341	.632	.519	.660	.390	.320	.621	.864

^aFirst floor

Table 24. Kerma Transmission Factors for Prompt and Delayed Gamma Rays at Location 4A/E Relative to the Free-field Kerma in Hiroshima

Ground Range	Orientation							
	0°		90°		180°		270°	
	PG ^a	DG	PG	DG	PG	DG	PG	DG
700 m	.661	.540	.574	.562	.425	.363	.640	.601
1000	.739	.580	.550	.539	.352	.263	.666	.585
1500	.805	.663	.469	.439	.279	.229	.677	.597
2000	.843	.691	.410	.397	.251	.219	.708	.630

^aDose component

the street; note the decrease in TF on the first floor with increasing ground range beyond 1000 m as the lowered elevation angle allows more interception by the one-story house, while the TF for the second story increases, with less roof and more wall shielding. At 270°, the second story shifts from being primarily shielded by the roof to being shielded primarily by the wall (with a large window in the shielding wall) as the ground range increases.

Comparison of Delayed and Prompt Radiation Transmission Factors. The variation in the prompt and delayed gamma-ray TF for location 4A/E is shown in Table 24. The TF for prompt gamma rays are slightly larger than those for delayed gamma rays due to the harder spectrum of the prompt gamma rays produced by neutron capture in the air.

House Secondary Gamma Rays. The TF approach is less useful for understanding the behavior of secondary gamma rays produced by neutron capture in the house. The TF in this case (see above) is the ratio of the kerma in the shielded location due to the secondary gamma rays produced in the house to the free-in-air kerma due to neutrons at the same point in space. Since the gamma rays are produced in the house materials mainly by thermal neutron capture reactions, the level of production is largely dependent on the *number* of incident neutrons and is relatively insensitive to the spectrum. The FIA kerma from neutrons, however, is spectrum sensitive. Thus, at Hiroshima, where the entire neutron spectrum shifts drastically with ground range, the TF for the secondary gamma rays produced in the house undergo a

Table 25. Kerma Transmission Factors for Secondary Gamma Rays Produced at Location 2A/E-180° Relative to the Free-field Kerma in Hiroshima and Nagasaki

Ground Range	House Gamma ray Transmission Factor ^a	
	Hiroshima	Nagasaki
700 m	.405	.157
1000	.286	.150
1500	.192	.139
2000	.150	.126

^aRatio of gamma-ray kerma from house secondary gamma rays to FIA neutron kerma.

dramatic change that has little to do with the type of transport effects being discussed. It has to do with the changes in the neutron kerma per unit fluence as the spectrum changes with ground range.

The effect is illustrated in Table 25. The TF for secondary gamma rays produced in a house at Hiroshima decreases by nearly a factor of three from 700 to 2000 m ground range, while for the relatively constant spectrum at Nagasaki, the TF decreases only 20% over the same ground range.

The TF for the secondary gamma rays produced in houses do not change much with orientation, since the thermal neutrons "flood" the house (the fluence is nearly isotropic and nearly the same all over the house), and the gamma rays they produce arrive at the detector from all directions.

Tenement House Cluster Calculations

In Figure 9 detector locations are shown inside the two-story tenement houses of the tenement cluster for which Monte Carlo calculations were performed. In addition, several locations in the A and B houses in the tenement cluster were calculated to compare with results from the six-house cluster. The calculations provide a large data base for the study of shielding in tenement houses that was used in the development of the shielding models for the revised dosimetry system (discussed later). The tenement cluster model also provided the opportunity to cross-compare results from two cluster models for consistency. Selected results from the computations to illustrate various shielding situations follow.

Results for "typical" tenement house locations on the first floor are given in Table 26. For the 0° orientation, these locations were shielded by adjacent houses sharing a common wall, and at 270° they were shielded by tenement houses across the street. A comparison of first- and second-floor locations is shown in Table 27. The location on the first floor of tenement house 3 (3T/B 0°) was shielded primarily by the wall, the second floor location (3T/G 0°) by the roof, and the gamma-ray attenuation to the ground floor is less. The locations in house 4T show more attenuation for the first floor locations because of the presence of 3T.

Because of the built-up nature of Japanese residential neighborhoods, many survivors in houses were also shielded by adjacent houses. A comparison of TF for adjacent shielding by the two-story house B and the tenement house is shown in Table 28. Detector 8T/D 0° is shielded by house B and detector 4T/D 0° is shielded by a tenement house. The data in

Table 26. Comparison of the Kerma Transmission Factors at Two First-floor Tenement House Locations Relative to Free-field Kerma, Hiroshima at 1500 m

Location	Transmission Factor		
	Neutrons	Gamma rays	
		Prompt	Delayed
4T/B 0°	0.274	0.491	0.317
4T/D 0°	0.256	0.477	0.348
4T/B 270°	0.280	0.439	0.375
4T/D 270°	0.219	0.390	0.309

Table 27. Comparison of Kerma Transmission Factors on Different Floors in a Tenement House Relative to the Free-field Kerma, Hiroshima at 1500 m

Floor	Location	Neutrons	Gamma rays	
			Prompt	Delayed
1	3T/B 0°	0.418	0.795	0.605
2	3T/G 0°	0.525	0.655	0.564
1	4T/B 0°	0.274	0.491	0.317
2	4T/G 0°	0.416	0.513	0.444

Table 28. Comparison of the Effect of Mutual Shielding by Two-story House B and Two-story Tenement House on the Kerma Transmission Factor Relative to Free-field Kerma, Hiroshima at 1500 m

Location	Two-Story House (B)	Tenement House
	8T/D 0°	4T/D 0°
Transmission Factor		
Neutrons	0.256	0.256
Prompt gamma rays	0.444	0.477
Delayed gamma rays	0.374	0.348

the table indicate that there is little difference in the shielding. However, because tenement houses share common walls, several houses in a row may exhibit large adjacent shielding. This is illustrated in Table 29, which shows the variation in TF along a row of tenement houses aligned end-to-end towards the hypocenter. Since the free-field fluence of neutrons is less directional than that of gamma rays, the decrease in TF due to more interceding houses is less pronounced for neutrons than for gamma rays.

Several detector locations were in the kitchen and bath annexes to the tenement house. These locations are interesting from the standpoint of the nine-parameter coding procedure. TF for annex locations are given in Table 30. The TF vary a great deal with orientation toward the burst point because of the potential for shielding by the primary house (270° orientation), by adjacent annex buildings (0 and 180° orientations), and by partial shielding

Table 29. Comparison of the Effect of Multiple Tenement House Shielding on the Kerma Transmission Factor Relative to Free-field Kerma, Hiroshima at 1500 m

Number of Houses Interceding	Location	Transmission Factor		
		Neutrons	Gamma rays	
			Prompt	Delayed
0	3T/D 0°	0.441	0.795	0.652
1	4T/D 0°	0.256	0.477	0.348
3	6T/D 0°	0.250	0.277	0.243

Table 30. Comparison of the Effect of Shielding for Locations in the Annex of Tenement Houses on the Kerma Transmission Factors Relative to Free-field Kerma, Hiroshima at 1500 m

Location	Transmission Factor		
	Neutrons	Gamma rays	
		Prompt	Delayed
4T/E 0°	0.336	0.546	0.476
90°	0.396	0.623	0.564
180°	0.328	0.441	0.415
270°	0.248	0.311	0.257
4T/F 0°	0.412	0.587	0.543
90°	0.406	0.555	0.577
180°	0.305	0.435	0.354
270°	0.263	0.269	0.235

from a building a distance away (90° orientation).

The tenement cluster contains two houses of Type A and one house of Type B that were used in the six-house cluster. The presence of these houses in the tenement cluster provides the opportunity to check the consistency of the TF between the two clusters for similar shielding situations. This comparison is made in Table 31 for locations and orientations that provide similar, though not identical, shielding configurations. Except for the first case in the table, the results from the two clusters are within 10%.

Street Locations in Six-House Cluster

The 26 street locations in the six-house cluster shown in Figure 4 were used to generate a data base for globe shielding analysis. This analysis will be described later; here selected results are presented to indicate the magnitude of the shielding for street locations, the variations among different locations in the street, and the differences with shielding for locations inside houses.

Transmission factors computed from this data base for various locations and orientations at 1000 m ground range at Hiroshima are shown in Table 32. Groups of cases are separated to highlight features of the TF. The first group (cases 1 and 2) in Table 32 shows the difference in shielding for a situation with only a two-story house present between the detector and the

HOUSE AND TERRAIN SHIELDING

Table 31. Comparison of Similar Shielding Situations in the Six-house Cluster and the Tenement Cluster on the Kerma Transmission Factor Relative to Free-field Kerma, Hiroshima at 1500 m

Cluster	Location	Transmission Factor			
		Neutrons	Gamma rays		
			Prompt	Delayed	
T	1A/G 0°	0.645	0.795	0.669	
6H	3A/G 180°	0.552	0.706	0.650	
T	7B/G 0°	0.386	0.552	0.448	
6H	6B/G 180°	0.365	0.554	0.459	
T	7B/G 270°	0.430	0.646	0.617	
6H	6B/G 270°	0.391	0.660	0.596	
T	2A/E 0°	0.414	0.507	0.481	
6H	4A/E 90°	0.386	0.469	0.439	

Table 32. Selected Kerma Transmission Factors for Street Locations in the Six-house Cluster Relative to Free-field Kerma, Hiroshima at 1000 m

Case	Detector	Angle	Transmission Factor			Remarks
			Neutrons	Gamma rays		
				Prompt	Delayed	
1	2	270	0.56	0.51	0.37	Shielded by a single house (5B)
2	6	270	0.41	0.38	0.32	Same as Case 1 with entire cluster present
3	15	0	0.83	0.94	0.90	Locations down the street left to right, burst toward left end of street
4	6	0	0.51	0.63	0.58	
5	19	0	0.52	0.61	0.59	
6	2	0	0.73	0.88	0.77	Same as Case 4 with only House 5B in cluster present
7	19	0	0.52	0.61	0.59	Looking down street toward burst
8	19	45	0.52	0.53	0.51	Burst diagonally across row of 1-story houses
9	19	90	0.54	0.53	0.45	Shielded by 1-story house
10	19	135	0.64	0.78	0.72	Shielded diagonally by 1-story house
11	19	180	0.68	0.87	0.84	Little shielding, on edge of street toward burst
12	19	225	0.58	0.64	0.59	Shielded diagonally by 2-story house (see Case 10)
13	19	270	0.47	0.44	0.37	Shielded by 2-story house (see Case 9)
14	19	315	0.47	0.43	0.40	Shielded diagonally by row of 2-story houses (see Case 8)

burst point (case 1) and for a situation in which the detector is behind the same house but with the rest of the cluster of houses present (case 2). The presence of other houses clearly increases the attenuation.

The second grouping (cases 3, 4, and 5) presents a sweep down a street aligned towards the burst point. The case 3 location is at the edge of the street with little shielding towards the burst point. Cases 4 and 5 are in the middle of the street but their positions farther down the street permit more shielding by the houses on either side. Interestingly, case 5 results are not much different from case 4, even though there are more houses in front. Furthermore, these two locations do not show differences at the greater ground range of 2000 m. In Table 32, case 6 has only the single house 5B in the cluster present, for comparison to case 4.

Table 33. Kerma Transmission Factor at Street Location 19 in the Six-house Cluster Relative to Free-field Kerma, Hiroshima at 2000 m

Angle	Neutrons	Gamma rays	
		Prompt	Delayed
0°	0.52	0.56	0.54
45	0.51	0.35	0.35
90	0.54	0.45	0.39
135	0.67	0.81	0.76
180	0.73	0.91	0.90
225	0.61	0.71	0.70
270	0.47	0.45	0.36
315	0.46	0.34	0.32

Table 34. Comparison of Kerma Transmission Factors in a House and in the Open Relative to the Free-field Kerma, Hiroshima at 1500 m

Location		Neutrons	Gamma rays	
			Prompt	Delayed
In-House				
2A/E	0°	0.34	0.41	0.39
2A/E	180°	0.38	0.52	0.51
In-Open				
10	180°	0.55	0.40	0.40
24	0°	0.49	0.38	0.36
25	0°	0.66	0.49	0.50
26	0°	0.78	0.61	0.66

The last set of cases (7 to 14) in Table 32 presents results for a wide variety of situations through variation of burst point orientation for a single location in the cluster. This location is at the right hand side of the cluster with a two-story and a one-story house on opposite sides of the street. At the 45 and 315° orientations, the location is shielded from the burst point diagonally across a row of one- and two-story houses, respectively, and the difference in attenuation is apparent in the TF for the two orientations. The 90 and 270° orientations provide shielding by a one-story and by a two-story house, respectively. For comparison with results at a large ground range, Table 33 shows the same detector locations and orientations as cases 7 to 14, but at 2000 m ground range. Here, the orientations with substantial shielding (45, 90, 270, and 315°) show increased attenuation for gamma-ray component because the elevation angle to the burst point is lower.

Radiation TF for survivors in the street should be consistent with values computed for locations inside the houses, with any differences explainable by the changing nature of the shielding for the types of locations. A comparison of TF in the open and in houses is presented in Table 34. The orientation of the burst point is along the row of one-story houses (0 or 180°) for the cases in Table 34. The prompt and delayed gamma-ray TF for the inside and outside locations are within the same range, as expected. Notice that locations 24,

25, and 26 move farther away from the houses (Figure 4), and the TF increase consistently with reduced shielding. The neutron TF in the open are larger than those in the houses because the neutron field is less directional along the line of sight than the gamma-ray field and has a larger, downward directed skyshine component. The skyshine is shielded by the roof for locations in the house, but it arrives with little attenuation for outside locations.

Terrain Shielding

The hilly terrain at Nagasaki provided shielding for many survivors. These cases were analyzed with the globe technique. The variations in terrain have the potential to produce a wider range of attenuations than house shielding, and this range may be difficult to capture in a model. Under the constraint to use available computerized data (in this case, the globe data) for the shielding descriptions of survivors, a set of calculations using a simple "hill" to represent terrain shielding was performed and employed (as will be described later) for survivors shielded by terrain.

Table 35. Kerma Transmission Factors for Locations Near a Model Hill
Relative to Free-field Kerma, Nagasaki at 1000 m and 2000 m

Detector	Distance to Hill	Hill Slope	Ground Range 1000 m			Ground Range 2000 m		
			Neutrons	Gamma rays		Neutrons	Gamma rays	
				Prompt	Delayed		Prompt	Delayed
1	3 m	68°	0.65	0.25	0.39	0.61	0.13	0.22
2	3	43°	0.75	0.58	0.64	0.70	0.25	0.38
4	9	43°	0.85	0.75	0.77	0.80	0.36	0.51
6	15	43°	0.84	0.87	0.76	0.81	0.51	0.63
8	9	68°	0.76	0.55	0.69	0.72	0.25	0.40
10	15	68°	0.81	0.68	0.76	0.76	0.33	0.49

The hill selected for the terrain shielding calculations is a portion of a prolate spheroid exposed above the ground plane. The tips of the spheroid along the major axis are located below the ground plane and the axis is angled with respect to the ground plane so that the exposed portion exhibits a smoothly varying horizon, with different initial slopes. The hill is 80 m long, 18 m high, with slopes of 43 and 68° at either end. Detectors were located at 3 m intervals away from the hill out to 15 m to provide different shielding situations.

Selected results from the calculations for the hill model in Nagasaki at 1000 and 2000 m ground ranges are shown in Table 35. The neutrons exhibit less attenuation than the gamma rays for terrain shielding; this is the opposite of the results for house shielding. The neutron field is less directional and can shine down to the detector over the hill; whereas the hill intercepts more of the nearly line-of-sight gamma rays. For detectors in houses, the roof attenuates the incident neutron field.

The TF for delayed gamma rays are larger than those for prompt gamma rays, this also is the reverse of the house shielding results. In a house, the roof and walls attenuate all of the incident radiation. The delayed gamma rays from the debris, which are softer, are attenuated much more than the prompt gamma rays. In the open, the terrain blocks only a

Table 36. Comparison of Average Kerma Transmission Factors Relative to Free-field Kerma, Hiroshima at 1500 m

Source	Neutrons	Gamma rays	
		Prompt	Delayed
T65D (9 parameter)	0.32	—	0.90 ^a
Marcum estimate	—	0.55	0.45
In-house (This study)	0.40	0.54	0.47
In-open (This study)	0.67	0.67	0.65

^aTotal gamma-ray transmission factor.

portion of the incident gamma rays. The rising fireball raises the effective source height of the debris, reduces the portion blocked by terrain, and permits more of the delayed gamma rays to shine down on the detector.

To explore fully this type of shielding at Nagasaki, additional terrain models need to be developed. The simple hill model provides an indication of the magnitude of the shielding effect, but more realistic models, with different terrain features and locations on the hills, should be analyzed.

Summary of Calculations

During the course of development of shielding models for the revised dosimetry system, a data base of over 3,500 shielding calculations was produced for locations in two housing clusters representing actual locations in Hiroshima and Nagasaki at the time of the bombs and for a simple terrain model. These calculations employed state-of-the-art techniques that were validated with Operation BREN experiments (see Appendix 7-1). The number of data points far exceeds the number available to the developers of the T65D shielding models. A sensitivity analysis was performed to elucidate the effects of variations in house materials and the models on the resulting shielding.

Examination of the results for these locations indicated that the data base forms a consistent and defensible set of values from which to develop shielding models for the revised dosimetry system.

The averaged TF from the six-house and tenement cluster calculations for Hiroshima at 1500 m ground range are shown in Table 36 and compared with the T65D average values and the estimate made by Marcum.³ The data indicate that the Marcum conjecture is correct and very close to the averages obtained. A similar reduction in the TF for Nagasaki (the averaged values from the present study are nearly identical to those for Hiroshima) will occur from T65D to the new dosimetry. The increased gamma-ray shielding by Japanese houses is one of the major changes in the new dosimetry system.

HOUSE SHIELDING MODEL FOR NINE-PARAMETER DATA

The source of information for the nine-parameter shielding data for individual survivors at Hiroshima and Nagasaki is the RERF computer file CD465. This file contains the "nine parameters" and other data, shown in Table 37, that has been extracted from the more com-

Table 37. Shield Parameter Code (CD465)

Item No.	Description of Items	No. of Columns	Columns Used
Part I. Identification			
1.	Master file number	6	1- 6
2.	Sex and city of exposure	1	7
3.	Coordinates as to exact location ATB	8	8-15
Part II. Nine parameters and certainty of coding			
4.	Front Shielding (FS)	1	16
5.	Front Shielding Size (FSS)	1	17
6.	Unshielded (US)	3	18-20
7.	Lateral Shielding (LS)	2	21
8.	Internal Frontal Walls (IFW)	1	22
9.	Internal Lateral Walls (ILW)	1	23
10.	Height Above Floor (HF)	2	24-25
11.	Floor Number (FN)	1	26
12.	Slant Penetration (SP)	4	27-30
13.	Certainty of coding nine parameters	9	31-39
Part III. Other pertinent data			
14.	Completeness of shielding drawings prior to coding	1	40
15.	Attenuation factor (T57D) ^a	6	41-46
16.	Description of Japanese-type house	1	47
17.	Treatment of house	1	48
18.	Treatment of projection	2	49-50
19.	Elevation	1	51
20.	Grove	1	52
21.	Present coding disposition	1	59
22.	Sea Level	2	54-55
23.	Class of estimating dose	1	56
24.	Method of estimating dose	1	57
25.	Reserve columns	17	58-74
26.	Card design number	3	75-77
27.	Reserve columns	3	78-80

^aT57D refers to an earlier dosimetry system replaced by T65D.¹

plete shielding history for each survivor (discussed in Appendix 7-2). The nine parameters were originally formulated from the BREN experiments to relate radiation shielding to various physical characteristics of particular locations in Japanese-type houses.¹ The application of these nine parameters to actual survivor shielding situations required significant modification of the definitions of some parameters, because conditions in Japan differed from the relatively uncomplicated geometry of the BREN experiments. The relationship between the nine parameters, as used in actual Japanese survivor shielding situations and the radiation shielding was, therefore, not known. Before the CD465 data could be used in calculating the shielding of individual survivors, this relationship had to be determined.

The approach that was adopted rests on the assumption that the six-house and tenement clusters are representative of Japanese neighborhoods. This assumption is well supported by all test results to date, and is further strengthened by the analysis of the nine-parameter data reported here.

The relationship between the shielding and the nine parameters for the model clusters was determined by choosing a number of locations in each cluster for analysis. By convention, and to allow comparison with previous test results, some points in the six-house cluster

corresponded to those used in the BREN experiments for houses of similar floor plan. The nine parameters were assigned to combinations of location and orientation, using the floor plan of the two clusters, and the same procedures used by Japanese investigators when assigning the parameters to locations described in the survivor shielding histories. For each location and orientation TF were then calculated for each city at several ground ranges. Statistical analyses determined which parameters contained the most information about variation in TF. The results of these efforts allowed a set of shielding categories to be established. Each category represents a model shielding environment for calculating dose to individual survivors. The information on CD465 can be used to assign individual survivors to the appropriate category.

Definition of the Nine Parameters

It is difficult to give a definition of each of the nine parameters that is both concise and complete. In brief they are defined as follows:

FS. Front Shielding is 0 when no houses provide shielding, is 1 when an adjoining house shares a common wall, is 2 when an independent house provides shielding at a distance less than its height, and is 5 when an independent house provides shielding at a distance greater than its height but less than twice its height. One-story buildings are all taken to be 3.5 m in height and two-story buildings 6.0 m.

FSS. Front Shielding Size is 0 when no houses provide shielding, is 1 when there is a one-storied house within 7 m or a two-storied house within 6 to 12 m, and is 2 when there is a two-storied house within 6 m.

US. Unshielded is 100 unless FS=0 and the directional line to the bomb crosses an opening such as a window on the floor plan. Then its value is obtained by dividing the distance (in meters) from the survivor to the opening by 1.5 and rounding up to the next integer.

LS. Lateral Shielding is 0 when walls not on the directional line to the bomb contain openings and face no houses, is 1 when side walls have no openings and face no houses, is 2 when side walls face other buildings more than 3.5 m away but closer than 7 m for one-story buildings and 12 m for two-story buildings, is 3 when side walls face buildings less than 3.5 m away.

IFW. Internal Frontal Walls is the number of walls other than the outside wall through which the directional line to the bomb passes. The conditions that must be met are based on the distance from the survivor to the midpoint of a projection of the wall in the direction of the survivor.

ILW. Internal Lateral Walls is the number of walls other than those counted for IFW based on a similar set of projected-distance criteria. Most walls in typical houses meet these requirements.

HF. Height Above Floor is the height of the survivor above the floor in centimeters. It is usually taken to be 100 cm for standing and 30 cm for sitting survivors.

FN. Floor Number is 1 for one-story buildings, is 2 for the ground floor of multistoried buildings, and is 3 for upper floors of multistoried buildings.

SP. Slant Penetration is the distance in centimeters from the survivor to the point of incidence on an outside wall along the line-of-sight.

Assignment of Nine Parameters

Nine parameters were assigned to locations in both clusters on the basis of written instructions, dating from 1966, and supplemented by information obtained in Japan from those who had worked with survivor shielding histories. Comparisons of nine-parameter assignments made by SAIC with those made at RERF were conducted. Any differences in technique were resolved in favor of methods actually used for survivor histories.

Twenty-one separate points in the six-house cluster and 60 points in the tenement cluster were chosen for analysis. The six-house detector locations are shown in Figure 3, and the tenement house locations are shown in Figure 9. In order to allow comparison with existing data, some of these locations were points used in previous work with the cluster. Others were added to ensure adequate sample size. For many points, all the nine parameters were assigned. Following a sensitivity analysis (described below), a subset of the most significant nine parameters was assigned for 16 different orientations of the cluster with respect to the hypocenter at equal intervals of 22.5° . This rotation is justified because actual neighborhoods in the two cities were oriented randomly relative to the bomb. Rotation also allows the cluster to represent economically a large number of shielding situations. An example of the nine-parameter subset assignment and TF calculated at 1500 m ground range in the tenement cluster at Hiroshima is shown in Figure 31.

The resulting 336 locations in the six-house and 960 locations in the tenement cluster are each distinct in their nine-parameter assignments and have among them all combinations of the parameter values permitted for Japanese houses. The frequency of occurrence of each parameter in this set of locations is similar to that observed among the 10,706 survivors with cluster-like shielding histories. This correspondence indicates that the geometries of the cluster models are representative of Japanese neighborhoods in "nine-parameter space," as well as in physical space.

Variation of Transmission with Nine Parameters

Eight of the nine shielding parameters take on discrete, integer values that are not necessarily proportional to their influence on radiation shielding. To evaluate the importance of these parameters, a rank correlation analysis was used. TF were calculated for each location at a number of ground ranges. The locations were divided into subsets according to floor number (FN). For each subset, the rank correlation coefficients (RCC) and the RPCC were calculated for the six-house cluster for the remaining parameters against TF for the neutron, prompt gamma-ray, and delayed gamma-ray components. The results were consistent for all ranges tested at both cities.

The parameters FS, FSS, US, and SP are most strongly related to TF. The parameter SP consistently had the highest RPCC, followed by FS and FSS, with US sometimes significantly correlated at the 0.05 level or better. On the other hand, LS, HF, IFW, and ILW were never

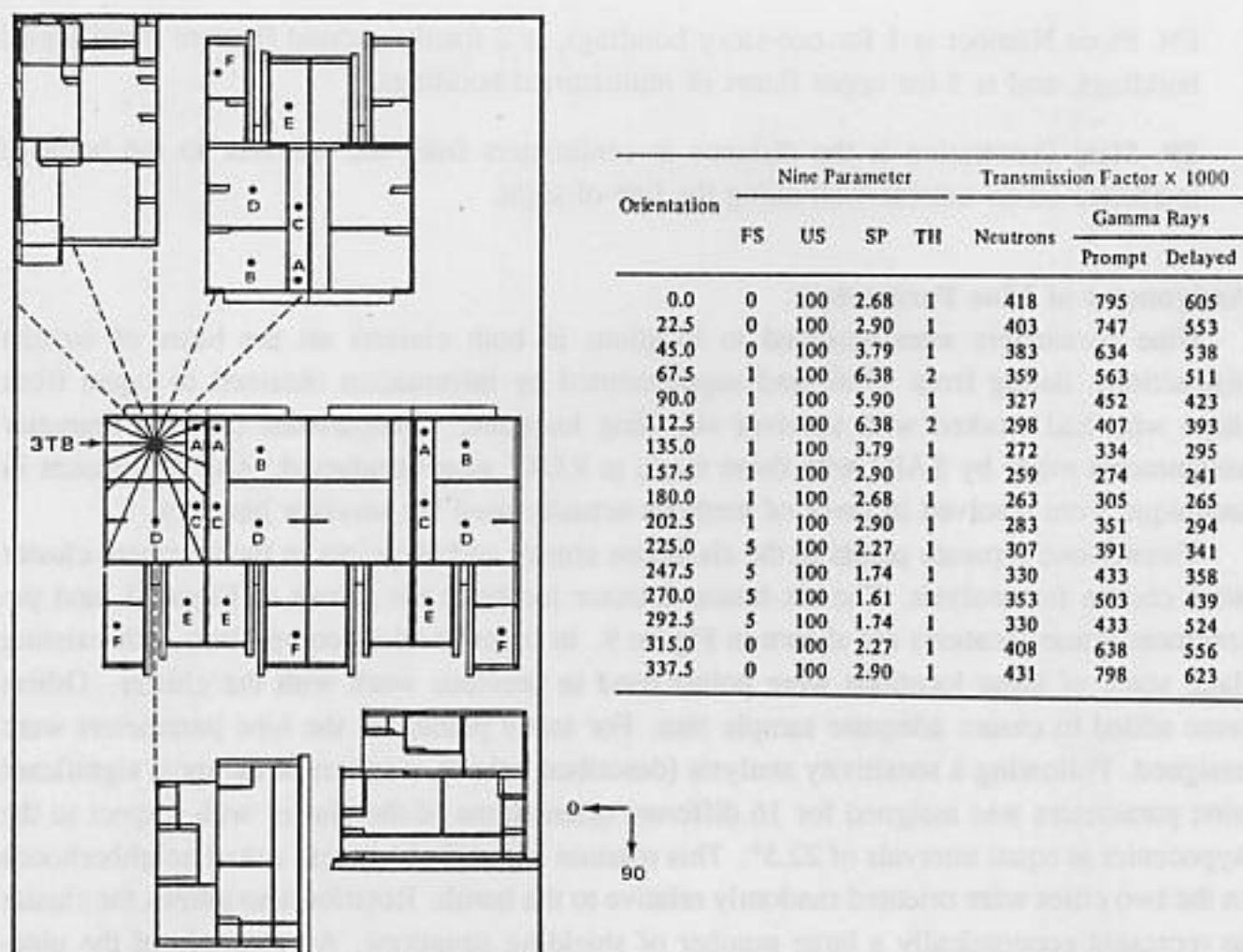


Figure 31. Results of calculations for location 3TB at 1500 m ground range at Hiroshima

significantly correlated with the TF. This is a consequence of the rules for evaluating these parameters. Locations with very different shielding characteristics often have the same value for LS so that important distinctions are missed. In contrast, assignment of ILW and IFW imposes distinctions that are unrelated to shielding. On the basis of these results, HF, LS, ILW, and IFW were not used in determining shielding categories for calculating doses to survivors.

Two of the remaining parameters, FS and FSS, are not independent quantities. They are closely related by their definitions, and so are highly correlated with each other. Consequently, they each explain the same variation in TF, and nothing is gained by using both parameters. Of the two, FS seems to have the greater resolution (i.e., it allows more cases to be distinguished). For this reason, FSS was not used in defining shielding categories, but FS was retained.

The importance of US in describing shielding was determined in the process of further analysis of SP. Since SP is a direct measure of the depth of a location within a building, it is also a gross measure of the amount of material shielding that location. It is reasonable to assume that the relationship between SP and TF will be different for cases where US is not 100, because these cases represent situations having an unobstructed opening in the direction of the bomb. There is less material shielding in these locations. Indeed, this effect

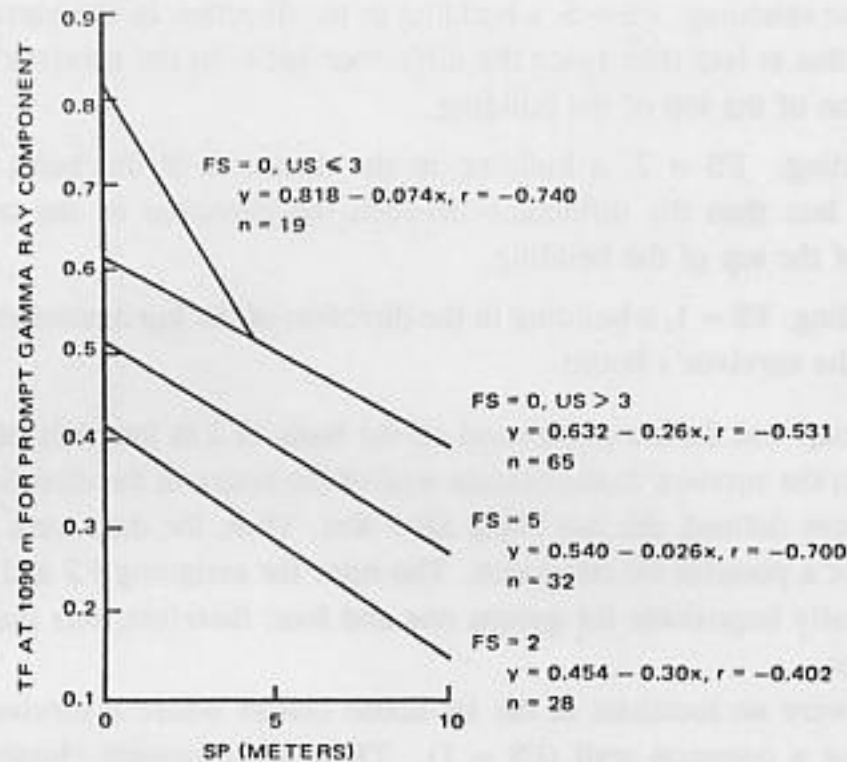


Figure 32. Regression of the transmission factor for gamma rays against SP for FN=1 in the six-house cluster

was observed.

Unlike the other parameters, SP is measured and recorded as a continuous variable. To get the maximum information from SP, a linear regression model was examined for each subset of locations having common values of FN, US, and FS. The result of several such regressions suggested that the slope of the TF versus SP curve was much steeper for small values of US. An example is presented in Figure 32 for the prompt gamma-ray component of the radiation field at 144 locations in the six-house cluster having FN = 1. The steepest slope is a consequence of the effect of an open window or door on shielding (for US ≤ 3 the survivor is close to an opening). The TF is large but drops rapidly as one moves deeper into the building. For US = 100, when no opening exists, the TF falls off more slowly from a smaller intercept. For US > 3, but not equal to 100, the relationship with SP is the same as if there were no opening at all. This pattern appeared for both cities and for all ranges although the regression equations varied somewhat for each city and range.

Survivor Shielding Categories for House Cluster Models

After testing several variations with regression analysis, the following shielding groups were defined for each floor number (FN) value:

1. Very low shielding. FS = 0, US < 3, no nearby buildings provide shielding in the direction of the burst, the survivor is within 4.5 m of an opening (window or door) that lies in the direction of the burst point.
2. Low shielding. FS = 0, US > 3, no shielding by nearby buildings, survivor is more than 4.5 m from an opening or there is no opening.

3. Intermediate shielding. $FS = 5$, a building in the direction of the burst point is within a distance that is less than twice the difference between the survivor's elevation and the elevation of the top of the building.
4. High shielding. $FS = 2$, a building in the direction of the burst point is within a distance less than the difference between the elevation of the survivor and the elevation of the top of the building.
5. High shielding. $FS = 1$, a building in the direction of the burst point shares a common wall with the survivor's house.

Each shielding group was further partitioned on the basis of 2 m intervals of SP, the line of sight distance from the survivor to the outside wall of the house in the direction of the bomb. Five SP groups were defined, the last being $SP > 8$ m. Thus, the data were partitioned into a $3 \times 4 \times 5$ matrix or a possible 60 categories. The rules for assigning FS and US made large values of SP virtually impossible for groups one and four; therefore, less than 48 categories actually had values.

In fact, there were no locations in the six-house cluster where a survivor was shielded by a house sharing a common wall ($FS = 1$). TF in the tenement cluster indicated that this shielding configuration could result in a variability in shielding different from $FS = 2$; therefore, the two distinct groups were created for high shielding. The shielding groups used in this analysis are (1) $FS = 0$, $US < 3$, (2) $FS = 0$, $US > 3$, (3) $FS = 5$, (4) $FS = 2$, and (5) $FS = 1$. Categorization on the basis of FN and SP partitioned all nine-parameter data into $3 \times 5 \times 5$ matrices.

Analyses were performed for the six-house cluster, for the tenement cluster, and for the combined data. Within each category, the average TF for prompt neutrons, prompt gamma rays, and delayed gamma rays were calculated. The number of data points in each category was tabulated. The variability of the TF was estimated by computing the FSD (standard deviation \div mean) for each dose component and shielding category. The results of this data generation and organization are discussed below.

Results of Calculations

The results are provided in Tables 38 to 46. Each table gives the number of cases, the average TF, and the FSD (when there is more than one case) for each category for a given FN. Results for the six-house cluster,* the tenement cluster, and the combined six-house and tenement clusters can be found with the following index:

Table Number for Transmission Factor Data

Floor Number	Six-house	Tenement	Combined
1	38	41	44
2	39	42	45
3	40	43	46

*These results for the six-house cluster differ slightly from previously published values because the TF was recomputed with the latest, updated free-field data.

Table 38. Mean Kerma Transmission Factors and Associated Fractional Standard Deviation for Floor Number 1 in the Six-house Cluster Relative to Free-field Kerma, Hiroshima at 1500 m

Group		Slant Penetration (SP) (M)									
		0 - 2		2 - 4		4 - 6		6 - 8		8 +	
		TF	FSD	TF	FSD	TF	FSD	TF	FSD	TF	FSD
1	Cases	8		13		1		0		0	
	FS=0 N ^a	0.586	0.20	0.433	0.22	0.361					
	US<3 G ^b	0.820	0.16	0.630	0.19	0.461					
	DG ^c	0.740	0.18	0.531	0.21	0.415					
2	Cases	8		12		34		16		2	
	FS=0 N	0.533	0.20	0.404	0.15	0.365	0.14	0.351	0.09	0.378	0.14
	US>3 G	0.723	0.14	0.578	0.09	0.511	0.16	0.490	0.12	0.443	0.07
	DG	0.658	0.20	0.500	0.13	0.453	0.17	0.427	0.12	0.423	0.03
3	Cases	13		8		11		2		0	
	FS=5 N	0.401	0.12	0.372	0.08	0.330	0.05	0.364	0.001		
	G	0.537	0.19	0.480	0.19	0.414	0.07	0.286	0.003		
	DG	0.514	0.20	0.447	0.20	0.363	0.12	0.282	0.05		
4	Cases	24		5		3		0		0	
	FS=2 N	0.334	0.19	0.314	0.09	0.303	0.02				
	G	0.469	0.19	0.381	0.23	0.318	0.12				
	DG	0.395	0.21	0.325	0.22	0.260	0.10				
5	Cases										
	FS=1 N										
	G										
	DG										

Dose component: ^aNeutrons, ^bPrompt gamma rays, ^cDelayed gamma rays.

Table 39. Mean Kerma Transmission Factors and Associated Fractional Standard Deviation for Floor Number 2 in the Six-house Cluster Relative to Free-field Kerma, Hiroshima at 1500 m

Group		Slant Penetration (SP) (M)									
		0 - 2		2 - 4		4 - 6		6 - 8		8 +	
		TF	FSD	TF	FSD	TF	FSD	TF	FSD	TF	FSD
1	Cases	7		7		4		0		0	
	FS=0 N ^a	0.550	0.19	0.369	0.16	0.360	0.10				
	US<3 G ^b	0.819	0.08	0.622	0.10	0.610	0.06				
	DG ^c	0.731	0.09	0.537	0.12	0.539	0.08				
2	Cases	6		3		18		18		7	
	FS=0 N	0.500	0.24	0.395	0.17	0.332	0.18	0.284	0.17	0.268	0.14
	US>3 G	0.684	0.14	0.645	0.16	0.535	0.16	0.473	0.16	0.413	0.16
	DG	0.627	0.16	0.532	0.16	0.465	0.19	0.410	0.17	0.340	0.20
3	Cases	7		2		11		6		0	
	FS=5 N	0.371	0.15	0.356	0.13	0.317	0.10	0.285	0.11		
	G	0.636	0.12	0.467	0.15	0.437	0.12	0.370	0.16		
	DG	0.579	0.12	0.417	0.12	0.386	0.12	0.297	0.14		
4	Cases	14		18		0		0		0	
	FS=2 N	0.211	0.21	0.280	0.12						
	G	0.349	0.18	0.377	0.21						
	DG	0.275	0.23	0.299	0.21						
5	Cases										
	FS=1 N										
	G										
	DG										

Dose component: ^aNeutrons, ^bPrompt gamma rays, ^cDelayed gamma rays.

HOUSE AND TERRAIN SHIELDING

Table 40. Mean Kerma Transmission Factors and Associated Fractional Standard Deviation for Floor Number 3 in the Six-house Cluster Relative to Free-field Kerma, Hiroshima at 1500 m

Group	Slant Penetration (SP) (M)									
	0 - 2		2 - 4		4 - 6		6 - 8		8 +	
	TF	FSD	TF	FSD	TF	FSD	TF	FSD	TF	FSD
1	Cases	6	4	3	0	0				
	FS=0 N ^a	0.626 0.05	0.517 0.05	0.472 0.06						
	US<3 G ^b	0.875 0.04	0.708 0.10	0.666 0.15						
	DG ^c	0.799 0.08	0.607 0.11	0.551 0.11						
2	Cases	5	1	8	6	2				
	FS=0 N	0.535 0.14	0.523	0.468 0.04	0.416 0.13	0.408 0.05				
	US>3 G	0.724 0.09	0.687	0.633 0.07	0.524 0.13	0.480 0.09				
	DG	0.652 0.16	0.589	0.536 0.06	0.429 0.20	0.402 0.11				
3	Cases	0	3	2	2	0				
	FS=5 N		0.394 0.02	0.425 0.03	0.438 0.03					
	G		0.383 0.05	0.520 0.03	0.395 0.03					
	DG		0.344 0.05	0.446 0.04	0.366 0.03					
4	Cases	6	0	0	0	0				
	FS=2 N	0.342 0.11								
	G	0.380 0.18								
	DG	0.324 0.15								
5	Cases									
	FS=1 N									
	G									
	DG									

Dose component: ^aNeutrons, ^bPrompt gamma rays, ^cDelayed gamma rays.

Table 41. Mean Transmission Factors and Associated Fractional Standard Deviation for Floor Number 1 in the Tenement Cluster Relative to Free-field Kerma, Hiroshima at 1500 m

Group	Slant Penetration (SP) (M)									
	0 - 2		2 - 4		4 - 6		6 - 8		8 +	
	TF	FSD	TF	FSD	TF	FSD	TF	FSD	TF	FSD
1	Cases	30	19	3	0	0				
	FS=0 N ^a	0.650 0.12	0.479 0.16	0.434 0.13						
	US<3 G ^b	0.862 0.09	0.635 0.20	0.530 0.15						
	DG ^c	0.807 0.10	0.571 0.18	0.457 0.13						
2	Cases	30	29	44	18	2				
	FS=0 N	0.518 0.11	0.439 0.18	0.431 0.10	0.401 0.08	0.439 0.09				
	US>3 G	0.702 0.12	0.607 0.20	0.534 0.12	0.477 0.11	0.574 0.04				
	DG	0.649 0.12	0.549 0.19	0.476 0.11	0.429 0.09	0.510 0.03				
3	Cases	19	6	2	0	0				
	FS=5 N	0.402 0.17	0.433 0.12	0.392 0.06						
	G	0.490 0.19	0.504 0.14	0.444 0.14						
	DG	0.468 0.20	0.486 0.14	0.414 0.16						
4	Cases	31	4	0	0	0				
	FS=2 N	0.395 0.14	0.341 0.05							
	G	0.530 0.23	0.329 0.04							
	DG	0.477 0.23	0.304 0.04							
5	Cases	31	16	4	0	0				
	FS=1 N	0.319 0.14	0.287 0.14	0.320 0.08						
	G	0.430 0.28	0.344 0.16	0.317 0.08						
	DG	0.367 0.29	0.277 0.17	0.281 0.06						

Dose component: ^aNeutrons, ^bPrompt gamma rays, ^cDelayed gamma rays.

HOUSE AND TERRAIN SHIELDING

Table 42. Mean Transmission Factors and Associated Fractional Standard Deviation for Floor Number 2 in the Tenement Cluster Relative to Free-field Kerma, Hiroshima at 1500 m

Group	Slant Penetration (SP) (M)									
	0 - 2		2 - 4		4 - 6		6 - 8		8 +	
	TF	FSD	TF	FSD	TF	FSD	TF	FSD	TF	FSD
1	Cases	20	10	6	0	0				
	FS=0 N ^a	0.531 0.23	0.425 0.18	0.366 0.21						
	US<3 G ^b	0.769 0.13	0.650 0.20	0.554 0.17						
	DG ^c	0.699 0.16	0.562 0.21	0.478 0.20						
2	Cases	10	25	38	24	7				
	FS=0 N	0.452 0.33	0.420 0.13	0.367 0.16	0.340 0.11	0.332 0.12				
	US>3 G	0.625 0.29	0.718 0.13	0.577 0.15	0.532 0.16	0.405 0.23				
	DG	0.549 0.30	0.625 0.18	0.489 0.17	0.442 0.15	0.353 0.20				
3	Cases	27	13	15	4	0				
	FS=5 N	0.329 0.14	0.325 0.12	0.250 0.13	0.303 0.11					
	G	0.493 0.17	0.425 0.18	0.416 0.08	0.336 0.15					
	DG	0.427 0.19	0.399 0.22	0.347 0.10	0.301 0.11					
4	Cases	10	10	0	0	0				
	FS=2 N	0.242 0.11	0.285 0.07							
	G	0.339 0.13	0.370 0.19							
	DG	0.297 0.18	0.327 0.14							
5	Cases	52	71	8	18	0				
	FS=1 N	0.250 0.12	0.281 0.15	0.268 0.14	0.279 0.13					
	G	0.384 0.23	0.431 0.22	0.438 0.13	0.450 0.15					
	DG	0.308 0.21	0.360 0.23	0.382 0.17	0.388 0.18					

Dose component: ^aNeutrons, ^bPrompt gamma rays, ^cDelayed gamma rays.

Table 43. Mean Transmission Factors and Associated Fractional Standard Deviation for Floor Number 3 in the Tenement Cluster Relative to Free-field Kerma, Hiroshima at 1500 m

Group	Slant Penetration (SP) (M)									
	0 - 2		2 - 4		4 - 6		6 - 8		8 +	
	TF	FSD	TF	FSD	TF	FSD	TF	FSD	TF	FSD
1	Cases	46	20	19	0	0				
	FS=0 N ^a	0.595 0.12	0.500 0.07	0.432 0.12						
	US<3 G ^b	0.794 0.13	0.707 0.09	0.569 0.13						
	DG ^c	0.749 0.11	0.598 0.07	0.493 0.10						
2	Cases	12	47	29	32	2				
	FS=0 N	0.548 0.11	0.500 0.10	0.481 0.08	0.434 0.08	0.447 0.02				
	US>3 G	0.714 0.15	0.625 0.11	0.627 0.12	0.540 0.12	0.489 0.01				
	DG	0.639 0.17	0.542 0.11	0.553 0.10	0.465 0.10	0.412 0.03				
3	Cases	5	8	1	0	0				
	FS=5 N	0.396 0.05	0.426 0.06	0.415						
	G	0.486 0.10	0.464 0.11	0.454						
	DG	0.407 0.06	0.409 0.08	0.428						
4	Cases	3	0	0	0	0				
	FS=2 N	0.385 0.03								
	G	0.402 0.08								
	DG	0.358 0.06								
5	Cases	15	45	20	0	0				
	FS=1 N	0.353 0.05	0.397 0.07	0.391 0.08						
	G	0.399 0.09	0.418 0.10	0.467 0.10						
	DG	0.336 0.08	0.367 0.10	0.419 0.08						

Dose component: ^aNeutrons, ^bPrompt gamma rays, ^cDelayed gamma rays.

HOUSE AND TERRAIN SHIELDING

Table 44. Mean Kerma Transmission Factors and Associated Fractional Standard Deviation for Floor Number 1 in the Combined Data Relative to Free-field Kerma, Hiroshima at 1500 m

Group		Slant Penetration (SP) (M)									
		0 - 2		2 - 4		4 - 6		6 - 8		8 +	
		TF	FSD	TF	FSD	TF	FSD	TF	FSD	TF	FSD
1	Cases	38		32		4		0		0	
	FS=0 N ^a	0.636	0.14	0.460	0.19	0.416	0.14				
	US<3 G ^b	0.853	0.11	0.633	0.20	0.513	0.15				
	DG ^c	0.793	0.12	0.555	0.19	0.447	0.12				
2	Cases	38		41		78		34		4	
	FS=0 D	0.521	0.14	0.429	0.18	0.402	0.14	0.378	0.11	0.408	0.14
	US>3 G	0.706	0.12	0.599	0.18	0.524	0.14	0.483	0.11	0.509	0.14
	DG	0.651	0.14	0.535	0.18	0.466	0.14	0.428	0.10	0.466	0.10
3	Cases	32		14		13		2		0	
	FS=5 N	0.401	0.15	0.398	0.13	0.339	0.09	0.364	0.001		
	G	0.509	0.19	0.490	0.17	0.418	0.09	0.286	0.003		
	DG	0.487	0.21	0.464	0.18	0.371	0.14	0.282	0.05		
4	Cases	55		9		3		0		0	
	FS=2 N	0.368	0.18	0.326	0.08	0.303	0.02				
	G	0.503	0.23	0.358	0.20	0.318	0.12				
	DG	0.441	0.24	0.315	0.18	0.260	0.11				
5	Cases	31		16		4		0		0	
	FS=1 N	0.319	0.14	0.287	0.14	0.320	0.08				
	G	0.430	0.28	0.344	0.17	0.317	0.08				
	DG	0.367	0.29	0.277	0.17	0.281	0.06				

Dose component: ^aNeutrons, ^bPrompt gamma rays, ^cDelayed gamma rays.

Table 45. Mean Kerma Transmission Factors and Associated Fractional Standard Deviation for Floor Number 2 in the Combined Data Relative to Free-field Kerma, Hiroshima at 1500 m

Group		Slant Penetration (SP) (M)									
		0 - 2		2 - 4		4 - 6		6 - 8		8 +	
		TF	FSD	TF	FSD	TF	FSD	TF	FSD	TF	FSD
1	Cases	27		17		10		0		0	
	FS=0 N ^a	0.536	0.22	0.402	0.19	0.363	0.18				
	US<3 G ^b	0.782	0.12	0.638	0.17	0.576	0.14				
	DG ^c	0.708	0.15	0.552	0.19	0.502	0.17				
2	Cases	16		28		56		42		14	
	FS=0 N	0.470	0.30	0.417	0.14	0.356	0.17	0.316	0.16	0.300	0.17
	US>3 G	0.647	0.24	0.710	0.14	0.564	0.16	0.507	0.17	0.409	0.20
	DG	0.578	0.26	0.615	0.18	0.481	0.18	0.428	0.16	0.346	0.20
3	Cases	34		15		26		10		0	
	FS=5 N	0.338	0.15	0.329	0.13	0.278	0.17	0.292	0.12		
	G	0.523	0.19	0.431	0.18	0.425	0.10	0.356	0.16		
	DG	0.458	0.22	0.401	0.21	0.363	0.12	0.299	0.13		
4	Cases	24		28		0		0		0	
	FS=2 N	0.224	0.18	0.282	0.10						
	G	0.345	0.16	0.375	0.20						
	DG	0.284	0.22	0.309	0.19						
5	Cases	54		71		8		18		0	
	FS=1 N	0.250	0.12	0.281	0.15	0.268	0.14	0.279	0.13		
	G	0.384	0.23	0.431	0.22	0.438	0.13	0.450	0.15		
	DG	0.308	0.21	0.360	0.23	0.382	0.17	0.388	0.18		

Dose component: ^aNeutrons, ^bPrompt gamma rays, ^cDelayed gamma rays.

Table 46. Mean Kerma Transmission Factors and Associated Fractional Standard Deviation for Floor Number 3 in the Combined Data Relative to Free-field Kerma, Hiroshima at 1500 m

Group	Slant Penetration (SP) (M)									
	0-2		2-4		4-6		6-8		8+	
	TF	FSD	TF	FSD	TF	FSD	TF	FSD	TF	FSD
1	Cases	52	24		22		0		0	
	FS=0 N ^a	0.578 0.11	0.503 0.07		0.437 0.12					
	US<3 G ^b	0.803 0.12	0.707 0.09		0.582 0.14					
	DG ^c	0.755 0.11	0.600 0.08		0.501 0.11					
2	Cases	17	48		37		38		4	
	FS=0 N	0.544 0.12	0.500 0.10		0.478 0.08		0.432 0.09		0.427 0.06	
	US>3 G	0.717 0.13	0.626 0.11		0.628 0.11		0.537 0.13		0.484 0.07	
	DG	0.643 0.16	0.543 0.11		0.549 0.09		0.460 0.12		0.407 0.08	
3	Cases	5	11		3		2		0	
	FS=5 N	0.396 0.05	0.418 0.06		0.421 0.03		0.438 0.03			
	G	0.486 0.10	0.442 0.13		0.498 0.07		0.395 0.03			
	DG	0.407 0.06	0.392 0.11		0.440 0.04		0.366 0.03			
4	Cases	9	0		0		0		0	
	FS=2 N	0.356 0.10								
	G	0.388 0.15								
	DG	0.336 0.13								
5	Cases	15	45		20		0		0	
	FS=1 N	0.353 0.05	0.397 0.07		0.391 0.08					
	G	0.399 0.09	0.418 0.10		0.467 0.10					
	DG	0.336 0.08	0.367 0.10		0.419 0.08					

Dose component: ^aNeutrons, ^bPrompt gamma rays, ^cDelayed gamma rays.

A comparison of TF averaged over all categories for each FN for the six-house cluster with the tenement cluster is shown in Table 47. The TF for the six-house and tenement clusters are consistent for a given floor. This indicates that shielding models derived from either cluster, given a sufficient number of data points, would not exhibit large differences when compared with the other cluster.

The tenement cluster data are examined and compared to the six-house cluster for each floor. Particular focus involves comparison of six-house data for FS = 2 with tenement data for FS = 1. The unique feature of the tenement houses is the common wall between each unit, permitting coding of FS = 1. In the preliminary DS84 dosimetry system, all nine-parameter situations with FS = 1 in tenement houses were calculated with the FS = 2 category.

Of the eighteen locations for which FN = 1 (single-story house) in the tenement cluster, eight are in the annexes (kitchen and bath) of tenement houses. The annexes were considered separate from the main two-story buildings as required by the nine-parameter coding rules. This partitioning is indicated by the Treatment of House (TH) parameter being equal to two. The TH parameter was coded along with the nine parameters and is used to record the way in which a structure was considered when coding the shielding parameters FS and LS. The shielding of one part of an extended structure was sometimes accounted for by dividing the structure into conceptually separate units. The parameter TH is 1 when a building is considered as one unit; is 2 when it is considered as two units; is 3 when considered as three or more units; and is 9 when unknown. The tenement house TF for FS = 2, and SP = 0 to

Table 47. Comparison of Kerma Transmission Factors for Six-house and Tenement Clusters Relative to Free-field Kerma, Hiroshima at 1500 m

	All Cases		FN = 1		FN = 2		FN = 3	
	6H	TEN	6H	TEN	6H	TEN	6H	TEN
Number	336	960	160	288	128	368	48	304
Neutrons								
Minimum	.174	.204	.231	.248	.174	.204	.308	.331
Maximum	.745	.783	.745	.783	.691	.746	.664	.728
Average	.374	.404	.385	.436	.324	.326	.468	.468
FSD	28%	29%	24%	26%	31%	29%	19%	18%
Prompt Gamma rays								
Minimum	.257	.222	.279	.222	.257	.252	.308	.332
Maximum	.986	.990	.986	.990	.932	.913	.932	.978
Average	.526	.545	.526	.564	.498	.496	.600	.585
FSD	28%	29%	26%	30%	30%	30%	28%	25%
Delayed Gamma rays								
Minimum	.193	.187	.229	.187	.193	.207	.261	.297
Maximum	.908	.940	.908	.940	.839	.859	.894	.893
Average	.458	.480	.464	.511	.427	.424	.521	.518
FSD	31%	32%	28%	32%	34%	33%	31%	27%

2, is higher than in the similar category for the six-house cluster. This is probably due to the smaller size of the annex and the smaller size of the adjacent shield (the other annex) than for the House A (single story, stand alone) situation in the six-house cluster. This result may warrant creating a new category when $TH \geq 2$, but additional data are required before a decision can be reached. For the FN = 1 cases, the six-house FS = 2 and tenement FS = 1 averages fall within one standard deviation of each other, but the tenement TF is consistently smaller. This is probably because of the close proximity (to the annex) of the large two-story common wall shield.

When FN = 2, the subject is on the first floor of a two-story house. Here the comparison of FS = 2 for the six-house and FS = 1 for the tenement cluster shows the reverse of FN = 1 results, because of the single wall thickness for the common wall and the smaller house size in the tenement situation. The tenement categories for FN = 2, FS = 1, SP = 0 to 2, and SP = 2 to 4 have 52 and 71 cases, respectively, yet the FSD for gamma rays is over 20%. This is due to the large variation in actual situations that fall within these categories. For $SP \leq 2$, the minimum (0.252) and maximum (0.548) values for prompt gamma rays occur at 3TA/157.5° and 3TC/180°, respectively; for SP = 2 to 4, the minimum (0.267) and maximum (0.685) occur at 3TD/202.5° and 3TD/45°, respectively. These locations and orientations exhibit diverse shielding situations that are undifferentiated in both our selected parameter model and in the full nine-parameter specification. From this standpoint alone, the separation of FS = 2 and FS = 1 seems warranted.

When FN = 3, the subject is on the second floor of a two-story house. TF for FN = 3 are higher than those for FN = 1, because FN = 1 cases are shielded in some instances by two-story houses that may not be close enough to appear in the nine-parameter data. Thus, averages over a series of locations for FN = 1 that fall into apparently unshielded categories

Table 48. Fractional Standard Deviations by Shielding Group for Kerma Transmission Factors of Prompt Gamma-Rays Relative to the Free-field Kerma, Hiroshima at 1500 m

Shielding Group		Combined Data		
		Floor Number		
		1	2	3
1	FS = 0 US = 3	0.22	0.19	0.17
2	FS = 0 US = 3	0.20	0.23	0.15
3	FS = 5	0.20	0.21	0.13
4	FS = 2	0.26	0.19	0.15
5	FS = 1	0.28	0.22	0.12

have implicit shielding from other houses in the cluster.

Table 48 presents the marginal FSD for prompt gamma rays for each of the five groups in which the data over all SP values have been averaged. Using (1) Table 48; (2) the FSD values in Table 47 for all cases averaged together and for each FN averaged together; and (3) the FSD values in Tables 44 to 46 for individual group/SP categories, construct the following table is constructed:

Typical FSD for Gamma-Ray Transmission

All cases combined	30%
By floor number	28%
By group	20%
By category	15-20%

This table shows that by partitioning the shielding cases into categories based on a nine-parameter subset, the FSD inherent in the variability of the shielding can be reduced from the 30% to the 20% range. Furthermore, since some categories have large FSD, due to their potential for a wider range of variation while others are smaller, this partitioning permits better estimates of the uncertainty of dose estimates for those subjects whose situations are identified using the nine parameters.

Note further that the uncertainty due to locating the survivor embodied in the use of nine parameters is larger than the estimated uncertainty from the house materials ($\approx 10\%$) and the Monte Carlo calculation statistical uncertainty ($\approx 5\%$).

Recommended Nine Parameter Model for the Dosimetry System

Analysis shows that, within the constraint to use only the available computerized nine-parameter data for survivors in typical Japanese houses, the shielding can be calculated to within about 20% uncertainty. This uncertainty arises from the imprecision of the nine-

parameter information in specifying the survivor's location with respect to factors impacting his shielding. It is expected that precise, state-of-the-art calculations for a set of actual survivor situations that happen to have the same nine parameters would exhibit variations of about 10 to 20%.

The partitioning of nine-parameter space into a set of categories that differentiate shielding effects appears to be a reasonable representation of this variation. There does not seem to be a basis to prefer or select one individual location or orientation from a category as indicative of all cases falling within the bounds of the category. Thus, the procedure is to form one leakage tape for each category in Tables 38 to 46 by averaging together all the cases from the data base from the six-house and tenement clusters that fall into that category. For example, the 78 cases that fall into group 2 with SP in the range 4 to 6 for FN = 1 (Table 44) are averaged together to form one leakage tape for the dosimetry system. The house shielding computations for survivors in the RERF data base whose nine parameters are in this category are performed by the dosimetry system with this averaged leakage tape. The uncertainty in calculating the shielding for this survivor is estimated by the FSD value for the category (in this example, 14% for neutron shielding).

The best verification of this nine-parameter model would be to perform shielding calculations of actual survivor configurations in state-of-the-art detail and to compare them with results from the dosimetry system model. These "benchmark" computations would indicate the presence of bias in the dosimetry system models and show whether or not the uncertainty estimates are realistic. House clusters should be selected for the benchmark calculations that have as many survivors as possible, since most of the effort in performing these calculations is producing the geometry model of the cluster.

Particle Leakage Tape for the Nine-Parameter Categories

The dosimetry system model requires particle leakage tapes for each of the categories in Tables 44 to 46. They are produced by combining leakage tapes from the detector locations for all the detector and orientation combinations in a given category. The number of combinations available for each category is given in these tables. The leakage tape for a given detector location is preprocessed to rotate all the particle directions to the required orientation prior to combining with other tapes. The combined leakage tape with leakage histories for the various detectors (at various orientations) is used in the dosimetry system in the same manner as a leakage tape for a single location except that orientation is no longer a parameter and results are not for a detector location but are for a nine-parameter category.

Since each primary leakage tape has 15 batches with 3,000 histories per batch, a combined tape may have a million histories, far more than needed to generate useful dose estimates. Because the time for calculation of the dose to an organ is directly proportional to the number of leakage histories, it was necessary to reduce the number on the combined tape.

One method for reducing the number, random rejection of histories with a corresponding increase in the weight of the histories surviving, would result in an unbiased dose estimate with the statistical uncertainty in the dose increasing by the square root of the reduction factor. However, one can make use of knowledge about how the average leakage tapes are coupled in the dosimetry system at a single implied orientation. Since the fluence contributing most to the dose arrives from the direction of the burst point, a direction-biasing method

was used that rejects particles that leak in directions where there is only a small amount of incident radiation in favor of those that leak in the burst point direction. Also, the maximum angle above the horizon from which particles arrive was chosen to be about 21.1° , changing slightly at different ranges and for different types and energies of radiation. The effect of these changes on the fluences was minor compared to the tremendous improvement in calculational uncertainty. With this biased reduction method, the number of leaking particles in each tape is around 75,000.

At all the ranges and cities, reducing the number of Monte Carlo histories required by introducing the directional bias in the selection gave improved statistics. The calculational efficiency for neutrons and gamma rays was about three times better. Calculations of gamma rays produced in the houses by neutrons, however, had only a slight improvement in efficiency. Furthermore, using the angle-differential fluence produced inside a house by this method results in significant uncertainty reduction when that fluence is coupled with the calculations for a phantom (Chapter 8). The reduction comes about because the fluences in the house have less statistical uncertainty in the directions that contribute most to the dose. The Monte Carlo statistical uncertainty in the coupling calculation is still much less than the other uncertainties associated with the calculation of house shielding.

SHIELDING MODEL FOR GLOBE DATA BASE SUBJECTS

The computerized data bases at RERF that provide survivor shielding information consist of the nine-parameter data and the globe data. Research to develop models to provide radiation fields for survivors who have globe data is described below. The globe data are available for about 20% of those proximally exposed and were used primarily for survivors in the open but shielded by houses or terrain.

Globe Data Base Description

The detailed description of the globe technique for calculating TF, given in Appendix 7-2, indicates how the globe data were derived from the shielding histories and how they were applied in the T65D dosimetry system for the calculation of TF. A summary of the globe technique and the globe data base is provided here to explain how the revised dosimetry system will calculate the radiation fields for survivors whose shielding is described by this technique.

The globe technique was developed prior to the BREN house shielding experiments in Nevada and the subsequent development of the nine-parameter technique for describing the shielding for survivors in Japanese houses. The development of the nine-parameter procedure resulted from the difficulty in using the globe technique for a large number of different situations arising from the house shielding. Strict application of the globe technique would have required scale models of each survivor's house and neighboring shielding to derive the globe parameters. In the final T65D system, however, the globe method was applied to three broad classes of survivors:

1. Survivors in the open shielded by Japanese houses.
2. Survivors in the open shielded by terrain features.
3. Survivors heavily shielded by concrete buildings.

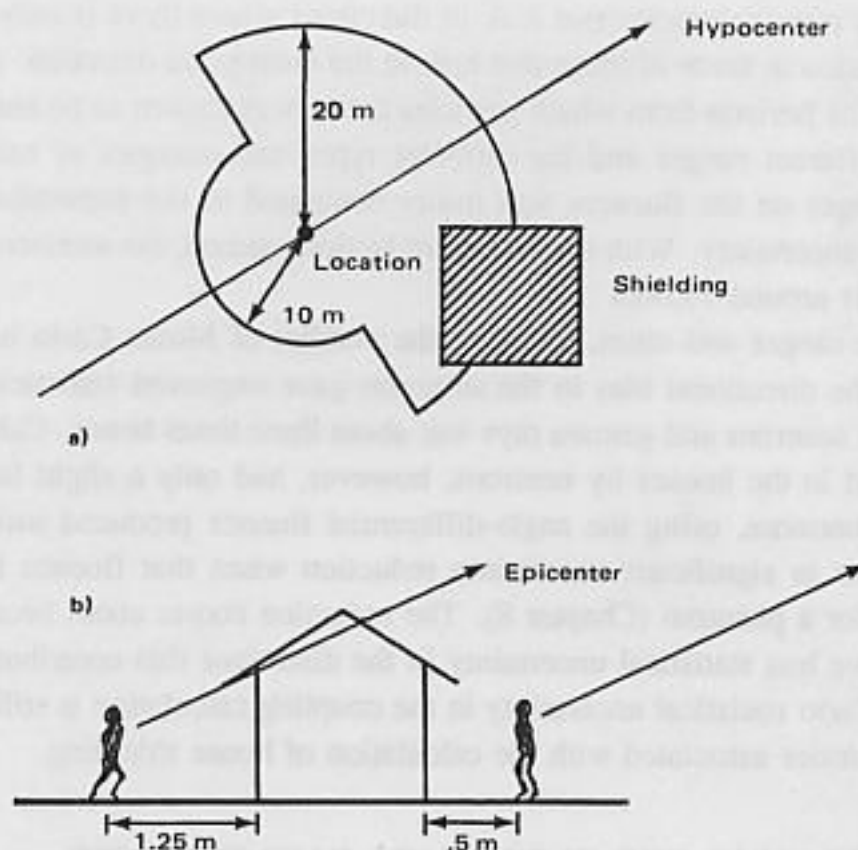


Figure 33. Depiction of conditions for globe cases. a) Shielding must be within 20 m in front or 10 m in back of location. b) Survivor must be more than 1.25 m from the front shielding or 0.5 m from the back shielding. Not shown the distance to the shielding object must be less than three times the height of the shield.

Of the approximately 4,500 survivors for whom the globe technique was used, 73% were in Hiroshima. Only 12% were located less than 1000 m from the hypocenter while 50% were located 1500 m or beyond. Furthermore, 84% were shielded by Japanese houses while just 8% were terrain shielded. All of those shielded by terrain were in Nagasaki and 77% of them were located beyond 1500 m from the hypocenter.

The development of the model in the revised dosimetry system to account for shielding for those survivors with globe data in the "open shielded by Japanese houses" and in the "open shielded by terrain features" categories is discussed. To qualify for the first category, the survivor must have been outside, with shielding present within 20 m in front or 10 m in back as shown in Figure 33. The shield height must have been at least one-third of the distance from the survivor to the shield. If the survivor was too close to the shielding house (less than 1.25 m in front or 0.5 m in back), as shown in Figure 33, his shielding assessment was performed with the nine-parameter method.

Unfortunately, the computerized globe data does not contain any information as to whether a survivor in the terrain-shielded class was also shielded by a house. The globe shielding description for a survivor inside a house and shielded by terrain does not reflect the additional shielding provided by the roof and walls of the house. This is also true for a survivor outside and shielded by terrain yet near a house. Given these caveats, it should

be mentioned that the number of survivors in such situations is small. However, since the actual shield configuration is recorded in the survivor shielding files, new data could be retrieved and codified to account for such shielding. The modular architecture of the new dosimetry system could be modified easily to improve the dosimetry for those survivors in such situations.

The globe data give the fraction of the incident radiation directed at a survivor's location that is shielded; that is, the fraction of the 4π solid angle subtended by some object such as parts of a Japanese house or a hill. Imagine a unit sphere with its polar axis the line between the survivor and the bomb burst point. This unit sphere is then partitioned into 18 latitudes (polar angle intervals) of 10° separation. Now depress the horizontal plane containing the center of the unit sphere 4° in the vertical plane containing the polar axis. All points on this sphere above this depressed plane are called above the horizon; all points below, are called below the horizon. The globe data consists of 36 numbers that give the fraction of the polar space above and below the horizon, respectively, that is blocked in each of the polar intervals. Note that, depending on the angle of the source-detector axis (which is ground-range dependent), the first few polar intervals may lie completely above the horizon and the last few polar intervals may lie completely below the horizon. Since the globe data are dependent on the ground range and the height of the burst, identical locations at different ground ranges in either city will result in different globe parameters. Additional data given in the globe data file for survivors in the open and shielded by Japanese houses, such as the distance, in the front or the back, to the house was useful in deriving the shielding model for the new dosimetry system.

One of the major drawbacks of the globe data for deriving detailed radiation fields for shielded survivors is the lack of azimuthal information concerning the solid angle blocked. Thus, a person standing near a corner of the house such that the space blocked and unblocked divides vertically may have globe parameters similar to those of a person shielded horizontally by a single-story house. Although the globe data may be similar in these two cases, the TF and kermas may be quite different. Furthermore, there is no accounting for the depth of the shielding. A survivor in front of a row of two-story houses may have the same globe parameters as a survivor who stands in front of a single two-story house.

Objectives of the Globe Data Model

There are several objectives for the model for survivors having globe data for their shielding descriptions. The primary objective, of course, is to exploit the available computerized data to its fullest but to consider carefully the inherent errors and biases in the data base. Quantification of the precision or bias in the resulting model for the revised dosimetry system can be achieved by making detailed state-of-the-art calculations for survivor situations that have globe data and comparing the results to those generated by the model used in the dosimetry system. Another primary objective is to assure consistency in the treatment of survivors with globe data with other shielding descriptions, notably the nine-parameter technique. The T65D system has a marked inconsistency in the TF derived from the nine-parameter and globe techniques. This is not surprising, since the nine-parameter and globe techniques were derived using different bases and different approaches. In the revised dosimetry system consistency is maintained by using the same techniques and data

in deriving the radiation fields at the survivors locations.

Development of the Model for Globe Data Survivors

A data base was generated for the analysis of potential techniques for using globe information in the revised dosimetry system. This data base consisted of a series of 26 calculations for street locations in the six-house cluster and 10 calculations for locations near a modeled hill. The street locations were chosen to provide a variety of different situations encountered in the actual shielding histories in Hiroshima and Nagasaki. The street locations for which calculations were made are shown in Figure 4, and the terrain locations are shown in Figure 34. In addition, other calculations were made for locations at various distances away from a two-story house (house B model) to examine globe data for a single house. The additional points are identical to the points representing the sweep across the street in front of house 5B in the six-house cluster. Modifications were made to the standard adjoint Monte Carlo shielding analysis procedure to permit calculation of the globe data for each of the survivor locations, ground ranges, and orientations chosen for examination. This modification consisted of writing an additional file that gives the starting direction cosines for each Monte Carlo adjoint history and indicates whether this source direction is blocked or unblocked. The source location is blocked if, on extension of the ray to the cluster boundary, it encounters a wall, roof, or hill. It is unblocked if it encounters only air on its way to the boundary. A code was written to use this information to calculate the globe parameters.

The adjoint transport calculations were carried out for each of the locations specified in Figures 4 and 34 and for those near the single house using the same radiation transport codes that were used in generating the nine-parameter models. The leakage tapes obtained from the adjoint transport calculations were then folded with the free-in-air fields for a series of ground ranges and cluster orientations to generate a data base of TF for neutrons, prompt gamma rays, delayed gamma rays, and secondary gamma rays induced by neutrons in the house and ground. As in the nine-parameter model development, kerma TF were used to study the shielding variation with globe data. The ground ranges and orientations used in the calculations are given in Table 49. Overall, the data base consisted of 2,304 different ($36 \text{ locations} \times 4 \text{ ground ranges} \times 8 \text{ orientations} \times 2 \text{ cities}$).

Since the globe data can be calculated for each ground range and orientation, the model development consisted of heuristic examination of various methods to manipulate the free-field and shielded-field information to exhibit consistency and provide reduced variation in the TF as functionals of the globe parameters.

The simplest and most straightforward approach (the "direct" method) would be to construct the energy- and angle-differential fluence for the shielded field from incident fluences lying within the polar angle intervals of the globe analysis. Although conceptually simple, this method has potential drawbacks. Although the incident radiation is forward peaked along the line of sight from the bomb, the contribution from multi-scattered neutrons and gamma rays is important. Thus, some of the shielded radiation field in any angular interval is unrelated to the free field in the same interval. Additional complications arise because the lack of azimuthal information in the globe data forces assumptions about the azimuthal distribution of the blocked portion in any polar interval. Additionally, the direct method may introduce inconsistencies with the techniques used in the nine-parameter models because the

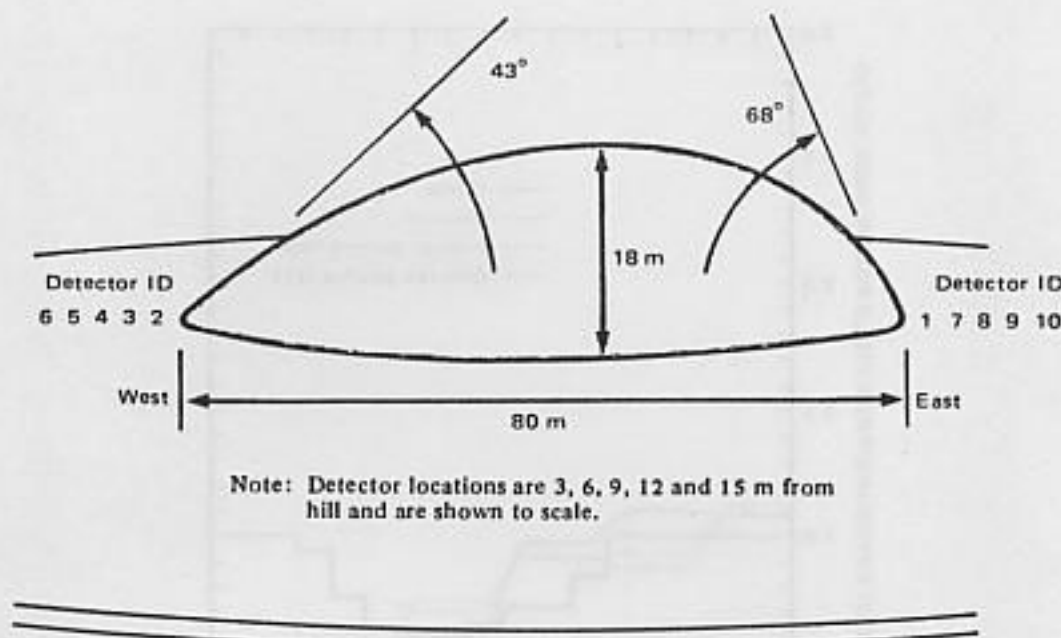


Figure 34. Terrain model and location of detectors for globe shielding study

Table 49. Ground Ranges and Orientations in the Data Base for the Globe Analysis

Ground Range	Orientation (Direction to Burst)
700 m	0° (West)
1000	45°
1500	90° (South)
2000	135°
	180° (East)
	225°
	270° (North)
	315°

direct method would provide a shielded field "artificially" constructed, not based on transport calculations for given situations.

Nevertheless, an examination of the direct method was made by calculating the ratio of the kerma produced by the radiation actually in a globe polar bin to the kerma produced by the radiation in that bin in the free field (a very specific, angular dependent TF) and comparing it to the unblocked fraction given by the globe technique. Plots of these factors are presented for selected cases in Figures 35 to 40. The curve labeled "globe" is the unblocked fraction from the special data saved in the Monte Carlo run. The curves labeled neutron, prompt gamma, and delayed gamma are the values:

$$\frac{\text{kerma due to shielded radiation in a globe bin}}{\text{kerma due to free field in the same globe bin}} \times \frac{1}{\text{TF}} \quad (2)$$

where TF is the kerma TF for the entire 4π -field and is used to normalize the values for plotting purposes. In analyzing these plots, only the relative variation between the globe

HOUSE AND TERRAIN SHIELDING

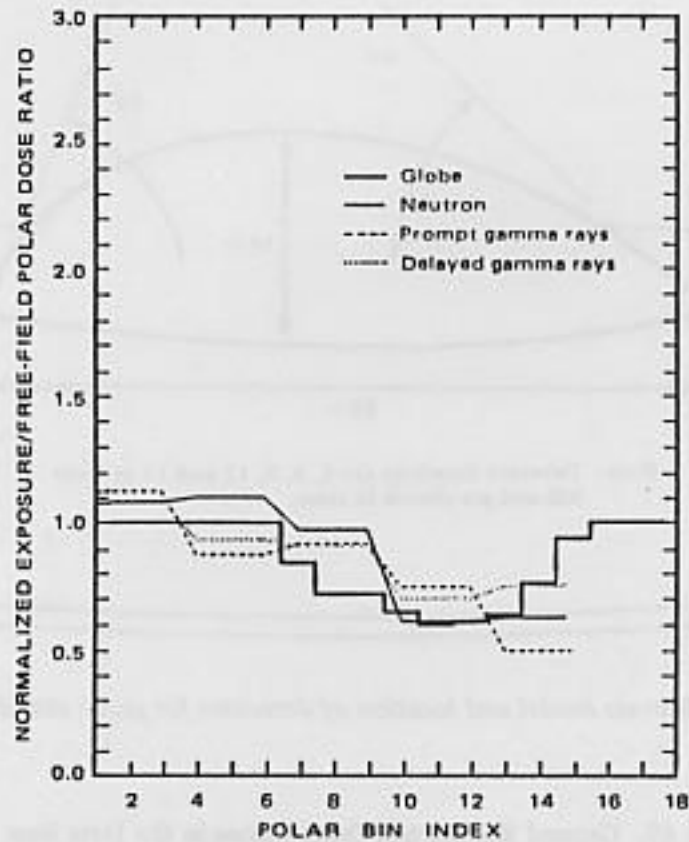


Figure 35. Polar dependent transmission factors for a location shielded from the back, Hiroshima, 700 m

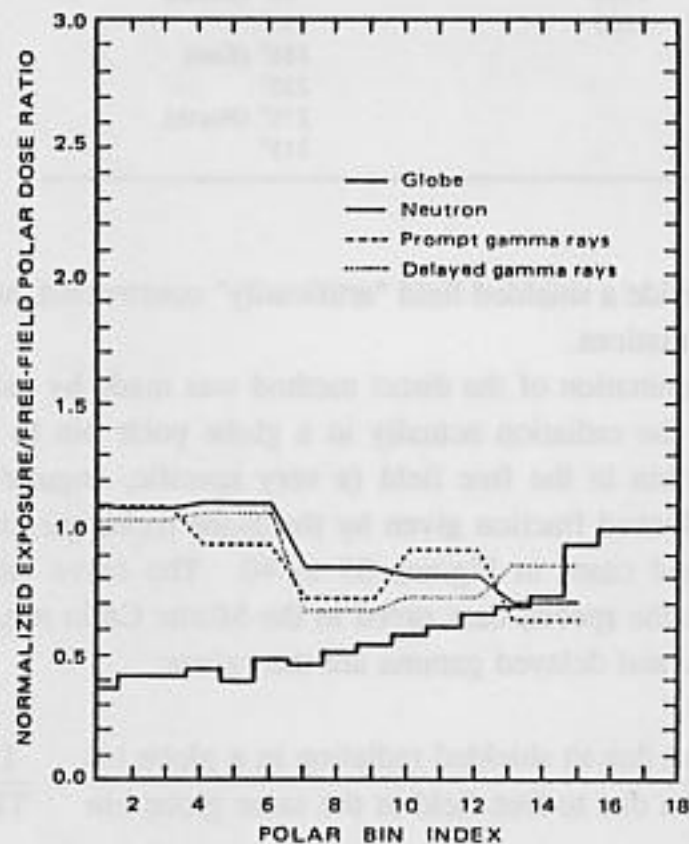


Figure 36. Polar dependent transmission factors for a location shielded from the front, Hiroshima 700 m

HOUSE AND TERRAIN SHIELDING

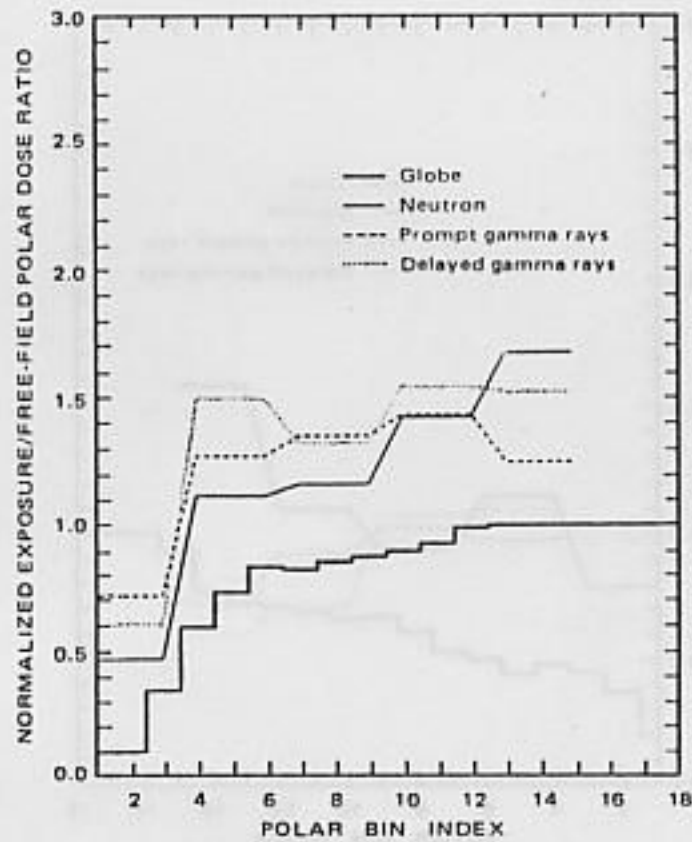


Figure 37. Polar dependent transmission factors for a location shielded from the front, Hiroshima 700 m

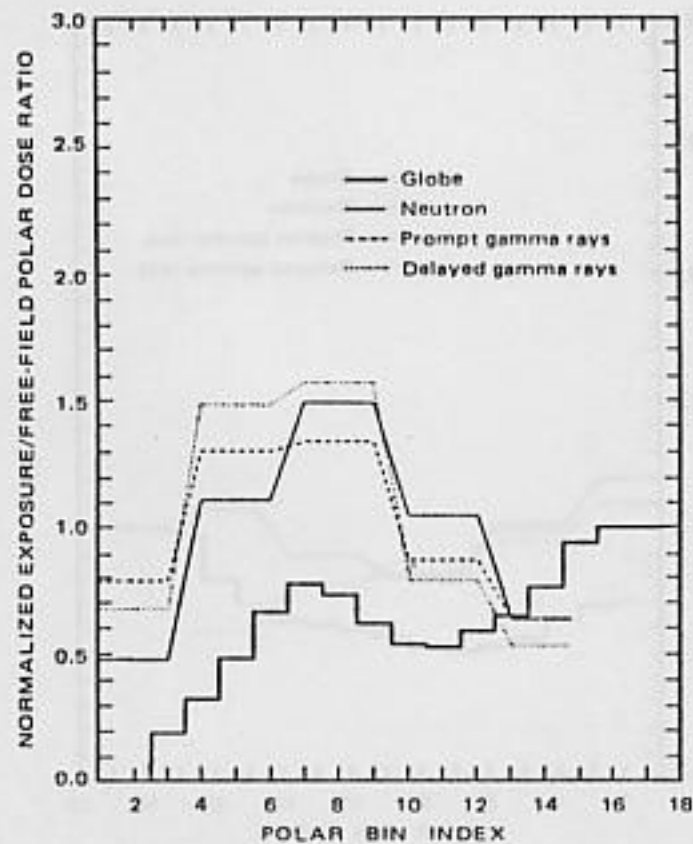


Figure 38. Polar dependent transmission factors for a location shielded from the front and back, Hiroshima, 700 m

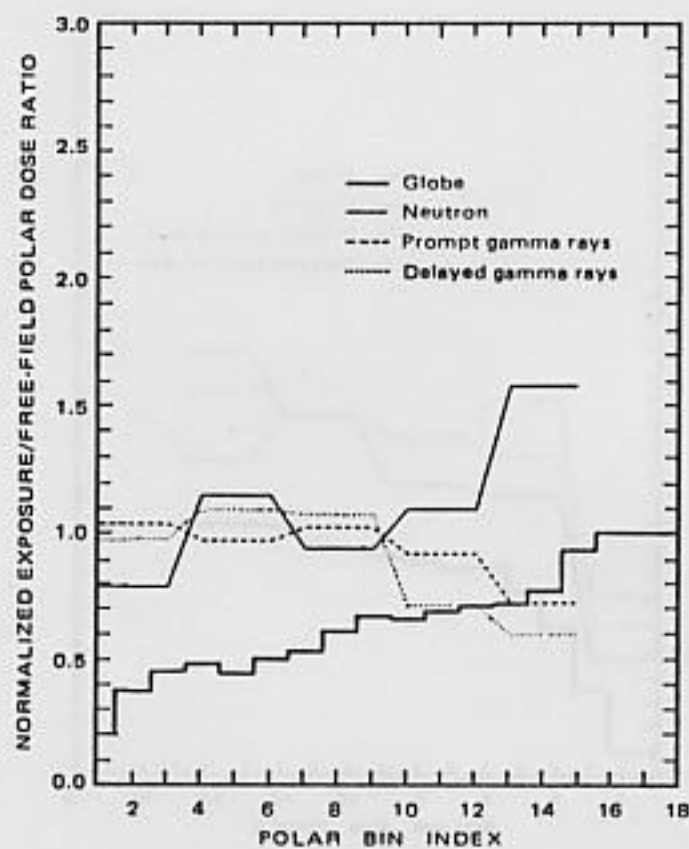


Figure 39. Polar dependent transmission factors for a location shielded from the front and back, Hiroshima, 700 m

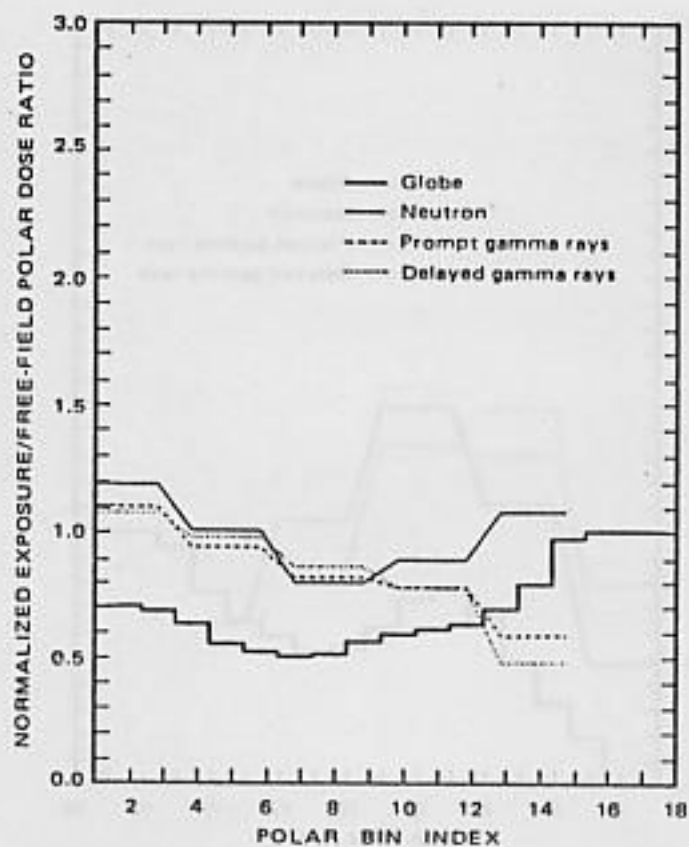


Figure 40. Polar dependent transmission factors for a location shielded from the side, Hiroshima, 700 m

data and the actual relative TF are important; the difference in magnitude between data in different figures is irrelevant to the discussion at hand.

If the relative variation between the actual ratio and the unblocked fraction were constant, or nearly so, the direct method would be a potential candidate for the revised dosimetry system. Figures 35 and 36 show the comparison for the survivor in the open blocked by a single house. For this situation, the correlation appears to be reasonably good only for the back-shielded situation shown in Figure 35. The front-shielded situation of Figure 36 is highly noncorrelated because of the scattering of the azimuthally asymmetric shield presented house 5B at this orientation. Figures 37 to 39 are situations in which survivors were in streets surrounded by several houses. The poor correlation is primarily due to back-scatter and side-scatter from houses, not accounted for in the globe parameters.

The approach of choice is an indirect or inferred method that uses the globe data to infer a position from a series of street (terrain) positions. The radiation field of the survivor is then calculated using the leakage tape from the shielding calculation for this position in a method similar to the procedure for survivors assigned nine parameters. The problem then involves derivation of the functionals on the globe data that best characterize these positions. Several approaches were tried; the one that gave the best results used the "neutron free-field weighted unblocked fraction", denoted here by WUBF. The WUBF is defined by the equation:

$$WUBF = \frac{\sum_i \{ \Phi_i^A \Delta\Omega_i^A (1 - B_i^A) + \Phi_i^B \Delta\Omega_i^B (1 - B_i^B) \}}{\sum_i \{ \Phi_i^A \Delta\Omega_i^A + \Phi_i^B \Delta\Omega_i^B \}} \quad (3)$$

where the superscripts A and B indicate the portion above or below the depressed globe horizon and

- Φ_i = the free-field neutron fluence in the globe polar interval i ,
- $\Delta\Omega_i$ = the fraction of the solid angle in polar interval i , and
- B_i = the blocked fraction in polar interval i .

The neutron and gamma-ray TF computed for each of the ground ranges and orientations were plotted against the WUBF to ascertain if there were a consistent trend in the variation of TF with WUBF. Some of the results are shown in Figures 41 to 46 for the house shielding cases and in Figure 47 for the terrain shielding (only Nagasaki is shown for the terrain shielding because there were no survivors with globe data due to terrain in Hiroshima). These figures show the TF for neutrons, prompt gamma rays, and delayed gamma rays at selected ground ranges. The solid line is the linear regression representing the best fit to the data, while the dashed lines represent lines with 15% larger and 15% lower slopes than the regression line. The plots exhibit the fact that most of the TF fall within $\pm 15\%$ of the regression of TF versus WUBF. The regression curves only serve to guide the eye in examining the data. They are not meant to represent, in any way, models for globe shielding.

Initial efforts at selecting a variable to correlate with the individual TF focused on a gamma-ray weighting scheme because the gamma rays are the most important (in producing dose) component of the free field at the ground ranges of interest. However, the globe data,

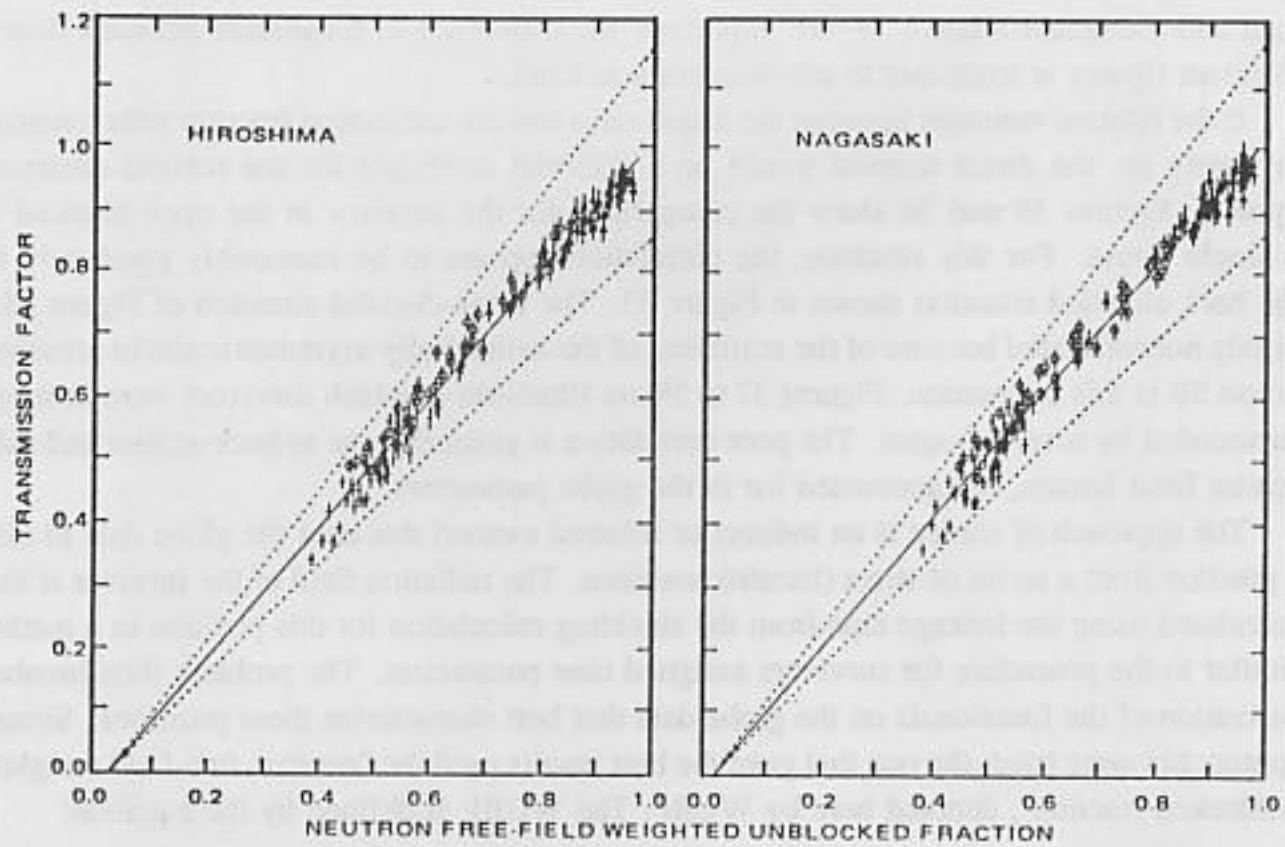


Figure 41. Transmission factors for prompt neutrons vs WUBF for all front- and back-shielded categories, Hiroshima and Nagasaki, 700 m

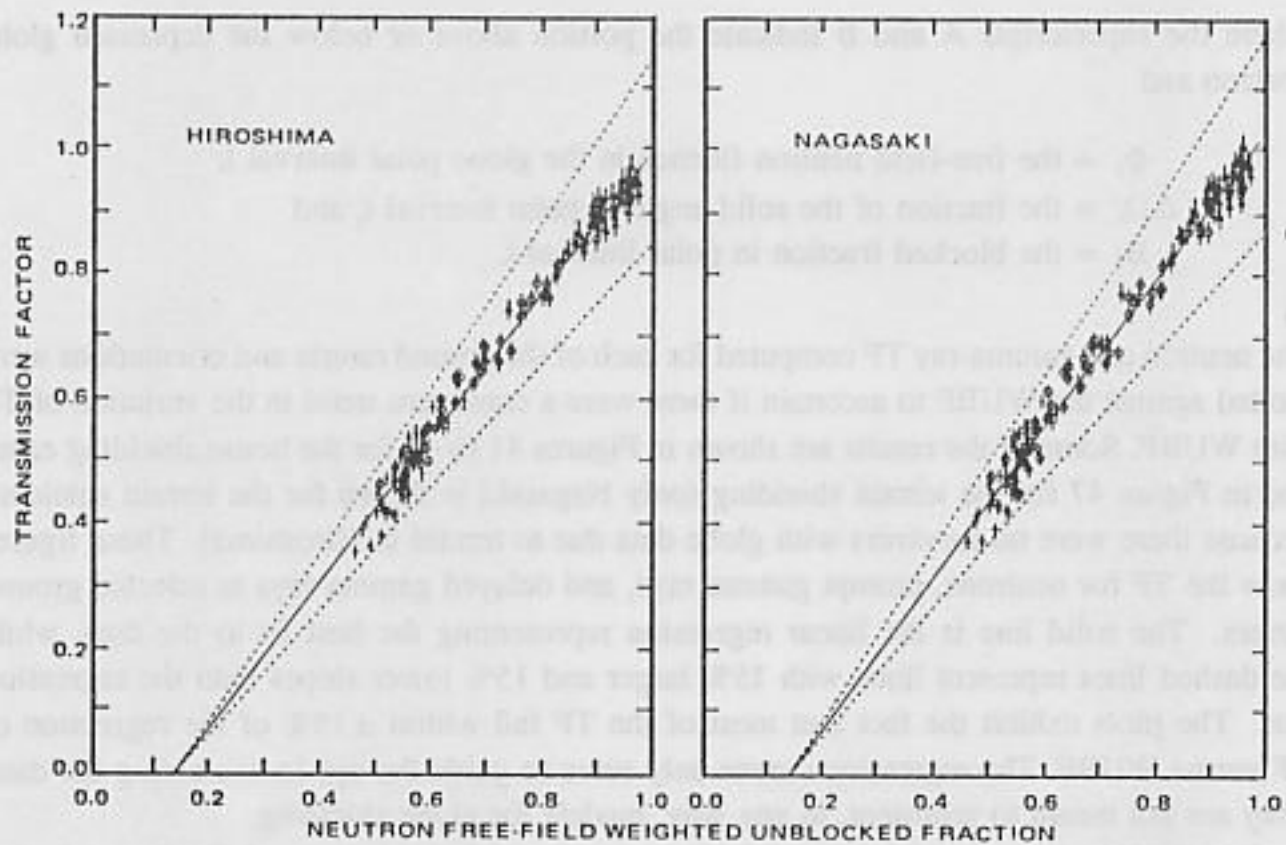


Figure 42. Transmission factors for prompt neutrons vs WUBF for all front- and back-shielded categories, Hiroshima and Nagasaki, 1500 m

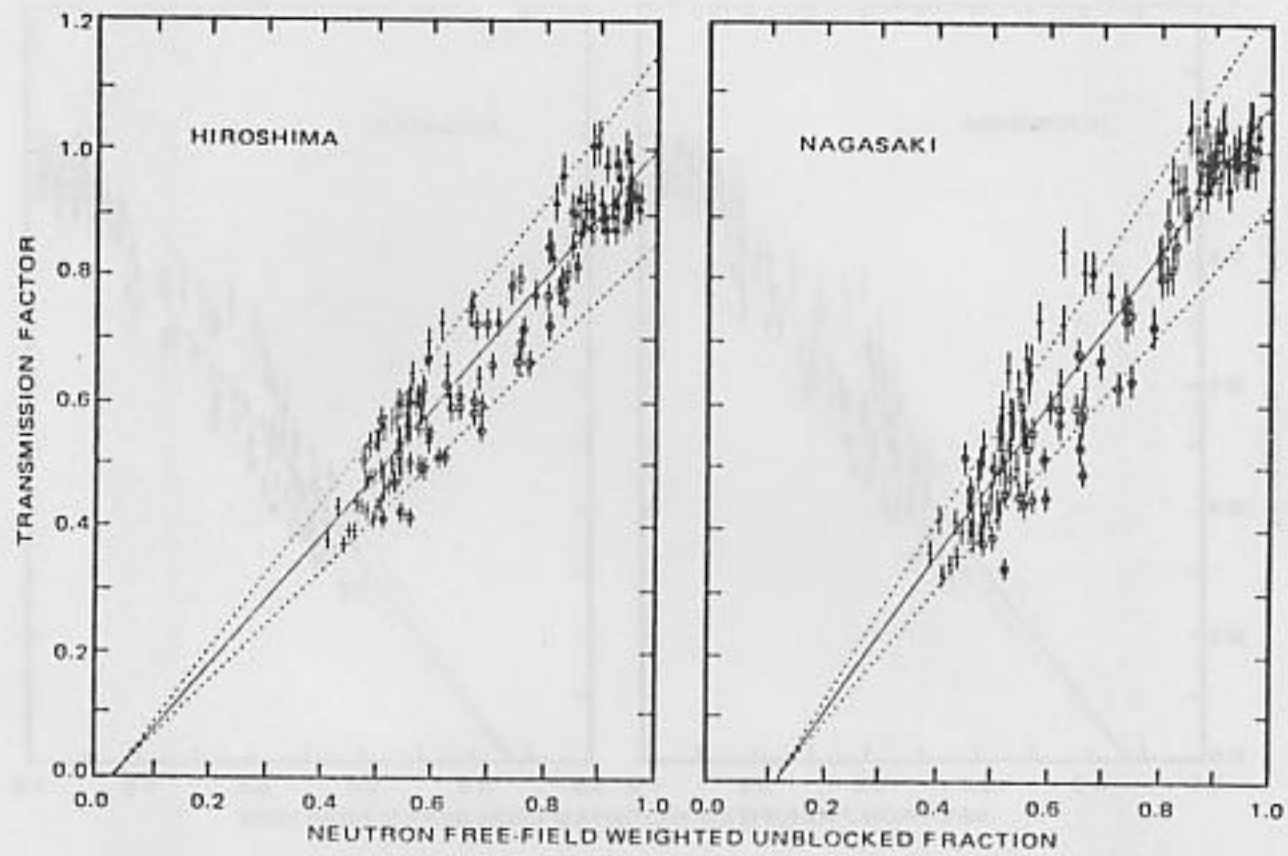


Figure 43. Transmission factors for prompt gamma rays vs WUBF for all front- and back-shielded categories, Hiroshima and Nagasaki, 700 m

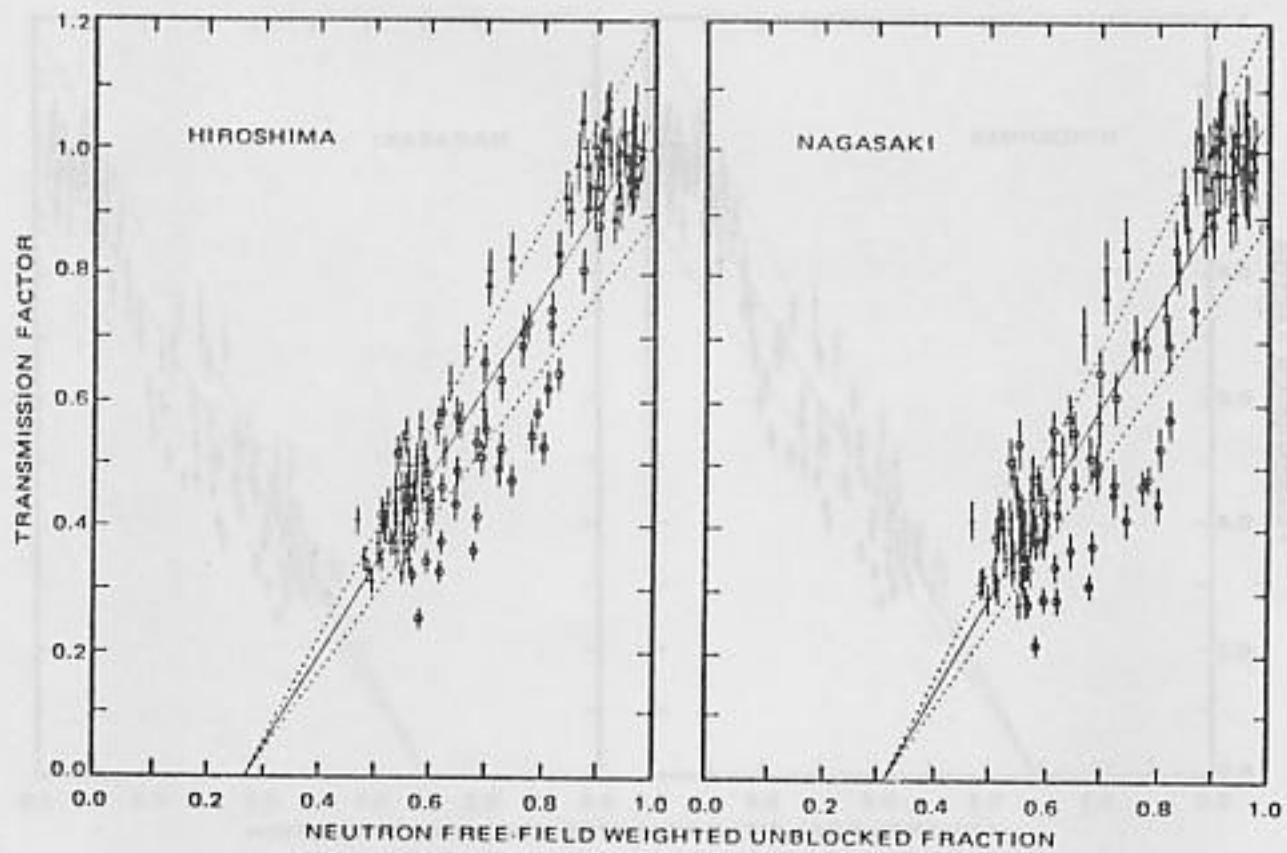


Figure 44. Transmission factors for prompt gamma rays vs WUBF for all front- and back-shielded categories, Hiroshima and Nagasaki, 1500 m

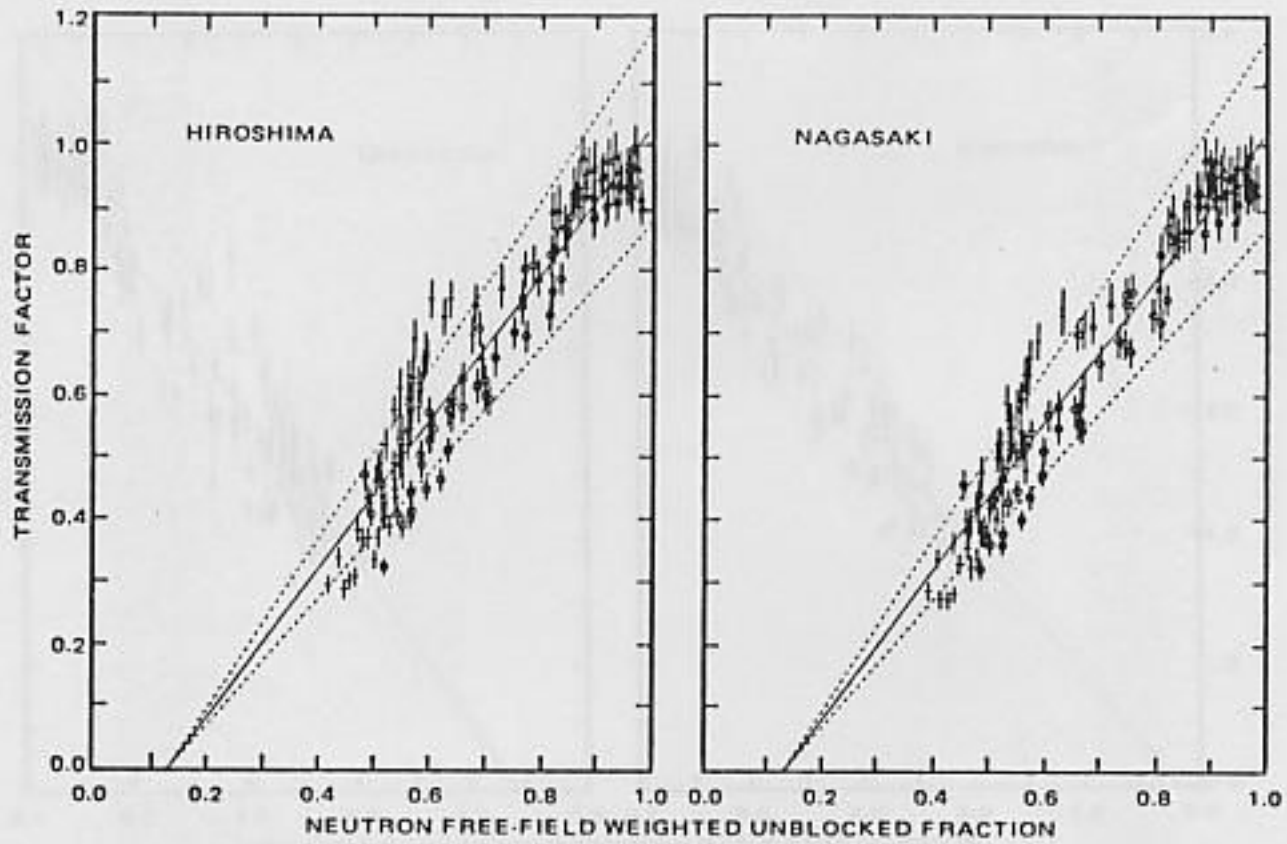


Figure 45. Transmission factors for delayed gamma rays vs WUBF for all front- and back-shielded categories, Hiroshima and Nagasaki, 700 m

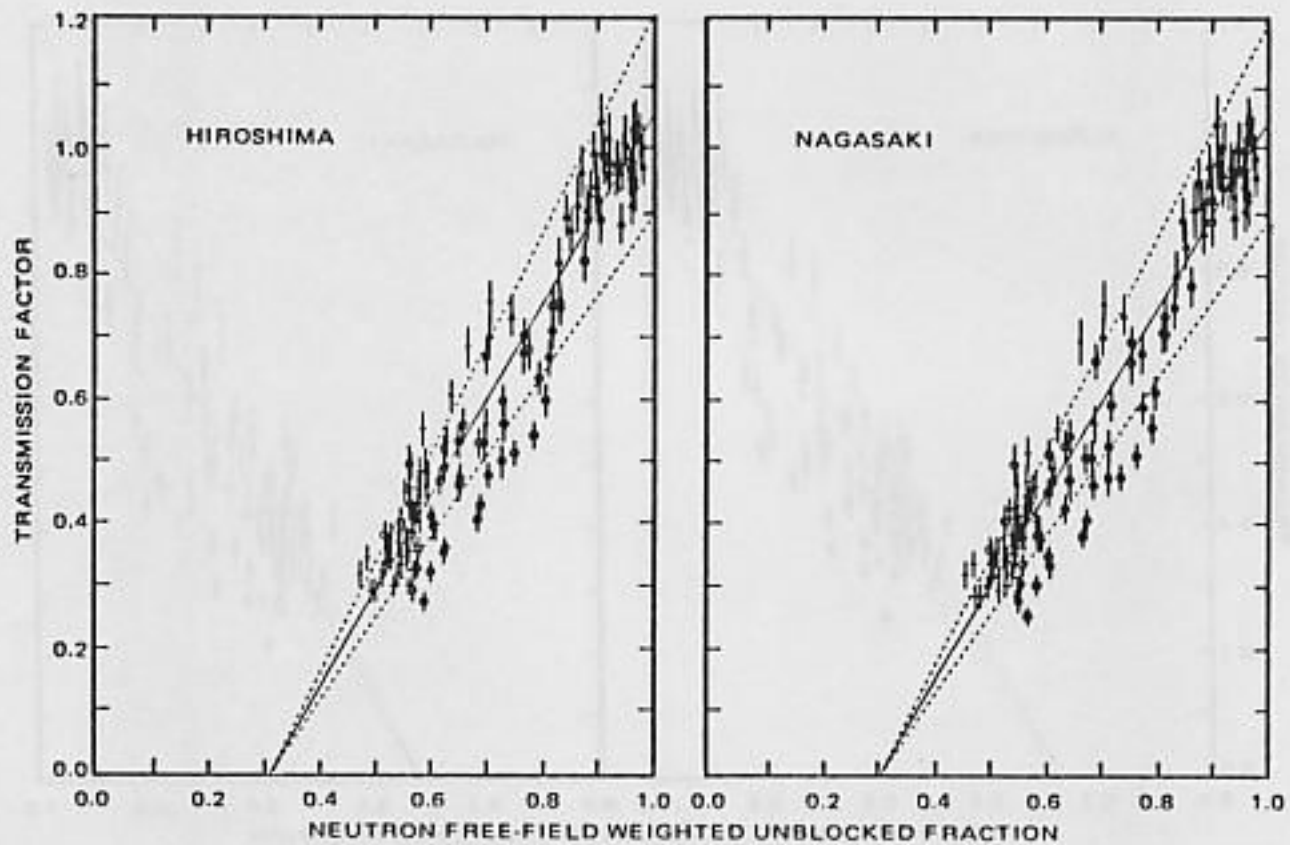


Figure 46. Transmission factors for delayed gamma rays vs WUBF for all front- and back-shielded categories, Hiroshima and Nagasaki, 1500 m

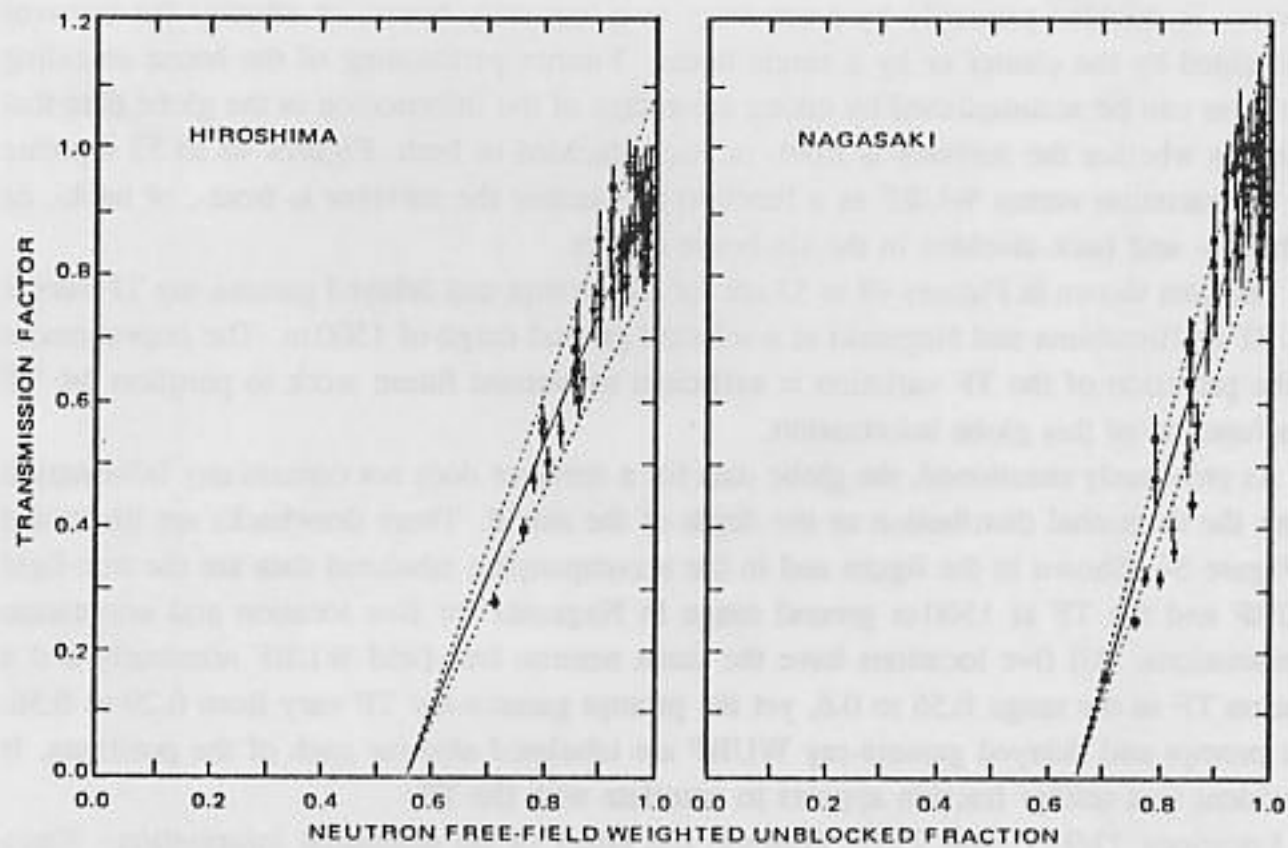


Figure 47. Transmission factors for prompt and delayed gamma rays vs WUBF for all terrain shield categories, Nagasaki, 1500 m

lacking any azimuthal information, is only a gross indicator of the shielding surrounding the survivor. The weighting of the globe data, in effect, filters for the more important incident directions. However, the preliminary results, using gamma-ray distributions, were not as good as those using neutrons, because the incident gamma-ray distribution is too peaked to act as a reliable filter. The neutrons are a better choice, because their angular distribution is more isotropic than either the prompt or delayed gamma rays. The reason for choosing a single variable, as opposed to separate variables for each component (e.g., a "prompt gamma-ray free-field weighted unblocked fraction" for the prompt gamma-ray fields) is the need to choose a single location for all components.

The correlation between the neutron WUBF and neutron TF at both Hiroshima and Nagasaki (Figures 41 and 42) is very good. The TF for the prompt gamma rays (Figures 43 and 44) show more variance with the neutron WUBF than do the delayed gamma-ray TF (Figures 45 and 46). This is because the delayed gamma rays are from a moving source, which tends to reduce the anisotropy of the angular distribution.

Figure 47 shows the TF for terrain shielding at 1500 m for prompt and delayed gamma rays versus neutron WUBF (note that all terrain shielded survivors were at Nagasaki and most were beyond 1500 m). The different effective source heights of the prompt and delayed gamma rays accounts for the different slopes of the regression lines. The more anisotropic character of the prompt gamma rays accounts for the larger variation in the degree of correlation seen for them as compared to the delayed gamma rays.

The data presented in Figures 41 to 47 lump all the locations together, whether the

survivor is shielded primarily by a one-story or a two-story house, or whether the survivor is shielded by the cluster or by a single house. Further partitioning of the house shielding data base can be accomplished by taking advantage of the information in the globe data that indicates whether the survivor is front- or back-shielded or both. Figures 48 to 53 separate out the variation versus WUBF as a function of whether the survivor is front-, or back-, or both front- and back-shielded in the six-house cluster.

The data shown in Figures 48 to 53 are for the prompt and delayed gamma-ray TF versus WUBF at Hiroshima and Nagasaki at a selected ground range of 1500 m. The improvement in the precision of the TF variation is sufficient to warrant future work to partition the TF as a function of this globe information.

As previously mentioned, the globe data for a survivor does not contain any information about the azimuthal distribution or the depth of the shield. These drawbacks are illustrated in Figure 54. Shown in the figure and in the accompanying tabulated data are the free-field WUBF and the TF at 1500 m ground range in Nagasaki for five location and orientation combinations. All five locations have the same neutron free-field WUBF nominally and a neutron TF in the range 0.56 to 0.6, yet the prompt gamma-ray TF vary from 0.29 to 0.56. The prompt and delayed gamma-ray WUBF are tabulated also for each of the positions. It is evident that neither fraction appears to correlate with the TF.

Locations 21/315° and 22/0° illustrate the effect of no azimuthal information. Since neutrons are fairly isotropic at 1500 m, small changes in orientation do not significantly change the shielding for outside locations. However, since the gamma rays are much more directional, any change which unblocks an important portion of the shielded space can significantly alter the TF. This is seen most clearly at location 22/0°, where the incident forward-most radiation is blocked by the two-story house, as opposed to location 21/315°. Even though location 21/315° is closer to the house, the incident radiation is no longer completely blocked in the most forward directions.

Locations 15/225° and 24/45° (Figure 54) illustrate the effect of no information about the depth of the shield. At 1500 m ground range, the burst point is 18.5° above the horizon, and a portion of the incident radiation must traverse the houses. Locations 15/225° and 24/45° appear to be similar shielding situations, in that approximately one-half of the surrounding space is unobstructed, and the immediate shielding structure is a single-story house. The highly directional gamma rays must traverse through the two-story houses at location 15/225° whereas at 24/45° they are blocked by the single-story house only. This results in the disparate prompt and delayed gamma-ray TF tabulated in Figure 54.

It is this inability to obtain any azimuthal or depth of shield information from the globe data that is responsible for the variations in gamma-ray TF for a given WUBF. This inherent deficiency in the shield description by the globe data is, therefore a limiting factor in using the globe data in determining survivor radiation fields.

Globe Model Used in the Revised Dosimetry System

As a result of the analysis described above, a model was devised for those survivors who were in the open but shielded by Japanese houses or by terrain. The WUBF is precomputed for 26 locations in the house cluster plus 10 locations in the terrain model for 8 different orientations at 45° intervals for every 250 m ground range from 700 to 2000 m at Hiroshima

HOUSE AND TERRAIN SHIELDING

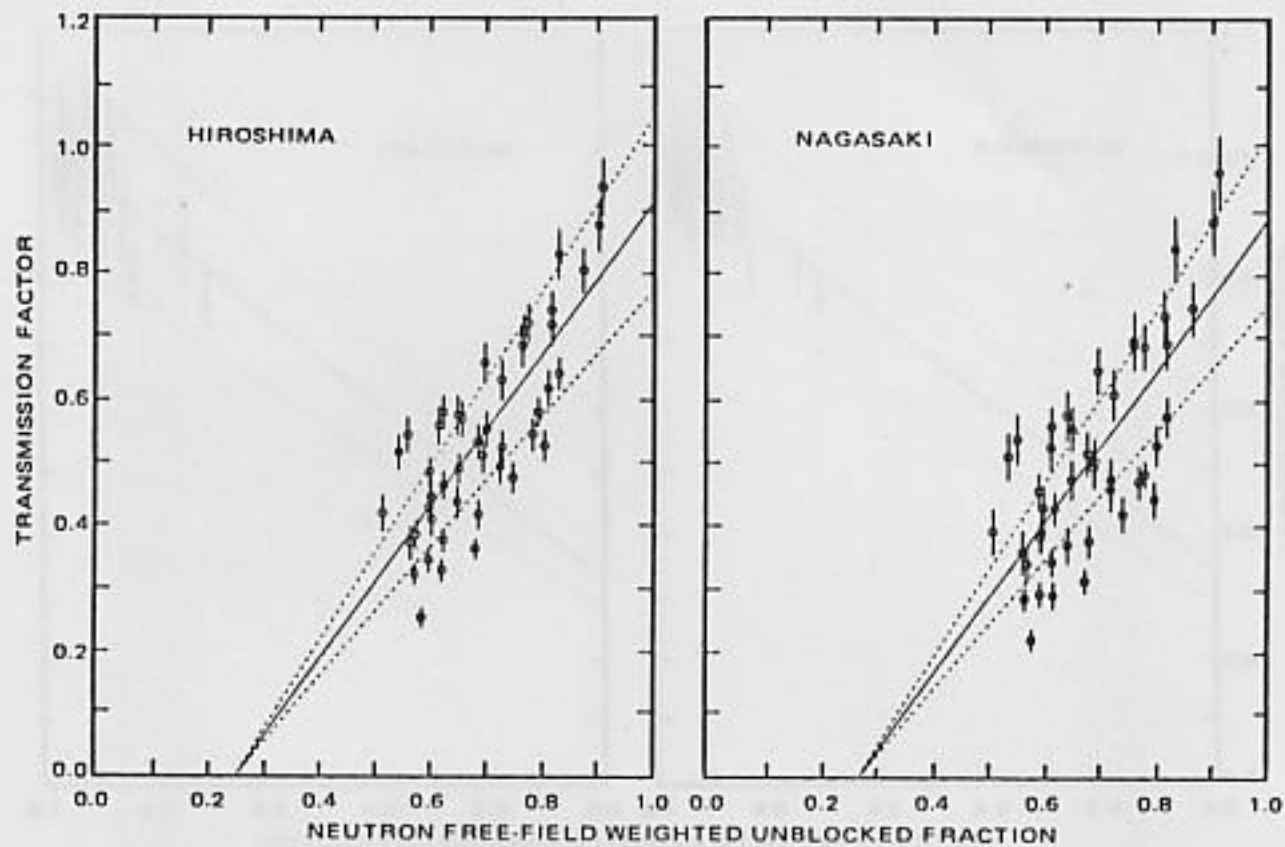


Figure 48. Transmission factors for prompt gamma rays vs WUBF for front shielding, Hiroshima and Nagasaki, 1500 m

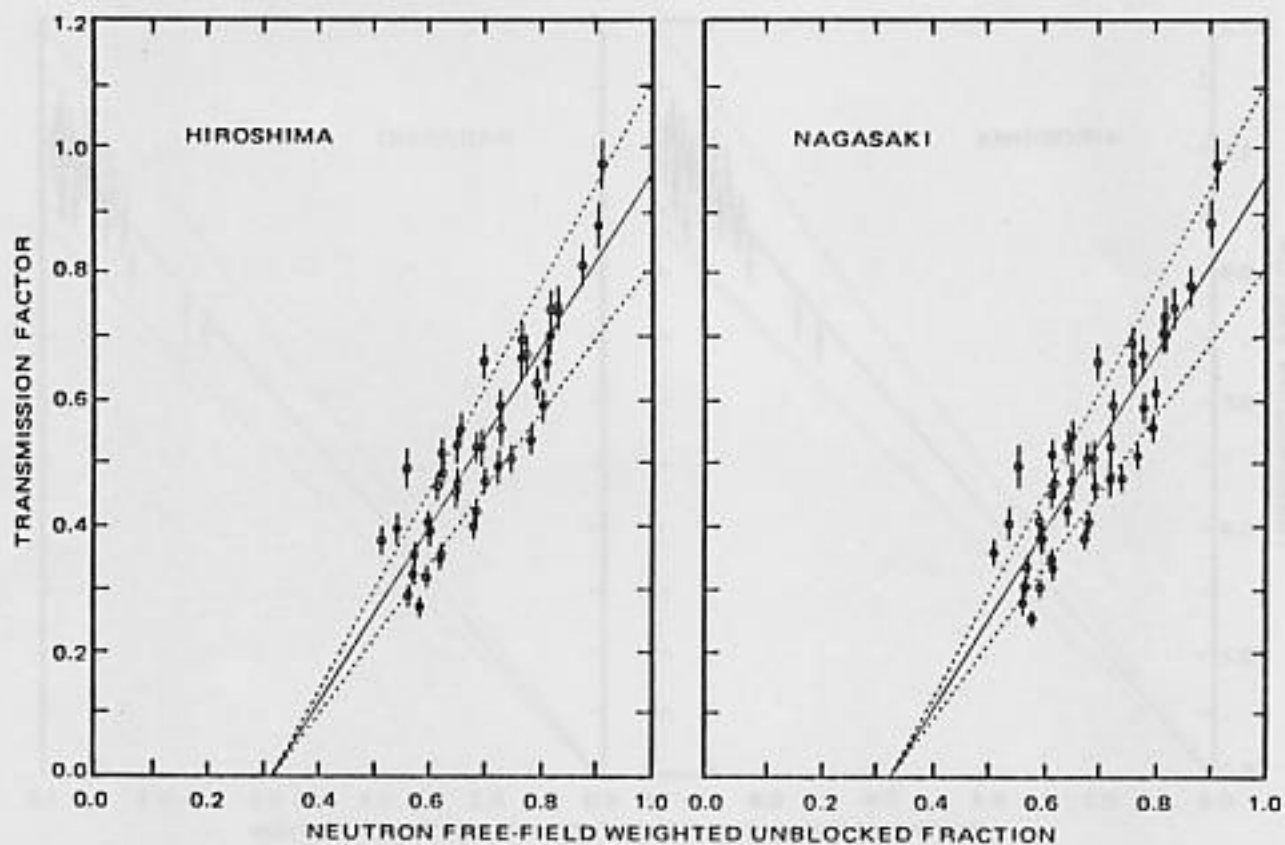


Figure 49. Transmission factors for delayed gamma rays vs WUBF for front shielding, Hiroshima and Nagasaki, 1500 m

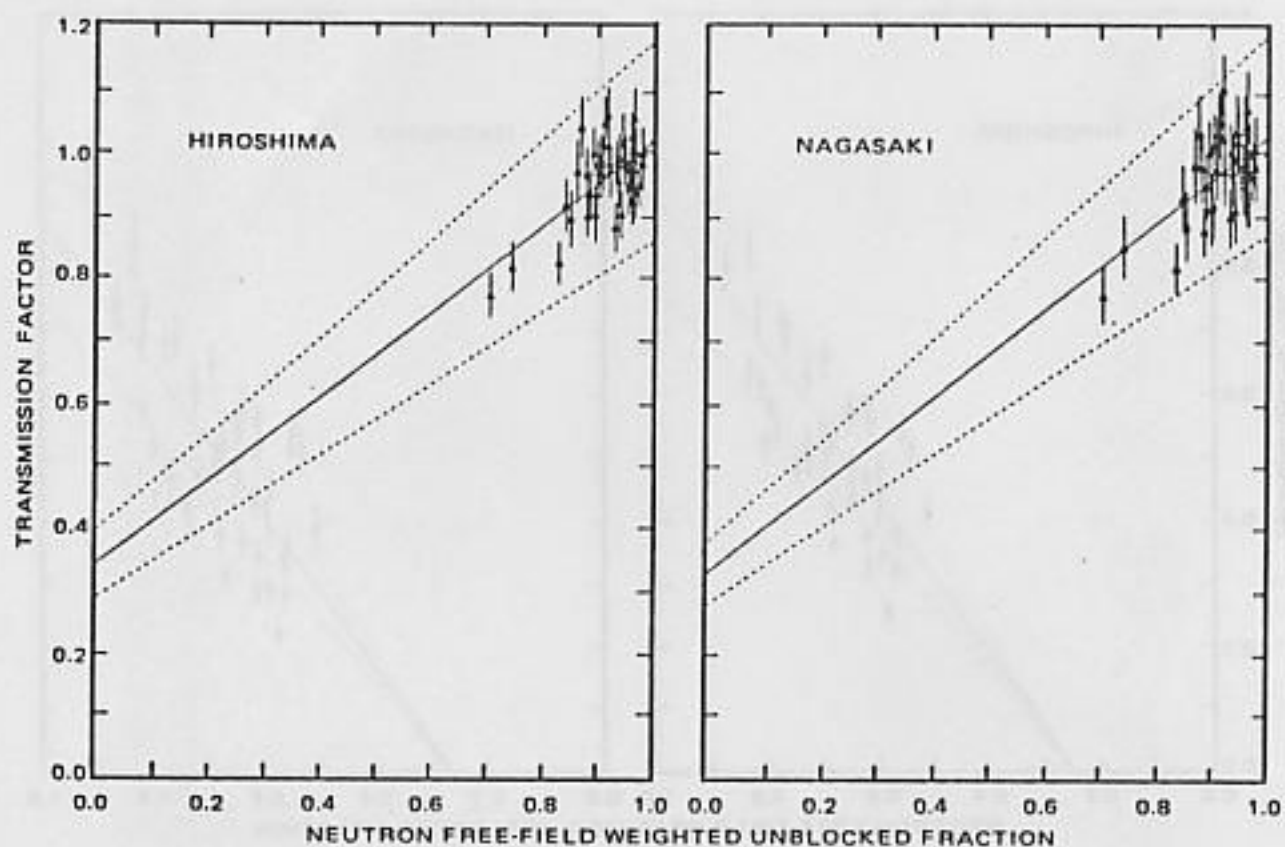


Figure 50. Transmission factors for prompt gamma rays vs WUBF for back shielding, Hiroshima and Nagasaki, 1500 m

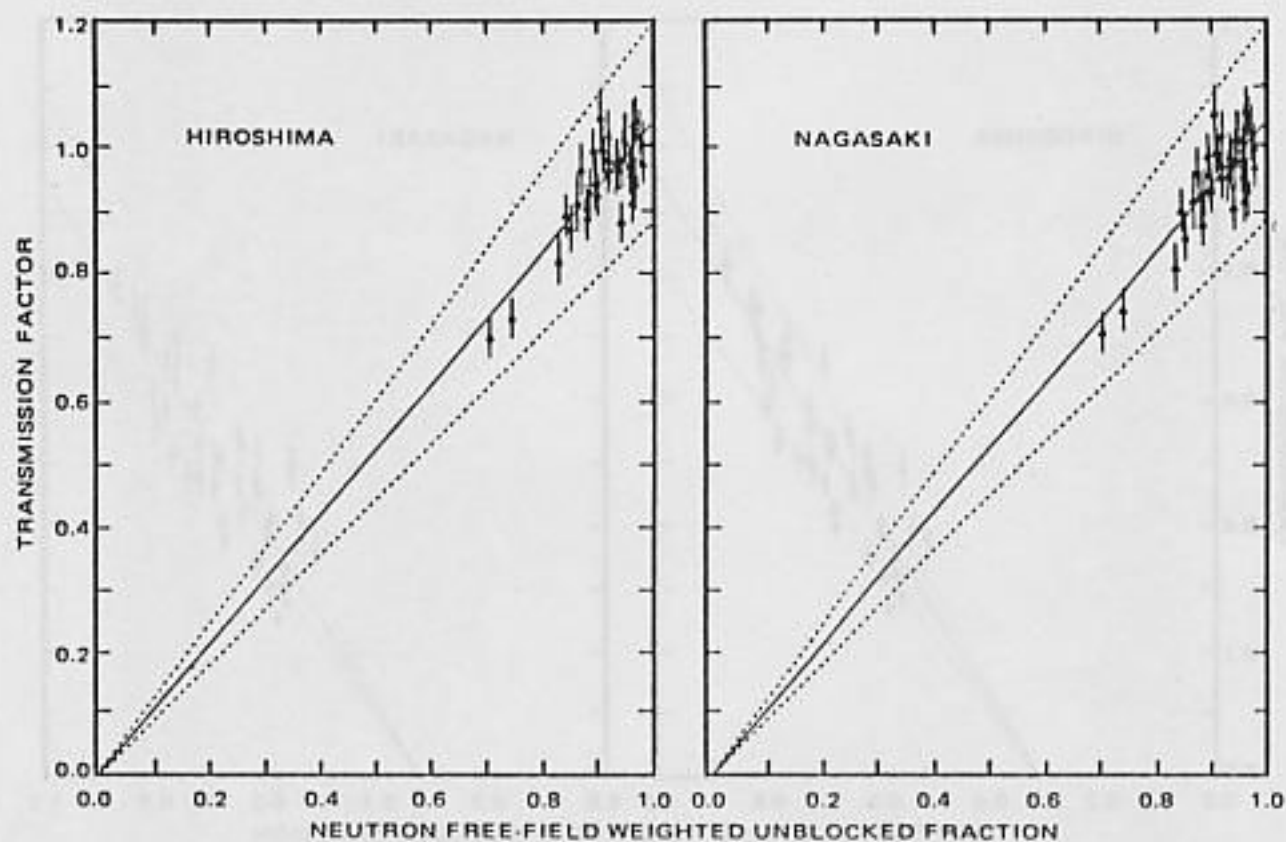


Figure 51. Transmission factors for delayed gamma rays vs WUBF for back shielding, Hiroshima and Nagasaki, 1500 m

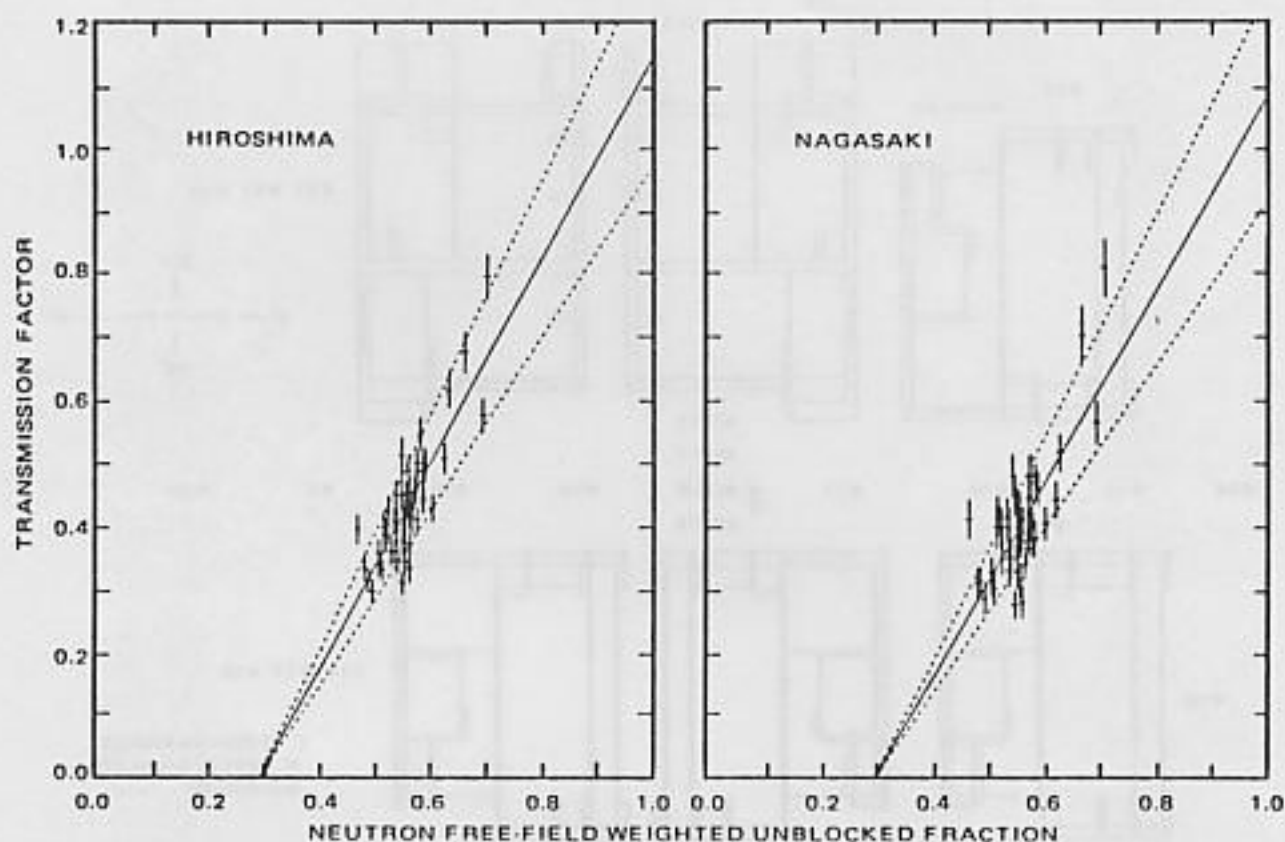


Figure 52. Transmission factors for prompt gamma rays vs WUBF for front and back shielding, Hiroshima and Nagasaki, 1500 m

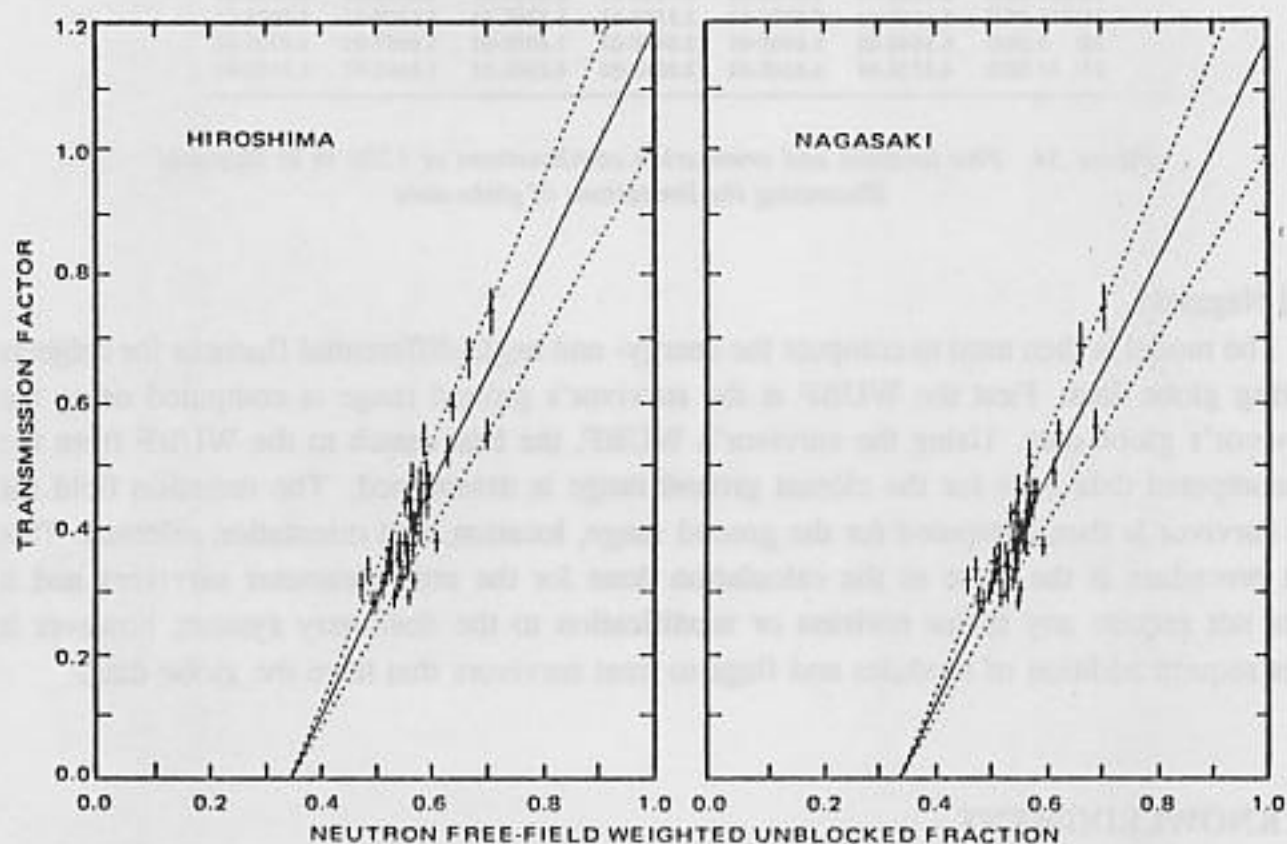
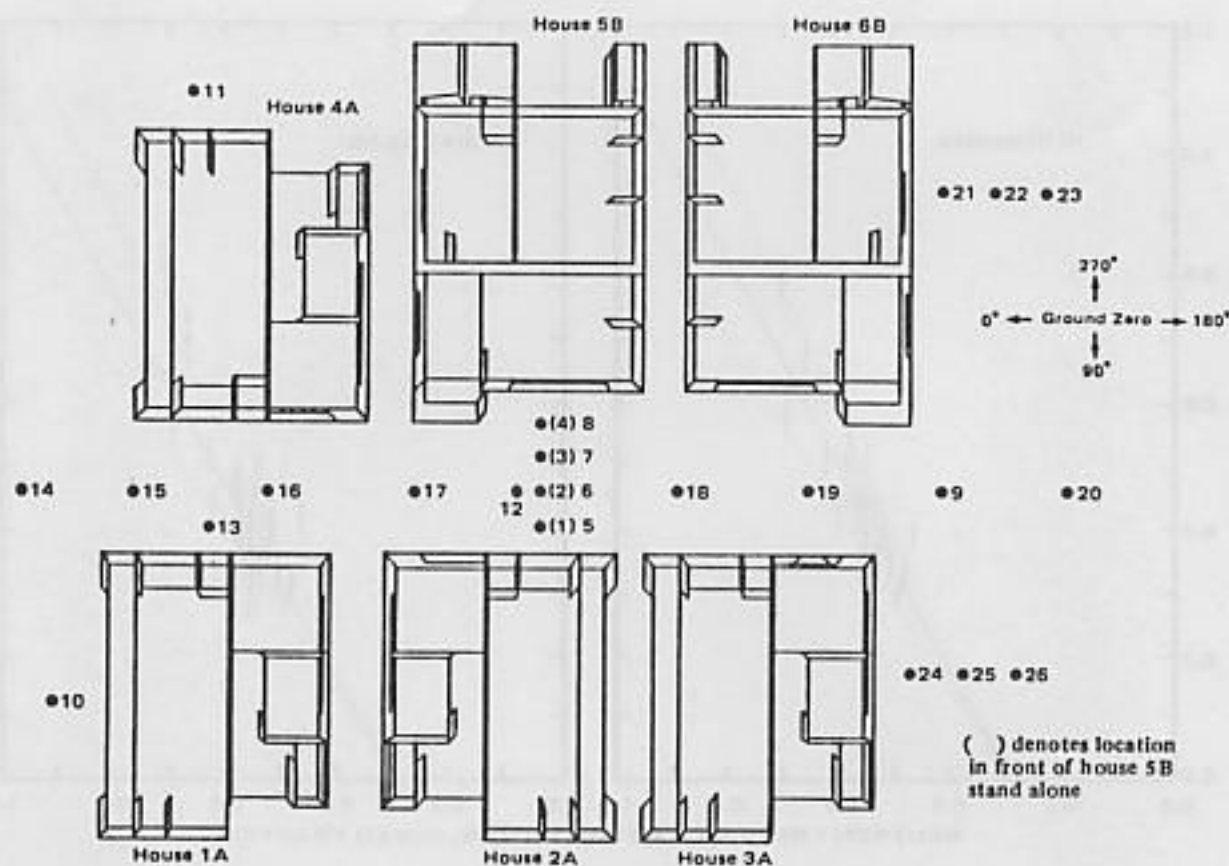


Figure 53. Transmission factors for delayed gamma rays vs WUBF for front and back shielding, Hiroshima and Nagasaki, 1500 m



Location and Orientation	Neutron		Prompt Gamma		Debris Gamma	
	WUBF	TF	WUBF	TF	WUBF	TF
2/315 DEG	6.161E-01	6.040E-01	2.205E-01	5.560E-01	3.252E-01	5.110E-01
15/225 DEG	6.186E-01	5.640E-01	2.592E-01	2.880E-01	3.591E-01	3.320E-01
21/315 DEG	6.150E-01	5.600E-01	2.518E-01	5.220E-01	3.576E-01	4.500E-01
22/ 0 DEG	6.164E-01	5.650E-01	2.045E-01	3.400E-01	3.095E-01	3.470E-01
24/ 45 DEG	6.212E-01	5.820E-01	2.282E-01	4.230E-01	3.446E-01	4.650E-01

Figure 54. Five location and orientation combinations at 1500 m in Nagasaki illustrating the limitations of globe data

and Nagasaki.

The model is then used to compute the energy- and angle-differential fluences for subjects having globe data. First the WUBF at the survivor's ground range is computed using the survivor's globe data. Using the survivor's WUBF, the best match to the WUBF from the precomputed data base for the closest ground range is determined. The radiation field for the survivor is then computed for the ground range, location, and orientation selected. This last procedure is the same as the calculation done for the nine-parameter survivors and it does not require any major revision or modification to the dosimetry system; however it does require addition of modules and flags to treat survivors that have the globe data.

ACKNOWLEDGMENT

The research to reassess the dosimetry of the survivors of the Hiroshima and Nagasaki atomic bombs was a multinational effort with many scientists contributing to the various

phases of the program. With regard to the reevaluation of the house shielding of the survivors that is reported here, special credit should be given to Mr. Hiroaki Yamada (deceased), Mr. Yoshio Okamoto, Dr. Dale L. Preston, and Dr. Hiroo Kato of the Radiation Effects Research Foundation. During our several visits to RERF at both Hiroshima and Nagasaki, this group worked tirelessly to explain the survivor shielding data, to demonstrate how it was generated, to provide special statistical analyses of the data, to seek out experts in Japanese house construction, and to provide complete access to all the available shielding files. The working group is pleased to acknowledge the contributions of Takashi Maruyama, National Institute of Radiological Sciences.

REFERENCES

1. Auxier, J. A., 1977. *Ichiban: Radiation Dosimetry for the Survivors of the Bombing of Hiroshima and Nagasaki*. Washington: Department of Energy, TID-27080.
2. Loewe, W. E. and Mendelsohn, E., 1981. Revised dose estimates at Hiroshima and Nagasaki. *Health Physics* 41:663-666.
3. Marcum, J., 1981. *House Attenuation Factors for Radiation at Hiroshima and Nagasaki*. Marina del Rey, CA: R & D Associates, unpublished report.
4. Milton, R. C. and Shohoji, T., 1968. *Tentative 1965 Radiation Dose Estimation for Atomic Bomb Survivors*. Hiroshima: Radiation Effects Research Foundation, report ABCC-TR-1-68.
5. Woolson, W. A., Marcum, J., Scott, W. H., and Staggs, V. E., 1982. Building transmission factors. In *Reevaluations of Dosimetric Factors, Hiroshima and Nagasaki*, V. P. Bond and J. W. Thiessen, Eds., pp. 179-196. Washington: Department of Energy report CONF-810928.
6. Woolson, W. A., Scott, W. H., and Wilson, C. W., 1984. Delayed radiation models for atomic bomb survivor dosimetry. In *Second U.S.-Japan Joint Workshop for Reassessment of Atomic Bomb Radiation Dosimetry in Hiroshima and Nagasaki*, pp. 67-71. Hiroshima: Radiation Effects Research Foundation.
7. Conover, W. J., 1980. *Practical Non-Parametric Statistics*, 2nd edition. New York: John Wiley.